ECE L10 11012016 ECE 4242/6243 PART II Notes
Chapter 7: Semiconductor Lasers

7.1. Introduction:

Chronology of some early lasers: Some of the first lasers (Kuhn [1]) include 1) Optically pumped ruby laser by T. Maiman (May 1960); 2) He-Ne laser by A. Javan et al. (December 1960); 3) GaAs lasers by three groups (1962) operated at liquid He; 4) CO_2 laser by C.K.N. Patel (1964); 5) Geusic et al. Nd:YAG laser (1964); 6) Bridges, Argon ion laser (1964), 7) GaAs-AlGaAs heterostructure lasers at room temperature by I. Hayashi et al (1968), 8). Excimer laser by N. Bassov et al. (1970). Gordon Gould is credited with the first laser invention recorded in 1957. Schalow and Townes published their first theoretical paper on lasers in 1958.

We need to understand the mechanisms of light emission before we start discussing <u>L</u>ight <u>A</u>mplification by <u>S</u>timulated <u>E</u>mission of <u>R</u>adiation (LASER). Light is emitted when electrons belonging to higher energy states make transitions to lower energy states. Not always the photons are emitted. Some time electron falls down to lower levels via surface states, collisions, and other scattering mechanisms that are nonradiative. This helps define the quantum efficiency η_q as $\tau_{nr}/(\tau_{nr} + \tau_r)$. Here, τ's are the average lifetime for radiative for nonradiative transitions, described in Chapter 4 (LEDs).

Transitions are between discrete energy states in atoms and molecules, and from upper band (conduction band) of states to lower band (valence band) of states in semiconductors. The difference in the lower and higher energy states is determined by allowed states via the selection rules. In molecules the transitions due to the vibrational or rotational states create very small energy difference as in gases (CO_2, NH_3; the CO_2 emits around 10.6 microns and the NH_3 produces microwaves). In others, the difference could be large such as in argon, neon, and nitrogen due to electronic transitions. Generally, electrons are first pumped up to higher energy states using gas discharge (transferring energy from the DC or RF electric field), optical pumps (arc lamps and lately the diode lasers), chemical reactions, and current injection. The downward transitions of electrons produce photons. This is well known in neon tubes, He-Ne lasers, argon lasers, and excimer lasers (used in Lasik procedures for correcting eye lenses).

Another form of transitions is due to free carriers and excitons (bound electron and hole pairs). Excitons are described in the LEDs Chapter 4. That is, electron injection from the conduction band (higher energy states) of an n-semiconductor into a p-semiconductor across the n-p junction causes either electron-hole recombination and light emission or formation of electron-hole pairs which are bound via the Coulombic attraction. The collapse of excitons results in the emission of photons. That is, when electron and hole recombine a photon of energy [($h\nu - E_{ex}$) is produced; generally, exciton binding energy is small (4-6 meV) in GaAs, Si, InP and Ge]. However, it is higher in ZnSe, GaN and other low dielectric constant semiconductors. Similar is the situation in polymer and organic semiconductors, which are known to exhibit higher binding energy. Exciton binding energy is reduced with increased electron and hole concentrations, which causes screening to counter the coulomb attraction. The binding energy of excitons can be increased by confining the constituent electrons and holes in quantum wells, wires, and dots.

Summary of Lasing: Regardless of transition type, the emitted photons are spontaneous and thus incoherent. That is the process of electron falling to a lower energy level, or electron-hole recombination, or exciton decay, or changes in vibrational or rotational modes of molecules are spontaneous. Therefore, emitted photons have no phase correlation among them. However, in the presence of large photon density [$\rho(h\nu)$] the photons stimulate electrons and holes to recombine producing photons. This results in stimulated emission. The stimulating photons are of similar wavelength and phase as the emitted photons. The magnitude of photon density needed to stimulate photons, in general, does not exist in light emitting systems. This requires special effort to build photon density. It is done in two ways:

(1) forming a resonator or cavity with at least two reflecting mirrors (the mirrors are implemented by introducing a reflecting surface or using distributed Bragg Reflectors (DBRs),

(2) distributed feedback (DFB) of photons in the lasing layer with the presence of a diffraction grating in one or both of the cladding layers.

In cavity type structures, the feedback is provided by the end mirrors, and in distributed feedback type structures, the feedback is provided continuously by a grating adjacent to the medium where lasing is taking place. Both cavity type and DFB lasers are further divided into two categories: (1) edge emitting, and (2) surface emitting lasers (SELs). Surface emitting lasers are also known as vertical cavity surface emitting lasers (VCSELs).

Cavity can be constructed by using distributed Bragg reflectors (DBR) or gratings which serve as a mirror. This gives a DBR laser shown in Fig. 55 which results in a very narrow line width. DBR mirrors are also used to fabricate a vertical cavity used in surface emitting laser (Fig. 56).

Examples of some laser structures are reproduced below.

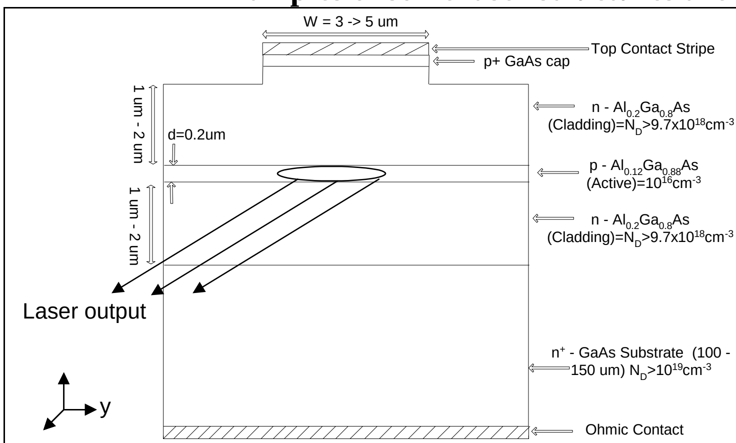

Fig .28. An edge-emitting cavity laser with ridge.

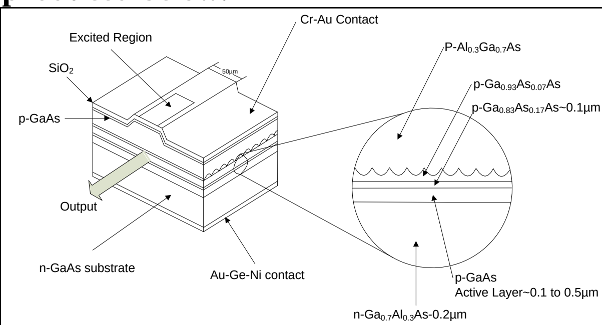

Fig .48 Distributed feedback (DFB) edge-emitting laser (first order grating).

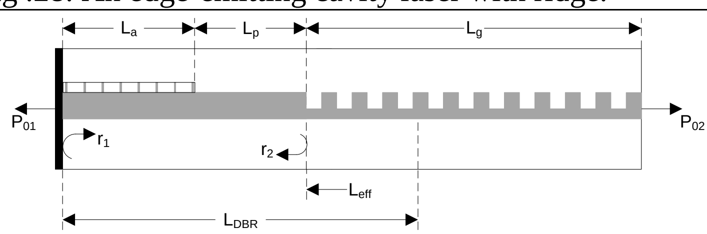

Fig. 55 Cavity formed by one conventional mirror and one distributed Bragg reflector (DBR).

Fig. 56 (right panel): In a vertical cavity surface emitting laser (VCSEL) the cavity thickness is multiple of half wavelengths and DBRs are quarter wavelengths with high and lower index of refraction.

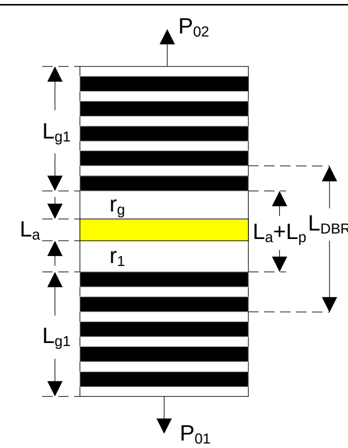

Fig. 56 VCSEL with DBR reflectors.

7.1.1 General Conditions of Lasing:

The general condition is based on the thermal equilibrium condition that in a medium, rate of emission is equal to the rate of absorption. [Reference A. Yariv]

Rate of emission = Rate of absorption

Since the emission is of two types: Spontaneous and Stimulated, the condition is rewritten as:

Rate of spontaneous emission + rate of stimulated emission =Rate of absorption

$$A_{21}N_2 + B_{21}\,\rho(h\nu_{12})\,N_2 = B_{12}\,\rho(h\nu_{12})\,N_1 \qquad (1)$$

Here, A and B are coefficients, known as the Einstein's coefficient. N_2 and N_1 are the number of electrons in the upper (energy E_2) and lower (energy E_1) levels. The above equation is true under equilibrium condition. Since we want stimulated emission to dominate, we would compare its rate with respect to the other two processes.

(1) Rate of stimulated emission (2nd term on left in Eq. A) >> rate of absorption (term on right).

$$B_{21}\,\rho(h\nu_{12})\,N_2 \gg B_{12}\,\rho(h\nu_{12})\,N_1 \qquad (2)$$

Or, $(N_2/N_1) \gg 1$ **Condition known as population inversion.** (3)

(Using Planck's distribution law, we can show that $B_{12}=B_{21}$).

Under equilibrium number of atoms (e.g. Ne atoms in He-Ne laser) having electrons in higher energy state E_2 is lower than Ne atoms in lower energy state E_1. This is a consequence of statistics (N is proportional to $e^{-E/kT}$ such as Maxwell-Boltzmann statistics). So the condition Eq. 3 can be written as

$e^{-(E2 - E1)/kT} \gg 1$ **Negative temperature condition** (4)

This is sometimes referred to as negative temperature condition. That is, it is valid only when temperature is negative since E2>E1. Alternatively, it is valid under non-equilibrium conditions when we optically or electrically pump the lasing medium to have more atoms of Ne in E2 state.

(2) Rate of stimulated emission >> rate of spontaneous emission (first term in Eq. 1)

$$B_{21}\,\rho(h\nu_{12})\,N_2 \gg A_{21}N_2 \qquad (5)$$

$\rho(h\nu_{12}) \gg A_{21}/B_{21}$ **Positive feedback via cavity or DFB structure** (6)

Condition Eq. 6 means that the stimulating photon density is higher than a certain value which depends on coefficients. Enhanced photon density [Condition (2)] is achieved by implementing positive feedback by either using a resonant cavity or distributed feedback.

Condition #1 is achieved by having non-equilibrium situation where electrons are pumped into the upper level E_2 in higher number than E_1. Generally, at equilibrium, the number is proportional to exp[-E/kT]. This is based on the Maxwell-Boltzmann statistics.

We can introduce more carriers in the upper level by injection as in p-n junction. Later on we will derive more specific condition of lasing in semiconductor lasers.

Relation between B_{21} and B_{12}

For blackbody radiation, the photon energy density between $\nu, \nu + d\nu$

$$\rho(h\nu_{12})d\nu = \frac{8\pi n_r^3 h\nu^3}{c^3}\frac{d\nu}{e^{h\nu/kT}-1}$$

Sometimes written as = $\dfrac{8\pi n_r^3 h\nu^3}{c^3 \nu_g}\dfrac{1}{e^{h\nu/kT}-1}$

$$\frac{N_2}{N_1} = e^{-h\nu/kT}$$

$N_2 A_{21} + B_{21} N_2 \rho(h\nu_{12}) = B_{12} N_1 \rho(h\nu_{12})$ [Maxwell-Boltzmann Distribution]

$$N_2\underbrace{\left[A_{21} + B_{21}\frac{8\pi n_r^3 h\nu^3}{c^3}\frac{1}{e^{h\nu/kT}-1}\right]}_{\rho(h\nu_{12})} = B_{12} N_1 \underbrace{\left[\frac{8\pi n_r^3 h\nu}{c^3\left(e^{h\nu/kT}-1\right)}\right]}_{\rho(h\nu_{12})}$$

$$\frac{N_2}{N_1}\frac{A_{21}}{B_{12}} + \frac{N_2}{N_1}\frac{B_{21}}{B_{12}}\rho(h\nu_{12}) = \rho(h\nu_{12})$$

$$\rho(h\nu_{12}) = \frac{\dfrac{N_2}{N_1}\dfrac{A_{21}}{B_{12}}}{1 - \dfrac{N_2}{N_1}\dfrac{B_{21}}{B_{12}}} = \frac{e^{h\nu/kT}\dfrac{A_{21}}{B_{12}}}{1 - e^{h\nu/kT}\dfrac{B_{21}}{B_{12}}}$$

$$\frac{8\pi n_r^3 h\nu^3}{c^3}\frac{1}{e^{h\nu/kT}-1} = \frac{\dfrac{A_{21}}{B_{12}}}{e^{-h\nu/kT} - \dfrac{B_{21}}{B_{12}}}$$

The above relation is true if

1) $\dfrac{A_{21}}{B_{12}} = \dfrac{8\pi n_r^3 h\nu^3}{c^3}$

2) $B_{21} = B_{12}$

7.1.2 Conditions for Lasing in Fabry-Perot Cavity Lasers

Described next is an approach which determines the ratio of total transmitted electric field to the incident electric field strength for a lasing medium. The condition of oscillation is obtained by setting this ratio to approach infinity. That is, $E_o/E_i \rightarrow \infty$, similar to what we do in electronic circuits (gain of an amplifier $\rightarrow \infty$; this is shown in Fig. 1b). The electric filed E at any point z in the lasing cavity medium for a travelling plane wave can be written in terms of propagation constant γ and angular frequency ω:

$$\bar{E} = Ee^{-j\gamma z} \cdot e^{j\omega t} = Ee^{-j(\gamma z - \omega t)} \tag{7a}$$

where $\gamma = (n_r - j\kappa)k_0$ (7b)

A medium with loss is represented by a complex index n_c (= $n_r - j\kappa$).

The characteristics for the medium can be represented by a complex propagation constant γ.

Here, n_r is the real part of the complex index of refraction n_c, k_o is the free space propagation constant (=$2\pi/\lambda$) and κ is the extinction coefficient, which is related to the absorption coefficient α:

$$\kappa = \frac{\alpha\lambda}{4\pi} \tag{7c}$$

Here, α the absorption coefficient of the medium is related to light intensity I as

$$I(x) = I(x=0)e^{-\alpha x} \tag{7d}$$

Note that intensity of light is related to the power represented by the Poynting vector P, which in turn is related with electric and magnetic fields as

$$P = \mathrm{Re}\,[1/2(E \times H^*)] \tag{7e}$$

Using Eq.(7c), we can rewrite Eq. 7b for the propagation coefficient as

$$\gamma = n_r k_o - j\frac{\alpha\lambda}{4\pi}k_o$$

(8a)

Using $k_o = \dfrac{2\pi}{\lambda}$ and substituting in Eq. 8(a)

$$\gamma = n_r\frac{2\pi}{\lambda} - j\frac{\alpha\lambda}{4\pi}\frac{2\pi}{\lambda} = n_r\frac{2\pi}{\lambda} - j\frac{\alpha}{2} \tag{8b}$$

A more general form of Equation (8b) includes g, the gain coefficient of the lasing medium

$$\gamma = n_r\frac{2\pi}{\lambda} + j\frac{(g - \alpha)}{2}$$

(8c)

Figure 1(a) shows the electric field strength at various locations during successive passes. Hwere, t_1, r_1 are the coefficients representing electric field transmission and reflection from boundary #1 (representing one of the cavity walls at z =0) of the lasing medium, and t_2, r_2 are for boundary #2 or mirror 2. The length of the lasing medium along the direction of propagation z is L.

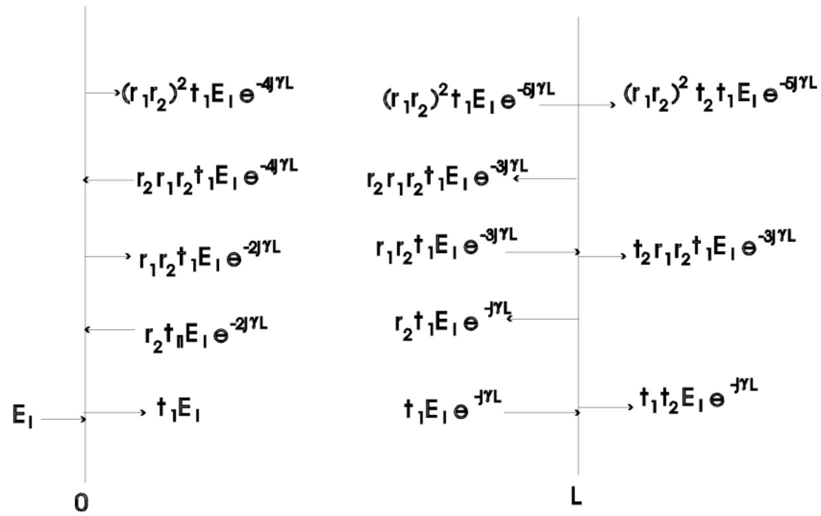

Fig. 1a. Electric field strength after many passes in a cavity of length L.

The electric field output E_o for the lasing cavity can be determined by adding all the components transmitted through side #2

$$
\begin{aligned}
E_o &= t_1 t_2 E_i e^{-j\gamma L} + t_1 t_2 r_1 r_2 E_i e^{-3j\gamma L} + (r_1 r_2)^2 t_1 t_2 E_i e^{-5i\gamma L} \\
&= t_1 t_2 E_i e^{-j\gamma L} [1 + r_1 r_2 e^{-2j\gamma L} + (r_1 r_2)^2 e^{-4j\gamma L} + \bullet\bullet\bullet]
\end{aligned} \tag{9}
$$

S=1+a+a^2+a^3+…..
S=1/(1-a)

Summing the series

$$
E_o = \frac{t_1 t_2 E_i e^{-j\gamma L}}{(1 - r_1 r_2 e^{-2j\gamma L})}
$$

$$
\frac{E_o}{E_i} = \frac{t_1 t_2 e^{-j\gamma L}}{(1 - r_1 r_2 E^{-2j\gamma L})} \tag{10}
$$

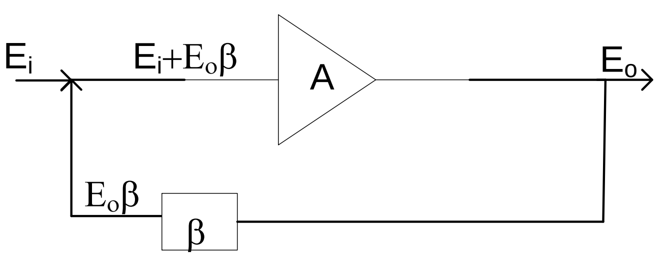

Fig. 1(b) Laser oscillator model with positive feedback β provided by the cavity mirrors.

The feedback of photon provided by the cavity can be modeled as an oscillator as shown in Fig. 1(b). Here,

$$E_o/E_i = [A/(1-A\beta)] \tag{11}$$

In Eq. 11 we have represented the amplification of light by the amplifier gain A, and the mirrors are represented by the feedback β. The condition of oscillation is when the denominator goes to 0. $A\beta = 1$.

Similarly, from Eq. 10, E_o approach infinite if the denominator becomes 0.

$$1 - r_1 r_2 e^{-2j\gamma L} = 0 \tag{12}$$

Equation (12) describes the condition of oscillation. Using Eq. 8c for γ in Equation (12), we can rewrite it as

$$1 - r_1 r_2 e^{-2j\left[n_r \frac{2\pi}{\lambda} + j\frac{(g-\alpha)}{2}\right]L} = 0$$

Using well known trigonometric identity: $1 \equiv 1 e^{-j2\pi m}, m \text{ is an integer}$, we can express Eq. 12 as

$$1 e^{-j2\pi m} - r_1 r_2 e^{(g-\alpha)L} e^{-2jn_r \frac{2\pi}{\lambda} L} = 0 \tag{13}$$

Equation (13) can be separated into two equations:

(a) Gain coefficient g from real part of Eq. 13

$$1 - r_1 r_2 e^{(g-\alpha)L} = 0$$

$$e^{(g-\alpha)L} = \frac{1}{r_1 r_2}$$

$$g = \alpha + \frac{1}{L}\ln\left(\frac{1}{r_1 r_2}\right) \tag{14}$$

Generally Equation (14) is written as $g = \alpha + \frac{1}{2L}\ln\left(\frac{1}{R_1 R_2}\right)$ (15)

Eq. 15 is also written as $g = \frac{1}{2L}\ln(\frac{1}{R_1 R_2}) + \alpha_f + \alpha_c + \alpha_d$, where $R_1 = r_1^2$ and $R_2 = r_2^2$. R_1 and R_2 relate to coefficient of reflection when intensity (or power density) is considered. Lower case r_1 and r_2 are electric field reflectivities.

Gain condition Eq. 15 states that lasing takes place when the gain coefficient g becomes equal to α (which represent all loss mechanism attenuating light intensity) and the term $\frac{1}{2L}\ln\left(\frac{1}{R_1 R_2}\right)$ (which represents photon power loss due to leakage through the two walls; which is the output).

(b) Phase condition from the imaginary part of Eq. 13

$$e^{-j2\pi m} = e^{\frac{-4jn_r\pi L}{\lambda}} \tag{16}$$

$$\boxed{L = \frac{m\lambda}{2n_r}} \tag{17}$$

In Equation (17) λ is the free space wavelength. Since λ in free space wavelength λ_L in medium is obtained by dividing λ by the index of refraction of the lasing medium;
$\lambda_L = \lambda/n_r$, and Eq. (17) can be written as

$$L = \frac{m\lambda_L}{2} \tag{18}$$

Phase condition Eq. 17 or Eq. 18 states that only those wavelengths are amplified by the cavity where integral half wavelengths fit the cavity length L. Wavelengths that are lasing are called cavity or longitudinal modes.

7.1.3 Resonant Cavity Modes and Mode Separation

Figure 2 shows schematically the cavity in which lasing is taking place, here the shaded faces represents the two reflecting walls.

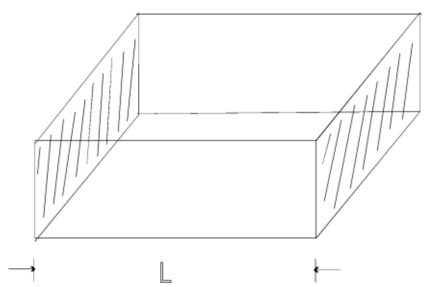

Figure 2. Cavity with parallel end faces

The condition of constructive interference in a Fabry-Perot Cavity is:

$$L = \frac{m\lambda}{2n_r} \tag{17}$$

Rewriting it,

$$m = \frac{2n_r L}{\lambda} \tag{19}$$

In a dispersive medium, index of refraction is a function of wavelength of operation. Since the cavity has many longitudinal modes, the index of refraction $n_r(\lambda)$ depends on λ. Note that many wavelengths can satisfy Equation (19) for different values of m.

We would next find out the separation Δm between successive modes (i.e. m and m±1, or m + Δm where Δm = ±1). Differentiate Equation (19) with respect to λ

$$\frac{dm}{d\lambda} = -\frac{2n_r L}{\lambda^2} + \frac{2L}{\lambda}\frac{dn_r}{d\lambda} = -\frac{2n_r L}{\lambda^2}\left(1 - \frac{\lambda}{n_r}\frac{dn_r}{d\lambda}\right) \tag{20}$$

$$d\lambda = -\frac{\lambda^2}{2L n_r}\left(1 - \frac{\lambda}{n_r}\frac{dn_r}{d\lambda}\right)^{-1} dm \tag{21}$$

Recognizing that m is an integer, dm will be written as Δm and correspondingly dλ as Δλ. The wavelength separation Δλ between successive modes is obtained by setting Δm = ±1.

$$\boxed{\Delta\lambda = \pm\frac{\lambda^2}{2L n_r}\left(1 - \frac{\lambda}{n_r}\frac{dn_r}{d\lambda}\right)^{-1}} \tag{22}$$

Equation (22) represents the wavelength separation between two successive cavity modes lasing in the vicinity of λ.

Figure 3 shows the emission spectrum highlighting cavity modes (also known as the longitudinal or axial modes) for the GaAs laser diode.

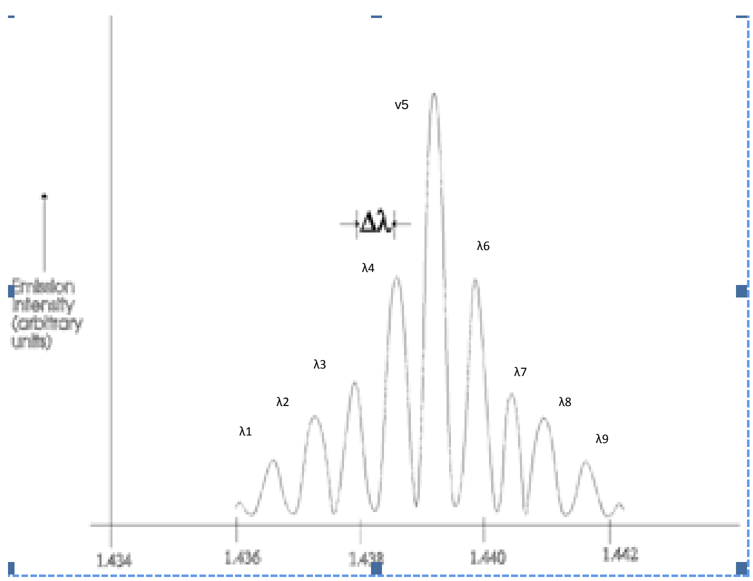

Fig. 3. Emitted intensity as a function of hv in eV

Example 1: Calculations of mode separation Δλ and frequency separation Δν in a GaAs laser

Method I-Simple approach: Operating wavelength for a cavity mode is λ= 0.85μm. The lasing wavelength is such that it satisfies the condition expressed by Eq. 31. So it is such that the corresponding photon energy hv> E_g. For a cavity of length L = 1000μm and index of refraction of the lasing layer is n_r = 3.59, we find from Equation (22) that $\Delta\lambda$=2.01 Å.

Once we know wavelength separation $\Delta\lambda$, we can also find out the frequency separation Δv between successive modes. (In this situation we use c = $\nu\lambda$ in Equation (19) and derive an equivalent relation for Δv). Δv is expressed in terms of speed of light and $\Delta\lambda$ as

$\Delta\lambda = \lambda_2 - \lambda_1 = c/v_2 - c/v_1 = c(\nu_1-\nu_2)/ v_2 v_1 = c\, \Delta v/ v_2 v_1$

Or, $\Delta v = (v_2 v_1 \Delta\lambda)/c = c\, \Delta\lambda/\lambda_2\lambda_1$

$\Delta v \sim c\, \Delta\lambda/ \lambda^2$

Substituting values of c, λ and $\Delta\lambda$, we get Δv=83.4GHz.

Method II: Compute the wavelength $\Delta\lambda$ and frequency $\Delta\upsilon$ separations between successive longitudinal or cavity modes for a GaAs laser diode with following parameters.

Operating wavelength λ=0.84 μm (in free space)

Cavity index of refraction n_r = 3.59

$d n_r/d\lambda = 2.5\ \mu m^{-1}$

Cavity length L = 200 μm

Compare the separation if cavity length is reduced to 25 μm.

Solution

$$\Delta\lambda = \pm \frac{\lambda^2}{2Ln_r}\left(1 - \frac{\lambda}{n_r}\frac{dn_r}{d\lambda}\right)^{-1}$$

λ = Operating wavelength in free space.

$$\Delta\lambda = \frac{(0.84*10^{-4})^2}{2*500*10^{-4}*3.59}\left(1 - \frac{0.84\mu m}{3.59}*2.5\mu m^{-1}\right)$$

$= 1.18\text{x}10^{-7}$ cm = 11.8 A°

Frequency separation between successive modes = $\Delta\upsilon$ (It is different from $\Delta\upsilon_s$)

$$\Delta\upsilon = \upsilon_1 - \upsilon_2 = \frac{c}{\lambda_1} - \frac{c}{\lambda_2} = c\frac{\lambda_2 - \lambda_1}{\lambda_1\lambda_2} = \frac{c\Delta\lambda}{\lambda_1\lambda_2}$$

Let λ_2 = 0.84 μm

$\lambda_1 = \lambda_2 + \Delta\lambda$

$\lambda_1 \lambda_2 \approx (\lambda_2)^2 = (0.84*10^{-4})^2$

$$\Delta\upsilon = \frac{3*10^{10}*1.18*10^{-7}}{(0.84*10^{-4})^2} = 5.017x10^{11}Hz$$

$$\Delta\lambda\Big|_{forL=25\mu m} = 8*\Delta\lambda\Big|_{L=200\mu m}$$

$$\Delta\upsilon\Big|_{forL=25\mu m} = 8*\Delta\upsilon\Big|_{L=200\mu m}$$

Cavity length L = 25 μm yields increased mode separation and therefore fewer axial modes.

In-homogenous mode separation: Because of dispersion (or different value of $dn_r/d\lambda$ for different cavity modes), we see that dn_r in λ_2-λ_1 is not equal to λ_3-λ_4. Hence the modes in Fig. 3 are not equally separated or in-homogenous.

7.1.4. Population inversion in semiconductor lasers: Equivalent Condition II for Lasing

This condition is based on the fact that the rate of stimulated emission has to be greater than the rate of absorption.

Rate of stimulated emission > Rate of absorption

$$B_{21} n_2 \rho(h\nu_{12}) > B_{12} n_1 \rho(h\nu_{12}) \tag{23}$$

The rate of stimulated emission is proportional to quantum mechanical coefficient B_{21} (which relates the probability per unit time that a stimulated transition takes place), n_2 is the number of electrons in the upper level, and photon density $\rho(h\nu_{12})$ that stimulates electrons to recombine with holes.

The electron concentration in the upper conduction band and their recombination is expressed by a product of joint density of states $N_j(E=h\nu_{12})$ *f(E) the probability that a level Ec1 is occupied * (1-f) the probability that a level E_{v1} in the valence band is unoccupied (or a hole is there+.

$$n_2 = \left[\frac{1}{1+e^{\frac{E_{c1}-E_{fn}}{kT}}}\right] * N_j(E = h\nu_{12}) * \left[1 - \frac{1}{1+e^{\frac{E_{v1}-E_{fp}}{kT}}}\right]$$

Here, probability f_e that the upper level E_2 or E_{c1} in the conduction band is occupied is

$$f_e = \left(\frac{1}{1+e^{\frac{(E_{c1}-E_{fn})}{kT}}}\right), \text{ } E_{fn} = \text{quasi-Fermi level for electrons.} \tag{24}$$

Probability f_h that a level E_1 or E_{v1} in the valence band is empty (i.e. a hole is there)

Here, again E_{v1} is a level in the valance band below E_v the valence band edge. Similarly, E_{c1} is the level in conduction band above conduction band edge E_c.

$$f_h = \left(1 - \frac{1}{1+e^{\frac{E_{v1}-E_{fp}}{kT}}}\right) \tag{25}$$

The rate of stimulated emission is:

$$= B_{21} * \left[\frac{1}{1+e^{\frac{E_{c1}-E_{fn}}{kT}}}\right] * N_j(E = h\nu_{12}) * \rho(h\nu_{12}) * \left[1 - \frac{1}{1+e^{\frac{E_{v1}-E_{fp}}{kT}}}\right] \tag{26}$$

Similarly, the rate of absorption:

Lower level VB Upper level (CB) (empty)

$$= B_{12} * \left[\frac{1}{1+e^{\frac{E_{v1}-E_{fp}}{kT}}} \right] * N_j(E = h\nu_{12}) * \rho(h\nu_{12}) * \left[1 - \frac{1}{1+e^{\frac{E_{c1}-E_{fn}}{kT}}} \right] \quad (27)$$

Using the condition that the rate of stimulated emission > rate of absorption; (assuming $B_{21}=B_{12}$), simplifying Equation (26) and Equation (27)

$$\frac{1}{1+e^{\frac{E_{c1}-E_{fn}}{kT}}} * \left[1 - \frac{1}{1+e^{\frac{E_{v1}-E_{fp}}{kT}}} \right] > \frac{1}{1+e^{\frac{E_{v1}-E_{fp}}{kT}}} * \left[1 - \frac{1}{1+e^{\frac{E_{c1}-E_{fn}}{kT}}} \right] \quad (28)$$

Further mathematical simplification yields

$E_{fn} - E_{fp} > E_{c1} - E_{v1}$ (29)

Note here, the energy of the emitted photon

$E_{c1} - E_{v1} = h\nu$ (30)

In addition, hν is greater than E_g as $E_g = E_c - E_v$ as shown in Fig. 4.

Fig. 4 schematically shows the energy levels E_{c1} and E_{v1}, band edges, and quasi-Fermi level locations. The photons hν ranging between these are not absorbed due to band-to-band transitions. This range is known as 'transparency condition'.

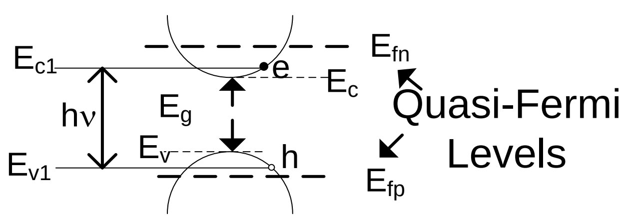

Fig. 4 Schematic showing band edges and quasi-Fermi level locations.

Combining Eqs. 29 and 30 we get

$$\boxed{E_{fn} - E_{fp} > h\nu > E_g} \quad (31)$$

Equation (31) is the equivalent of population inversion in a semiconductor laser. It is known as Bernard - Douraffourg condition and is also referred as condition of transparency.

For band-to-band transitions $h\nu \geq E_g$ and this is possible if the injected electron and hole concentrations push one of the quasi Fermi levels inside the conduction and/or valence band.

That is having the quasi Fermi level difference more than the energy gap

$$E_{fn} - E_{fp} > E_g \qquad (32)$$

This condition is used to find the injected carrier concentration needed in the active layer. This is further used to determine the cladding layer doping levels (see Example 2).

Definition of quasi-Fermi level

$$n = n_i e^{\frac{E_{fn} - E_i}{kT}} \quad \text{and} \quad p = n_i e^{\frac{E_i - E_{fp}}{kT}} \qquad \text{(Chapter 2)}$$

Example 2: Estimate the minimum injected electron concentration n_e needed to satisfy Bernard-Douraffourg condition in an n^+-p GaAs homojunction laser diode operating at 300˚K.

Given : n_i (at 300˚K) = 10^7 cm^{-3}, $E_g = 1.43$ eV.

The p-type concentration in the lasing layer (or active layer) can be assumed to be equal to n_e to maintain charge neutrality.

Solution: Bernard-Douraffourg states relates the difference between quasi Fermi levels (E_{fn}, E_{fp}) to the operating photon energy hυ.

$$E_{fn} - E_{fp} > h\upsilon$$

$$h\upsilon \approx E_c - E_v = E_g = 1.43 \text{ eV}$$

The electron concentration is related to the quasi Fermi level E_{fn} as

$$n = n_i e^{\frac{E_{fn} - E_i}{kT}} = n_e \qquad \text{(a)}$$

We have to determine n_e. Charge neutrality gives n = p in the active layer.

$$n = n_e + n_{p0} \approx n_e \text{ as } n_{p0} << n_e$$

$$p = p_e + p_{p0} \approx n_e \text{ (given in the problem)}$$

Therefore $p = n_i e^{\frac{E_i - E_{fp}}{kT}} = n_e$ (b)

Multiply Equations (a) & (b),

$$np = n_e^2 = n_i^2 e^{\frac{E_{fn} - E_{fp}}{kT}}$$

or $n_e = n_i e^{\frac{E_{fn} - E_{fp}}{2kT}}$ (c)

$$n_e\big|_{\min imum} = n_i e^{\frac{E_g}{2kT}} = 10^7 * e^{\frac{1.43}{2*0.0259}} = 9.75x10^{18} cm^{-3}$$

7.2 Threshold Current Density J_{th} in a semiconductor laser

An expression is derived for the minimum current density at which optical gain in a cavity overtakes losses in the cavity. One needs to differentiate the losses of photons under transparency or Bernard-Duraffourg condition.

7.2.1 Gain Coefficient, Threshold current Density, and Confinement Factor: The gain coefficient g is a function of operating current density and wavelength λ. Eq. (33) expresses it in terms of absorption coefficient $\alpha(h\nu_{12}) = \alpha_o$ involving band-to-band transition, and electron f_e and hole f_h distribution functions . This derivation is shown below

$$g = -\alpha_o(1 - f_e - f_h) \qquad (33)$$

Equation (33) is obtained by expressing net rate of stimulated emission, i.e. rate of stimulated emission minus the rate of absorption (Moss et al).

Ratio of the probability of photon emission and photon absorption is expressed as:
Probability of photon emission (stimulated and spontaneous) / Probability of photon absorption

$$= (n_\nu + 1)/n_\nu$$

Here, n_ν is the occupational probability or number of photons in a mode 'ν',

and $n_\nu = [1/\{\exp(h\nu/kT) - 1\}]$

Rate of stimulated emission is expressed as a product of probability $P(h\nu_{12})$ of a photon being absorbed or emitted, photon density $\rho(h\nu_{12})$ [which is equal to $n_\nu N_\nu \Delta\nu_s$, here N_ν is the mode density and $\Delta\nu_s$ the spontaneous line width], probability f_e that the upper level has an electron and probability f_h that the lower level has a hole. Probability that a photon is absorbed on emitted between two levels is $\alpha_o v_g$.

Rate of stimulated emission = $f_e f_h (\alpha_o v_g) n_\nu N_\nu \Delta\nu_s$ (34A)

N_ν= Mode Density= $N_\nu = \dfrac{8\pi n_r^2 \nu^2}{c^2 v_g}$, and v_g = group velocity of photons.

Rate of absorption = $(1-f_h)(1-f_e)\, \alpha_o v_g n_\nu N_\nu \Delta\nu_s$ (34B)

Net rate of stimulated emission = Rate of stimulated emission – rate of absorption

$$= [f_e f_h - (1-f_e)(1-f_h)]\, \alpha_o v_g n_\nu N_\nu \Delta\nu_s$$

$$= -[1-f_e-f_h]\, \alpha_o (v_g n_\nu N_\nu \Delta\nu_s) \qquad (34C)$$

The gain coefficient is defined as

$$g = -[1-f_e-f_h]\, \alpha_o \qquad (33)$$

Rate of spontaneous emission is expressed as: (**This is used to calculate α_o)**

$$R_c = \int r_\nu d\nu \equiv r_\nu \Delta\nu_s = f_e f_h (\alpha_o v_g) N_\nu \Delta\nu_s \qquad (35)$$

Equation (35A) gives

$$\alpha_o = \frac{r_\nu \Delta\nu_s}{f_e f_h v_g N_\nu \Delta\nu_s} \qquad (36)$$

The total rate of spontaneous emission is also expressed in terms of current contributing to carrier injection which recombine and produce photons. I/q is the electrons injected into p-region or hole injected in a p-n junction. Multiplying by η_q gives photons (spontaneous) emitted per second. Dividing by volume V of the lasing medium gives the rate of spontaneous emission per unit volume. Since I = J*A, we can also express in terms of current density J.

$$R_c = \frac{I}{q} \bullet \eta_q \bullet \frac{1}{V} = \frac{J}{q} \bullet \eta_q \bullet \frac{1}{d} \tag{37}$$

where: R_c = spontaneous rate per unit volume, η_q = quantum efficiency of photon (spontaneous) emission, d = active layer thickness, A = junction cross-section (A=LW, here L is the cavity length and W is the width of contact stripe).

Equations (33), (36) and (37) give

$$g = \frac{\left(\frac{J}{q}\right)\eta\left(\frac{1}{d}\right)(f_e + f_h - 1)}{f_e f_h v_g N_\nu \Delta\nu_s} \tag{38}$$

$$\frac{f_e + f_h - 1}{f_e f_h} = 1 - e^{\frac{h\nu - (E_{fn} - E_{fp})}{kT}} = z(T) \tag{39}$$

z(T) evaluation requires solving the charge neutrality condition along with other equations.

Substituting in Eq. (38) for $N_\nu = \dfrac{8\pi n_r^2 \nu^2}{c^2 v_g}$ (40)

and $\dfrac{f_e + f_h - 1}{f_e f_h}$ from Eq. (39), we get

$g = \dfrac{J\eta}{qd\, v_g \Delta\nu_s} \dfrac{c^2 v_g}{8\pi n_r^2 \nu^2}\left[1 - e^{\frac{h\nu - \Delta\zeta}{kT}}\right]$,	or	$J = \dfrac{8\pi n_r^2 \nu^2 e L_x \Delta\nu_s}{\Gamma \eta_q c^2 [1 - e^{\frac{h\nu - \Delta\zeta}{kT}}]} .g$ (41)

$$\Delta\zeta = E_{fn} - E_{fp} \tag{42}$$

The gain coefficient g is related to the current density J in Eq. (41). The condition of oscillation is obtained if we equate gain coefficient to its value in Equation (15). That is,

$$g = \alpha + \frac{1}{2L} \ln \frac{1}{R_1 R_2} \tag{15}$$

Here, α is the loss coefficient (which should not be confused with α_o) for photons with in E_{fn}-E_{fp}> $h\nu$ >E_g.

J ≡ J_{th} when Equation (15) is satisfied. Using Equation (15) and Equation (41)

$$\frac{J_{th}\eta}{qd\, v_g \Delta v_s}\frac{c^2 v_g}{8\pi n_r^2 v^2}\left[1-e^{\frac{h\nu-\Delta\zeta}{kT}}\right]=\alpha+\frac{1}{2L}\ln\frac{1}{R_1R_2} \tag{43}$$

Using $\left[1-e^{\frac{h\nu-\Delta\zeta}{kT}}\right]$=z(T)

$$J_{th}=\frac{8\pi n_r^2 v^2 qd\Delta v_s}{\eta c^2 z(T)}\bullet\left[\alpha+\frac{1}{2L}\ln\frac{1}{R_1R_2}\right] \tag{44A}$$

When the emitted stimulated emission is not confined in the active layer thickness d, Equation (44A) gets modified by Γ, the confinement factor (which goes in the denominator). This accounts for the loss of photons to the cladding layer.

$$J_{th}=\frac{8\pi n_r^2 v^2 qd\Delta v_s}{\Gamma\eta c^2 z(T)}\bullet\left[\alpha+\frac{1}{2L}\ln\frac{1}{R_1R_2}\right] \tag{44B}$$

In general the confinement is along transverse and lateral axes. It has two components $\Gamma=\Gamma_x\,\Gamma_y$.
The absorption coefficient α has many components

$$\alpha=\alpha_{FC}+\alpha_{Diffraction}+\alpha_S \tag{45}$$

Where, α_{FC} = free carrier absorption, $\alpha_{Diffraction}$ = diffraction loss, and α_S = scattering loss in the lasing medium.

Confinement factor

The confinement factor is defined below (Fig. 5): The cladding layers have lower index than GaAs active layer.

$\Gamma=\dfrac{\int_{-d/2}^{d/2} Pdx}{\int_{-\infty}^{\infty} Pdx}$. Here, P is the power at a point x in the active layer.

Confinement factor has various approximations in the transverse direction (perpendicular to the junction plane) as used in the design sets. Relations are tabulated below.

$\Gamma=2\pi^2 d^2(n^2_{active}-n^2_{clad})/\lambda^2$. General relation (Ref. Casey and Panish, 1978)

And for $Al_xGa_{1-x}As$-GaAs double heterostructure laser

$\Gamma=1-e^{-C\Delta n_r d}$, which is an empirical relation. (61)

<table>
<tr>
<td>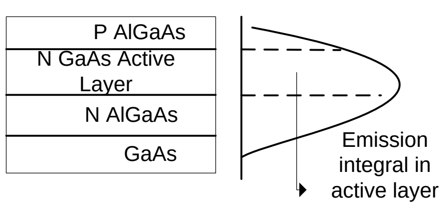

Fig. 5. Confinement of lasing mode due to lower index of refraction AlGaAs cladding layers</td>
<td>1. Transverse $\Gamma=2\pi^2 d^2(n^2_{active}-n^2_{clad})/\lambda^2$.
(λ is the free space wavelength.)
2. Given below is an empirical relationship generally used for AlGaAs-GaAs lasers.
$\Gamma=1-e^{-C\Delta n_r d}$, index difference between cladding and active layer is Δn_r, C is the constant which is dependent on material system.</td>
</tr>
</table>

Confinement factor is the ratio of active layer volume to mode volume for a cavity mode.

Rate equation for the electron density n and the photon density N_P

$$\frac{dn}{dt} = \frac{\eta_i I}{qV} - \frac{n}{\tau} - v_g g N_P$$

Where, I is the current and V is the volume of active layer (V=A*d, A=W*L, W=width, L=cavity length, d the active layer thickness).η_i is the injection efficiency, g the gain coefficient per unit length, and v_g the group velocity of mode.

$$\frac{dNp}{dt} = \Gamma v_g g N_P + \Gamma \beta_{SP} g R_{SP} - \frac{N_P}{\tau_P}$$

R_{SP} is the spontaneous electron recombination or photon emission rate, $R_{ST} = v_g g N_P$ is the stimulated photon emission rate, β_{SP} is the spontaneous emission factor.

The simultaneous solution of these equation gives time dependent characteristics of the laser.

Example 3. Evaluate the threshold current density J_{th} of a laser diode having an active layer thickness d = 0.2 μm, cavity length of 300 μm and cavity or contact width of 10 μm. In addition,

Internal quantum efficiency $\eta_q = 0.9$, Confinement factor $\Gamma = 0.5$

Reflectivity of cavity facets $R_1 = R_2 = 0.3$, Spontaneous emission line-width $\Delta\upsilon_s = 6.2\text{x}10^{12}$ Hz

$Z(T) \approx 0.8$.[Note that Z(T) depends on quasi Fermi levels which depend on forward biasing current and the emitting photon energy.]

Solution: The current density is expressed as

$$J_{th} = \frac{8\pi n_r^2 q d \Delta\upsilon_s}{\Gamma \eta_q Z(T)} \left(\frac{1}{\lambda^2}\right)\left(\alpha + \frac{1}{2L}\ln\left(\frac{1}{R_1 R_2}\right)\right) \qquad \left(\frac{\upsilon}{c}\right)^2 = \frac{1}{\lambda^2}$$

$$\frac{1}{2L}\ln\left(\frac{1}{R_1 R_2}\right) = \frac{1}{2x200x10^{-4}}\ln\frac{1}{0.3^2} = 60.2cm^{-1}$$

$$J_{th} = \frac{8\pi * 3.59^2 * 1.6*10^{-19} * 0.2*10^{-4} * 6*10^{12}}{0.8*0.9*0.5}\frac{1}{(0.84*10^{-4})^2}(20+60.2) = 196A/cm^2$$

Threshold Current Density as a function of temperature in homojunctions:

The current density J_{th} at which the lasing oscillations initiate is one of the important device parameters. It should be as small as possible. Figure 6 shows the J_{th} for homojunction GaAs laser as a function of T. Higher values of J_{th} make the device operation at room temperatures almost impossible because of heat sink/dissipation requirements. Heterojunction lasers are used to reduce the threshold current density (Section 5.2.4)

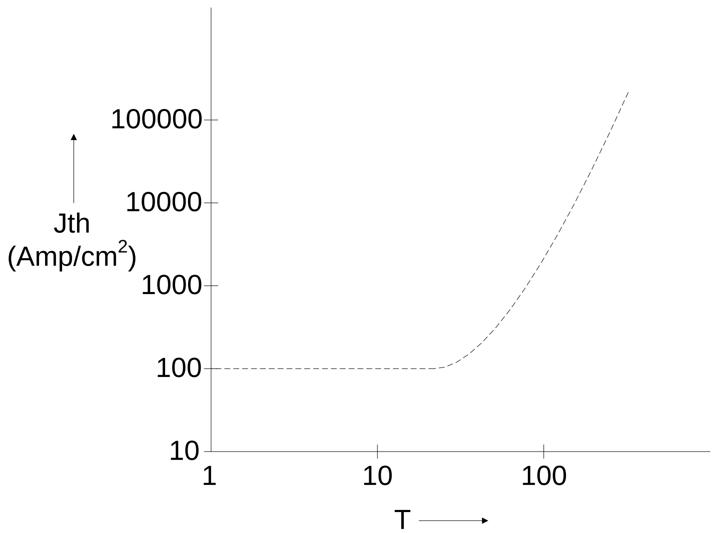

Fig. 6. J_{TH} versus Temperature

7.2.2 Threshold Current Density: Empirical Linear Model

Nominal current density J_{nom} is defined for a laser diode having an active layer thickness d = 1 μm and with a quantum efficiency $\eta_q = 1$. The actual current density, J, in a laser having an active layer thickness d and quantum efficiency η_q is

$$J = J_{nom} \bullet \frac{d}{\eta_q} \tag{46}$$

The gain g in a medium is plotted as a function of J_{nom} (see Figure4). It is empirically expressed as

$$g = \frac{g_o}{J_o}[J_{nom} - J_o] \tag{47}$$

J_o is the current density at which g=0. Equation (47) represents linear approximation of g as a function of J_{nom}. At threshold

$$g_{th} = \alpha + \frac{1}{2L}\ln\frac{1}{R_1 R_2} = \alpha + \frac{1}{L}\ln\frac{1}{R_1},\ R_1 = R_2 = R \tag{48}$$

Including the confinement factor Γ, we get

$$g_{th}\Gamma = \alpha + \frac{1}{L}\ln\frac{1}{R} \tag{49}$$

From Equation (47)

$$g_{th} = \frac{g_o}{J_o}[J_{nomth} - J_o] \tag{50}$$

From Equation (47) and Equation (50)

$$\frac{g_o}{J_o}[J_{nomth} - J_o] = \frac{1}{\Gamma}\left[\alpha + \frac{1}{L}\ln\frac{1}{R}\right] \tag{51}$$

Simplification of Equation (51) leads to

$$J_{nomth} = J_o + \frac{J_o}{g_o}\frac{1}{\Gamma}\left[\alpha + \frac{1}{L}\ln\frac{1}{R}\right] \tag{52}$$

Multiplying by $\frac{d}{\eta_q}$ we obtain $J_{nomth} \bullet \frac{d}{\eta_q} = \frac{J_o d}{\eta_q} + \frac{J_o d}{g_o \Gamma \eta_q}\left[\alpha + \frac{1}{L}\ln\frac{1}{R}\right]$ (53)

Using the defining Equation (46) we get

$$J_{th} = \frac{J_o d}{\eta_q} + \frac{J_o d}{g_o \Gamma \eta_q}\left[\alpha + \frac{1}{L}\ln\frac{1}{R}\right] \quad (54)$$

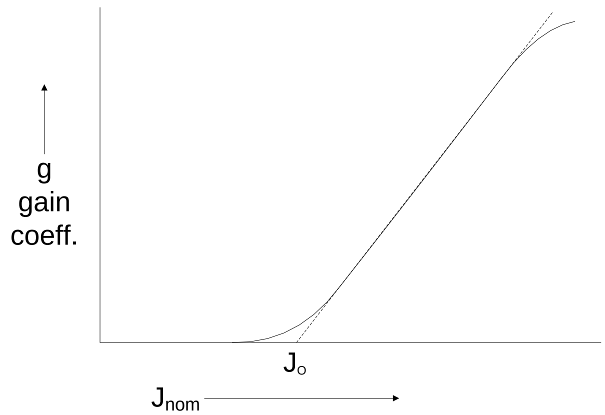

Fig. 7. Gain coefficient versus nominal current density (defined for a 1μm thick active layer).
The dashed line in Fig. 7 represents Eq. (47), where x-intercept is related to J_o, the slope is (g_o/J_o).

7.2.3 Reduction of Threshold Current Density in Heterostructure Lasers

Heterojunctions were used in 1969-70 to reduce J_{th}. The central concept in here is to reduce the active layer thickness d. Note that in homojunctions $d \cong 2L_n$ or $2L_p$, and we do not have much control on diffusion lengths once a material is chosen. In contrast, heterojunctions achieve reduction in d, and hence J_{th}, by

a. confining injected minority carriers
b. confining emitted photons.

Effect of active layer thickness 'd' on J_{th}: As we can see from the equation 44 for I_{th} (or J_{th}) it depends on active layer thickness d.

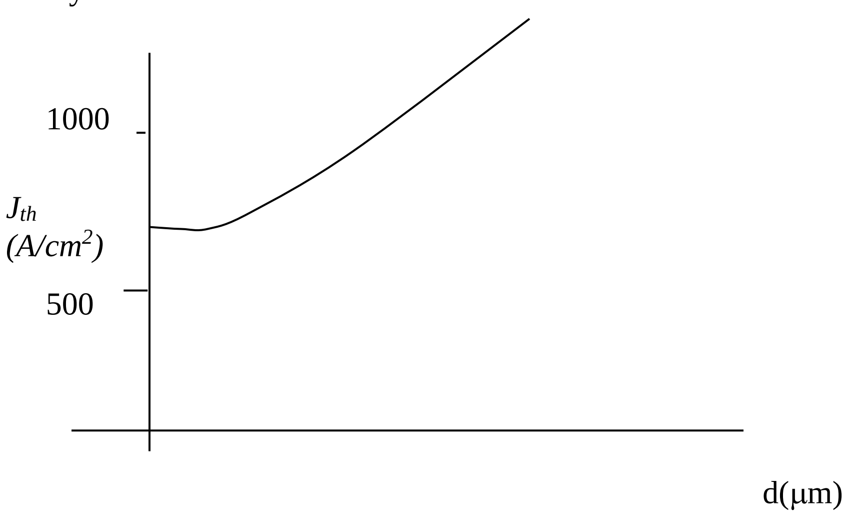

Fig. 8 Threshold current density as a function of active layer thickness.

Fig. 8 shows the effect of reducing active layer thickness d on threshold current density J_{th}.

Another aspect of reducing the active layer thickness is the reduction of the of confinement factor Γ. The photons are not confined in this thin layer as well as in a thicker layer.

7.3 Power output, Power-Current (P-I), Near-field, Far-Field Characteristics

Power output of a laser is expressed as a fraction of estimated photon energy density generated accounting for the losses due to mirrors R1 and R2.
(Ref: A. Yariv: Optical Electronics, publisher HRW)

$$P_{out} = \begin{pmatrix} \text{Power emitted by stimulated} \\ \text{emisssion in the cavity} \end{pmatrix} * (\text{Fraction lost due to mirrors})$$

$$= \left[\frac{(I - I_{TH})\eta_{\text{int}} h\nu}{q}\right] * \left[\frac{\frac{1}{2L}\ln(1/R_1 R_2)}{\alpha + \frac{1}{2L}\ln(1/R_1 R_2)}\right] \qquad (55)$$

where:

$$\boxed{\eta_{\text{int}} = \eta_{inj} * \eta_q} \quad \textit{Just like LEDs} \qquad (56)$$

Assume $n_{inj} \cong 1, \quad \eta_q = 0.9 \leftrightarrow 1.0$

External Differential Efficiency is defined as rate of change of power output per current over the threshold value.

$$\eta_{ex} = \text{external differential} \rightarrow \text{ quantum efficiency}$$

$$\eta_{ex} = \frac{d(P_{out}/h\nu)}{d[(I - I_{TH})/q]} = \text{Rate of increase of output power per increase in t} \qquad (57)$$

Power conversion efficiency

$$\eta_C = \frac{P_{out}}{V_{app} * I}$$

7.3.1 Optical power-current characteristics*:*

The laser diode emits spontaneously until the threshold current is exceeded (i.e. $I > I_{th}$ Fig. 9).

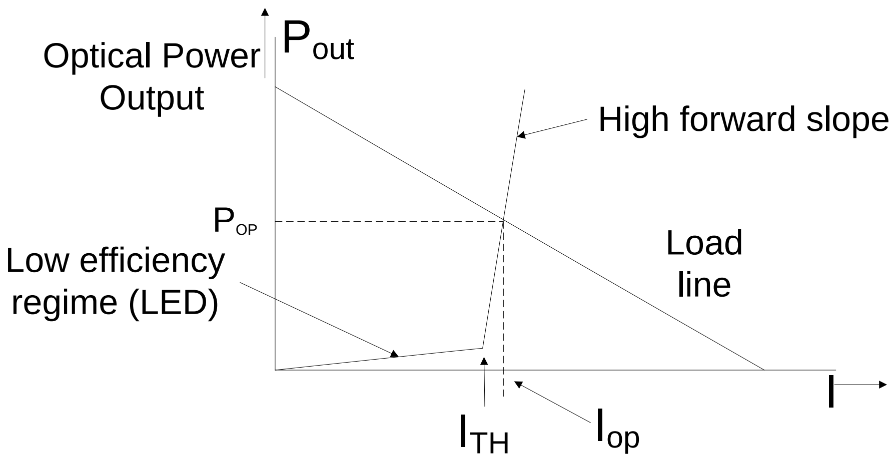

Fig. 9 Power output versus current (P-I) characteristic.

Note that ΔP_{out} is significant above ΔI increments above I_{th}. Fig. 10 shows the V-I characteristic.

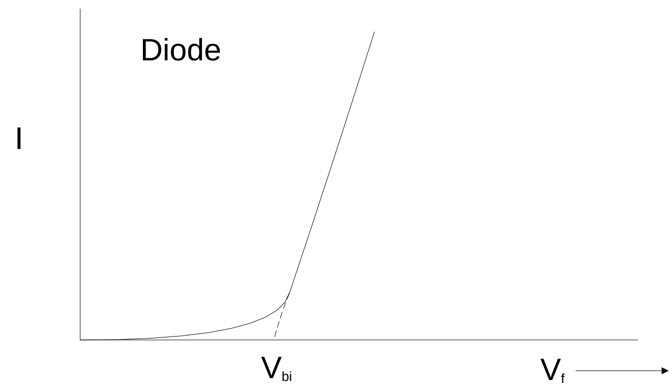

Fig. 10. V-I characteristics of a laser diode.

P-I Behavior as a function of temperature

The I_{th} value is a function of operating temperature. This is shown in Fig. 11.

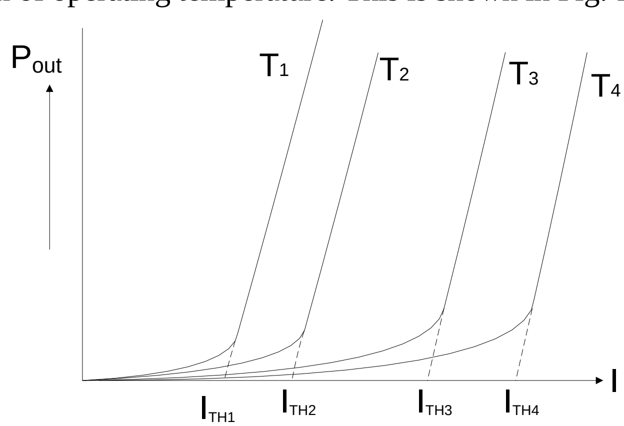

Fig. 11. Variation of threshold current density as a function of temperature.

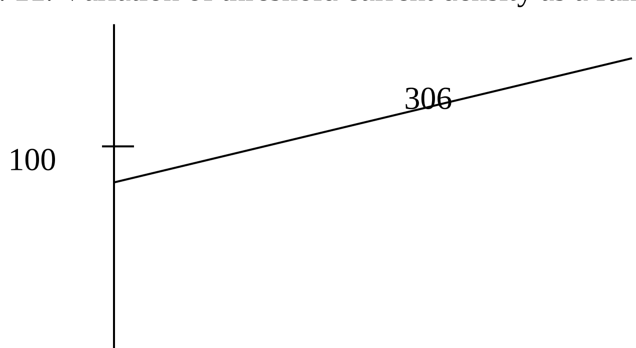

Log I_{TH} $\qquad$ $I_{TH} \propto Exp(T/T_0)$

Figure 12: Temperature variation of threshold current.

The temperature dependence of threshold current density is shown in Fig. 12. Temperature T_0 as defined $J_{TH}(T) \sim J_{TH}(0)\ exp\{T/T_0\}$. Higher the value of T_0, the less insensitive J_{TH} will be on T. See Section 5.7 on Quantum Dot lasers in which J_{TH} are temperature independent.

7.3.2 Near-field and Far-field Patterns and Beam Divergence: The active layer looks more like a thin slit and the output beam diverges significantly in the direction perpendicular to the junction plane. The divergence is not as severe in the plane parallel to the junction (see laser design). The order of lasing mode is determined by the near-field and far-field patterns. Near field is obtained by viewing the intensity distribution via a camera using an optical microscope. If there is only one spot with maximum intensity in the center and gradually decreasing along the x-(perpendicular or transverse to the junction plane) and y-(lateral or in the junction plane), we have a single mode operation. Observing two spots along x-axis means it is not a single transverse mode laser. The number of transverse and lateral modes depends on active layer thickness d and stripe width W. Far-field pattern is obtained by scanning a photodetector around the laser in a direction perpendicular to the junction plane. This is shown in Fig. 13. Pattern shown in figure 13(a) means there is only one fundamental or zero order modes. Figs. 13(b) and 13(c) show first and second order modes, respectively. Higher order modes are obtained when active layer thickness d is above a minimum value (see Design Level-2). This is schematically shown in Figs. 13(a) and 13(b). Fig. 14 shows the beam divergence angles perpendicular and parallel to the junction plane. That is, the angle at which the intensity is reduced by a factor of 2.

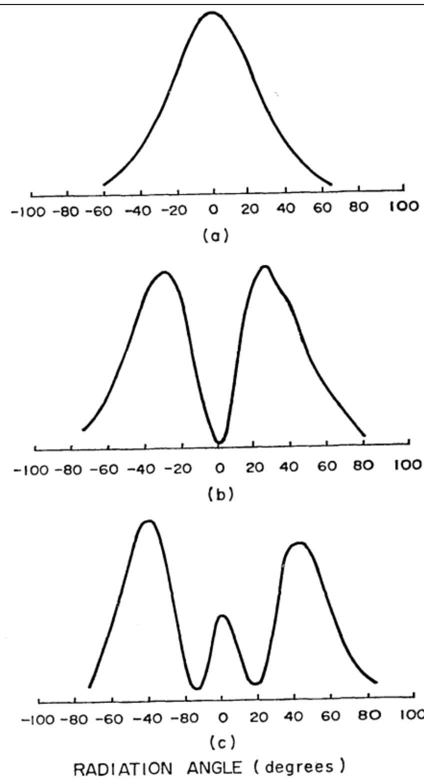

Fig. 13. Far-field pattern of a AlGaAs-GaSs laser [Yonezu, 1973].

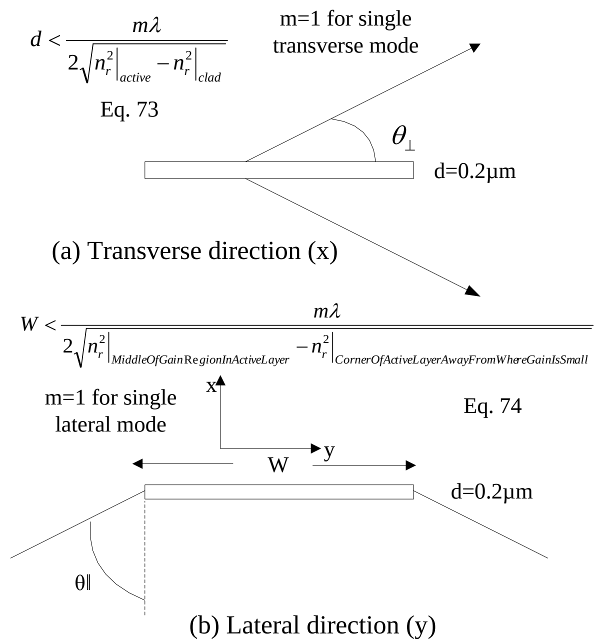

Fig. 14 (a) Beam divergence in transverse/perpendicular and (b) lateral directions.

... Yonezu et al ... Jap. J. Appl. Phys.
12, p 1585 (1973)

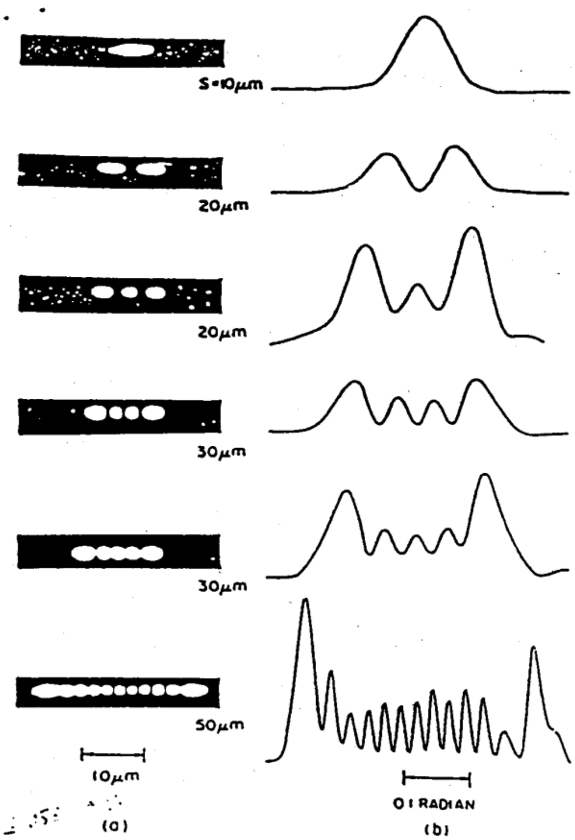

FIG 7.11-2 Modes along the junction plane as a function of stripe width S for planar stripe DH lasers. (a) Near-field patterns. (b) Far-field patterns (Ref. 103)

Fig. 14 (b)

Beam Divergence: ***(See also pages 341 - 343)***

As the active layer is reduced in thickness, the photons are not confined in this layer. This results in the lowering of confinement factor Γ.

In addition, the active layer looks more like a thin slit and the output beam diverges significantly (see laser design)

<u>Power Saturation due to thermal heating</u>

$I_{TH} \sim e^{T/T_0}$

T_0 – Characteristic Temperature

150-200K for AlGaAs-GaAs

40-70°K for InGaAsP

Near and far field path

$$D = \frac{2\pi d}{\lambda}\left(\mu^2 - \mu_c^2\right)^{\frac{1}{2}}$$

$\mu = n_r$ of active layer
μ_c = Cladding Index

Confinement factor (See also page 309 STEP C of Laser Design)

$$\Gamma_{trans} = \frac{D^2}{2 + D^2}$$

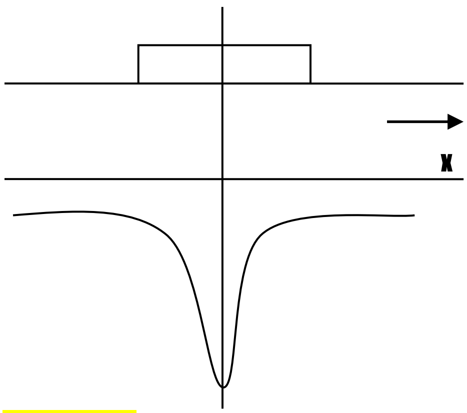

Fig. 14 (c)

$$\Gamma_{lateral} = \frac{W^2}{2 + W^2}$$

$$W = \frac{2\pi w}{\lambda}\sqrt{(\mu_l)^2 - (\mu_l^c)^2}$$

w is the width (2-3μ)

$$\Gamma = \Gamma_{lateral}\Gamma_{Trans}$$

Near field width, $w_\perp \cong d(2\ln 2)^{1/2}\left(0.321 + 2.1D^{-3/2} + 4D^{-6}\right)$

Far-field Beam Width, $\theta_\perp \cong \dfrac{0.65D(\mu^2 - \mu_c^2)}{1 + 0.15(1 + \mu - \mu_c)D^2}$

Good for D<2 which means d<0.3 μ for λ=1.5μ

Near-field, w||=same expression as $w_\perp$ for index-guided laser replaced d by w, D by w.

$$\theta_\parallel = \frac{\lambda}{w_{width}}$$

w= strip width
d = active layer thickness

7.4. Heterojunction Lasers

Reference is made to Chapter 2 where details of p-n heterojunctions including basic equations for built-in voltage, junction width, I-V equations are described.

7.4.1 Single and double heterojunctions:

NAlGaAs-pGaAs Single Heterostructure (SH): First we will analyze a single heterojunction (SH) such as N-AlGaAs-pGaAs (Fig. 15). This will be followed by the qualitative analysis of an N-AlGaAs/p-GaAs/P-AlGaAs double heterojunction (DH). Here, AlGaAs is the wider energy gap semiconductor and GaAs is the narrow gap semiconductor. We need to understand the following:

(1) Why the injection efficiency for a heterojunction is about ~1 even if the doping of N-AlGaAs layer is smaller than pGaAs as shown in Fig. 15,

(2) How the injected minority carriers are confined in a lower energy gap material in a double heterostructure (N-AlGaAs/p-GaAs/P-AlGaAs).

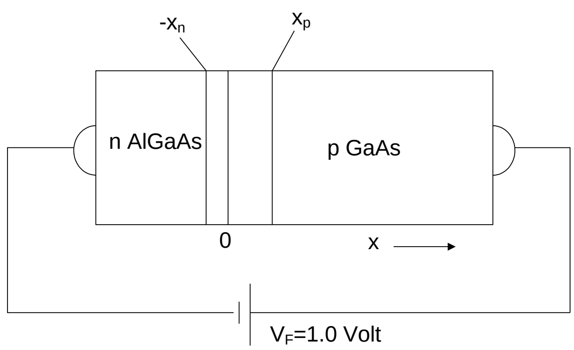

Fig. 15. A forward biased nAlGaAs-pGaAs single heterojunction diode.

$$J = q\left(\frac{D_n n_{i(GaAs)}^2}{L_n N_{A,GaAs}} + \frac{D_P n_{i(GaAs)}^2}{L_P N_{D,AlGaAs}}\left(\frac{m_{n1} m_{p1}}{m_{n2} m_{p2}}\right)^{\frac{3}{2}} e^{-\frac{E_{g2}-E_{g1}}{KT}}\right)(e^{\frac{qVf}{kT}} - 1) \quad (173/\text{Ch. } 2)$$

$$J = q\left(\frac{D_n n_{i(GaAs)}^2}{L_n N_{A,GaAs}} + \frac{D_P n_{i(GaAs)}^2}{L_P N_{D,AlGaAs}}\left(\frac{m_{n1} m_{p1}}{m_{n2} m_{p2}}\right)^{\frac{3}{2}} e^{-\frac{\Delta E_g}{KT}}\right)(e^{\frac{qVf}{kT}} - 1) \quad (174)$$

From Eq. (174) we can see that the second term, representing hole current density J_p injected from p-GaAs side into N-AlGaAs is quite small as it has [exp-(ΔE_g/kT)] term.

As a result $J \sim J_n(-x_N)$, and it is

$$J_n = q\left(\frac{D_n n_{i(GaAs)}^2}{L_n N_{A,GaAs}}\right)(e^{\frac{qVf}{kT}} - 1) \quad (175)$$ Chapter 2 page 162.

Similarly, the hole current $J_p(x=-x_N)$ is

$$J_P = q\left(\frac{D_P n_{i(GaAs)}^2}{L_P N_{D,AlGaAs}}\left(\frac{m_{n1} m_{p1}}{m_{n2} m_{p2}}\right)^{\frac{3}{2}} e^{-\frac{\Delta E_g}{KT}}\right)(e^{\frac{qVf}{kT}} - 1) \quad (176)$$

In an N-AlGaAs-pGaAs heterojunction, $J_p(-x_N)$ is negligible even if N_D in AlGaAs is comparable to N_A in pGaAs. This results in near unity injection efficiency in heterojunctions.
Injection efficiency $\eta_{inj} = I_n/(I_n + I_p)$, since the hole current I_p is very small due to $[\exp(-(\Delta E_g/kT)]$ term, the injection efficiency approaches **unity in heterojunctions**.

NAlGaAs-pGaAs-pAlGaAs Double Heterostructures (DH):
This treatment is to understand the confinement of injected electrons in pGaAs layer. This is the active layer where electrons and holes recombine emitting photons. The narrowness of this active layer (lower value of d) results in reduced threshold current density J_{TH}. The introduction of P-*AlGaAs layer results in reducing the number of minority holes at the pGaAs-PAlGaAs boundary* ***$x=x_p$ +d.*** Figure 16 shows a double heterostructure diode. The details of N-p heterojunction and p-P iso-type (same conductivity, p and P) heterojunction are shown in Fig. 17.

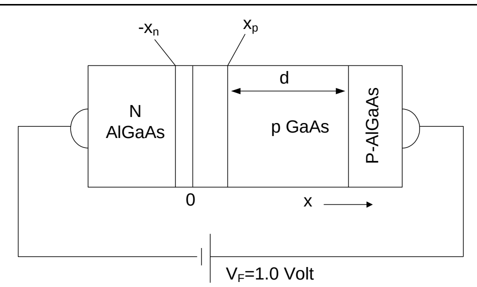

Fig. 16 Forward biased double heterostructure.

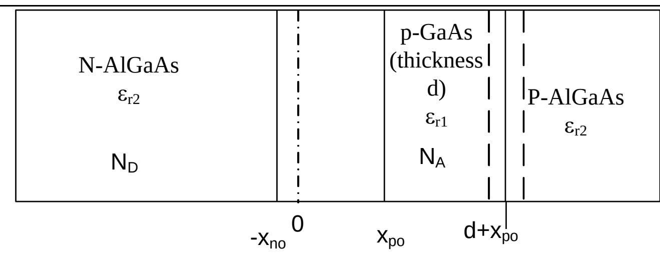

Fig. 17. A double heterostructure NAlGaAs-pGaAs-PAlGaAs diode.

7.4.2 Carrier Confinement in a Double Heterostructure (DH) laser

Electron confinement in p-GaAs active layer: The minority electron concentrations are shown in p-GaAs and P-AlGaAs in Fig. 16 for a NAlGaAs-pGaAs-pAlGaAs double heterostructure. Note that n_{e2} is determined by n_{p0} in P-AlGaAs which is given by $n_{p0}=n_i^2(\text{AlGaAs})/N_A$. Since n_i in AlGaAs is much smaller than in GaAs, therefore, the value of ne2 is much smaller than what it would have been if there was no P-AlGaAs. If n_{e2} is smaller (due to P-AlGaAs), it will result in smaller $n(x_p+d)$ value at the p-GaAs interface with P-AlGaAs. This means that injected electrons are confined to a higher degree in p-GaAs when P-AlGaAs layer is present. That is, P-AlGaAs forces all injected carrier to recombine in the active layer.

Holes confinement in p-GaAs: Similarly, we can show that holes present in p-GaAs layer cannot be injected into N-AlGaAs layer. Hence they are confined in the active layer. Since doping of P-AlGaAs layer is much higher than the active layer, the active layer p-GaAs cannot inject holes into P-AlGaAs cladding layer. Thus, both electrons and holes are confined in the p-GaAs active layer which is surrounded by two AlGaAs layers. This is known as carrier confinement.

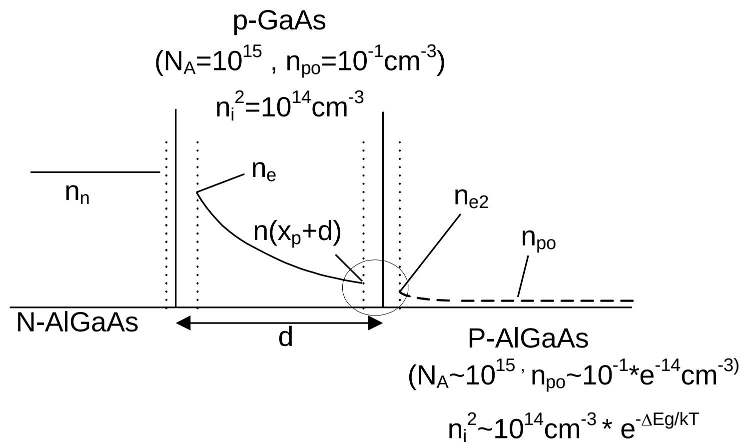

Fig. 18. Minority carrier concentration in p-GaAs and in p-AlGaAs. ($\Delta E_g = 0.35$eV)
The energy band diagram is given in Fig. 19.

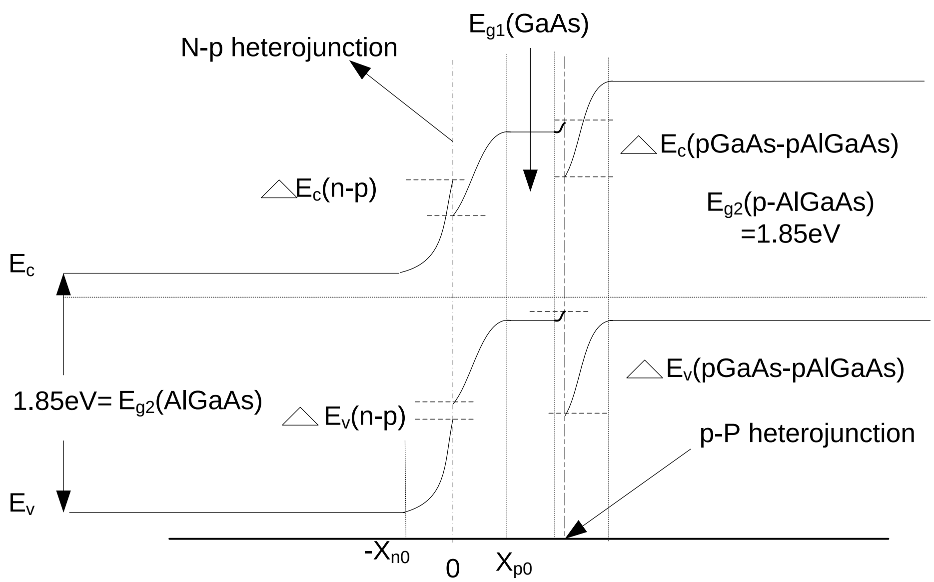

Fig. 19 Energy band diagram of a NAlGaAs-pGaAs-PAlGaAs double heterostructure diode

Figure 20 shows a p-AlGaAs-nGaAs-nAlGaAs DH laser structure. Here, n-GaAs is the active layer. Generally, this structure is realized on an n-GaAs substrate, and the p-AlGaAs layer has a thin p^+-GaAs cap layer. The heavy doped substrate and the cap layer serves to form Ohmic contacts. In addition, the substrate provides the mechanical support.

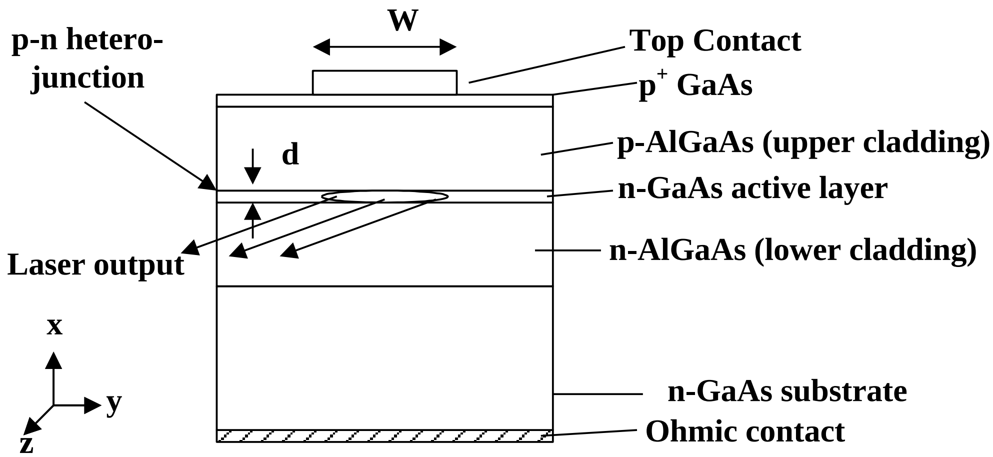

Fig. 20. AlGaAs-GaAs DH laser structure. The top contact is in the form of a stripe to confine the photon emission form a spot.

<u>Electron and Hole Confinement in P-AlGaAs-nGaAs-N-AlGaAs</u>

We have seen that in a PAlGaAs-nGaAs heterojunciton, the minority carriers are not injected from a lower energy gap (E_{g2}, n-GaAs) semiconductor into a larger energy gap (E_{g1}) semiconductor (P-AlGaAs). This is due to the band discontinuity ΔE_c (or ΔE_v for holes injection from pGaAs into N-AlGaAs in NAlGaAs-pGaAs heterojunctions).

Another property of a heterojunction, in this case isotype n-GaAs/N-AlGaAs, is that the injected minority holes from the P-AlGaAs emitter are confined into the nGaAs layer only. The nAlGaAs acts as a barrier for the hole transport. This confines the injected minority holes within the nGaAs active layer. To maintain the charge neutrality, equal concentration of electrons is supplied by the Ohmic contact on the N-side.

This aspect is illustrated in Fig. 21. Here, a p-n GaAs homojunction (Fig. 21A) is compared with a p-n double heterojunction (Fig. 21B). Once the electrons and holes are confined to the lower energy gap GaAs active layer, photons are emitted in this layer. The confinement of photons into a thinner (than homojunctions) active layer ensures reduced threshold current density J_{TH}. Homojunction Device A: Electrons are injected from the n-GaAs side into p-side. The injected minority electrons recombine with holes. The electron population declines by $1/e^2$ within a distance of $2L_n$ from the junction. Emitted photons are confined within a cavity of length L and thickness $2L_n$. The width of the cavity is determined by the contact stripe as shown in Fig. 21A.

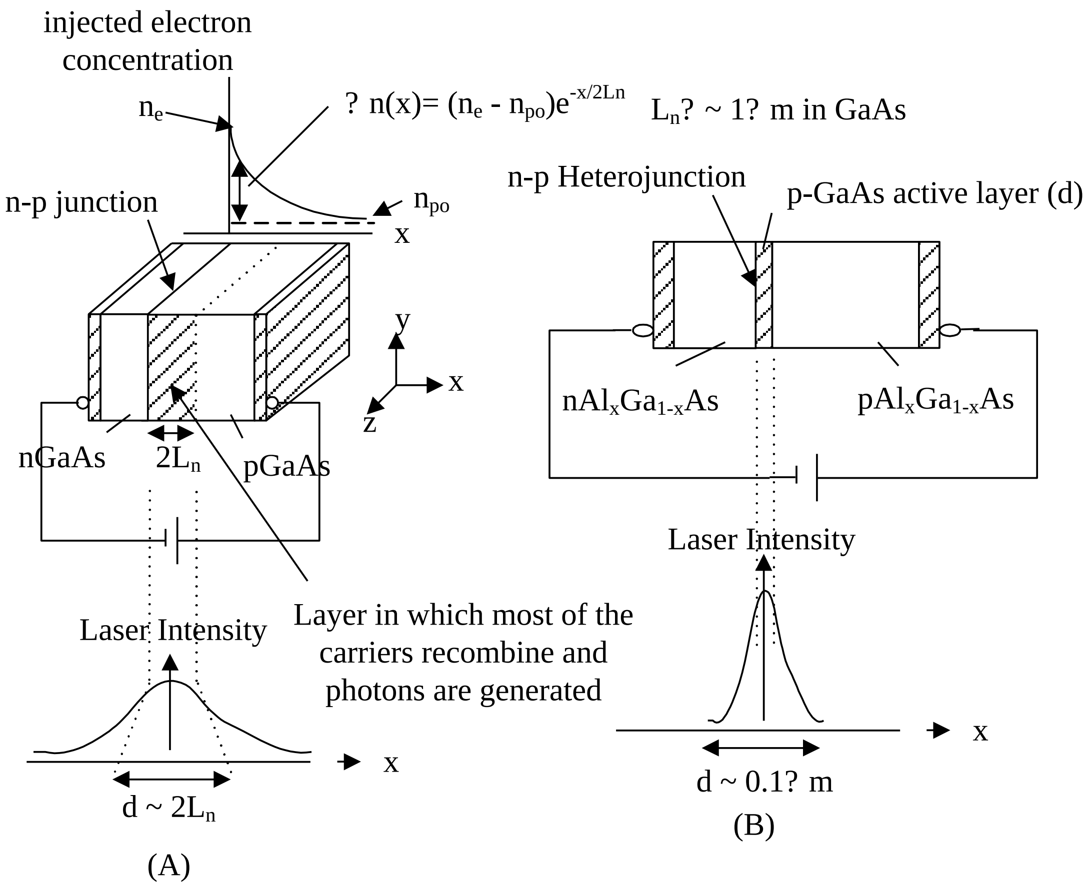

Fig. 21 Comparison of transverse lasing intensity distribution in: (A) an n-p GaAs homojunction, and (B) an N-p-P double heterojunction.

Double Heterojunction Device B: In contrast (to structure A), the injected electrons are confined to the p-GaAs layer of thickness d. The thickness of this layer can be made much smaller than $2L_n$. Typical value of d is 0.1 μm in double Heterostructures. In the case of quantum well lasers, grown by molecular beam epitaxy or MOCVD, this thickness could be in the range of 50 –100 Å.

As $d << L_n$, the threshold current density in DH and quantum well lasers is much smaller than homojunction lasers. How does this happen? The role of p-$Al_xGa_{1-x}As$ is crucial in the restriction of electrons in the p-GaAs region.

$E_{gpAlxGa1-xAs} > E_{gp-GaAs}$, we have assumed ΔE_g of 0.35 eV. Since $n_i^2|_{pAlGaAs} << n_i^2|_{pGaAs}$, we get a very small value of $n_{p0}|_{pAlGaAs} << n_{p0}|_{pGaAs}$. A reduced value of n_{po} in p-AlGaAs determines the value of injected excess electron concentration Δn_{e2}, which in turn determines the excess electron concentration n_e at pGaAs-PAlGaAs boundary. This is a qualitative explanation of injected electron confinement in p-GaAs.

7.4. 3. Photon Confinement in the Active Layer:

As is evident from waveguiding fundamentals, we need to sandwich the active layer between two lower index of refraction layers. AlGaAs fits that requirement. In addition, it is lattice matched to GaAs. In the laser design example, we have mentioned various methods for the calculation of modes in such a slab waveguide. Also we need to calculate the confinement factor Γ of the mode. Confinement factor also determines the J_{TH}. Generally, the confinement factor becomes smaller as the thickness of the active layer becomes narrower. This also depends on the index of refraction difference between the active and the cladding layers.

In this structure, p-AlGaAs and n-AlGaAs cladding layers (having lower index of refraction n_{r1}, depending on the Aluminum concentration) sandwich the nGaAs layer that has a larger index of refraction n_{r2}. As a result this causes wave guiding along the x-direction. Depending on the index difference Δn and the active layer thickness, the waveguide will support fundamentals or higher TE (transverse electric) modes. The mode confinement in DH structure increases the laser output intensity for the same injection current.

Example 4

a) What are the two general conditions for lasing?
b) Name the two conditions which express lasing in a cavity.
c) Sketch the optical power vs current characteristic (P-I), threshold current density vs temperature characteristic for a semiconductor laser.
d) Write an expression for optical power output for a laser diode.
e) Is the following statement true or false? "The laser beam diverges more in a direction perpendicular to the junction plane in the direction parallel to the plane of the junction (or lateral direction)"

Solution

(a) I. Population Inversion: $N_2 > N_1$ (General Case)

For semiconductors, it leads to Bernard – Douraffourg condition which is

$$E_{fn} - E_{fp} > h\upsilon > E_g$$

II. Build photon energy density ρ(hν)for positive feedback. This is represented by

a) $g = \alpha + \frac{1}{2L}\ln\left(\frac{1}{R_1 R_2}\right)$, b) $L = \frac{m\lambda}{2n_r}$, where λ is the free space lasing wavelength.

(b) See part II(a) and II(b) above.

(c) See below Figs. 9 and 11.

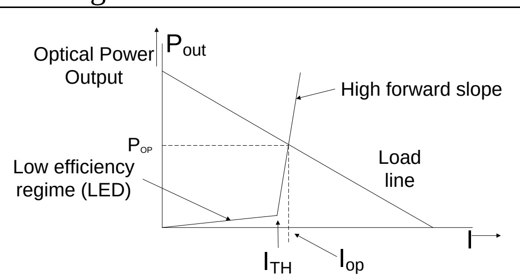

Fig. 9 P-I plot

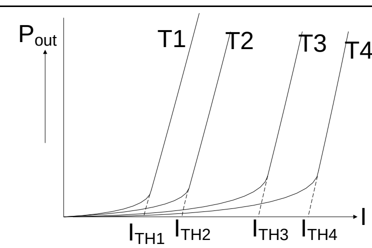

Fig. 11. Variation of threshold current density as a function of temperature.

Threshold current density as a function of temperature (see Fig. 12.

(d) $PowerOutput = \frac{(I - I_{th})\eta_{int} h\upsilon}{q} \frac{\frac{1}{2L}\ln\left(\frac{1}{R_1R_2}\right)}{\alpha + \frac{1}{2L}\ln\left(\frac{1}{R_1R_2}\right)}$

(e) True. $\theta_\perp \neq \theta_{||}$

Example 5 Determine the material for lasers operation at 505 nm and 1550 nm respectively. Provide the name and composition of semiconductors used for : (a) active layer (b) cladding layers (c) substrate. Justify your selection.

Solution: The material compositions are provided below in the table.

Operating Wavelength λ	505 nm or 0.505 μm	1550 nm or 1.55 μm
Corresponding Energy gap E_g (eV) (1.24 / λ(in μm))	2.455 eV	0.8 eV
Active layer material (Refer the chart)	$Zn_{0.8}Cd_{0.2}Se$	$In_{0.65}Ga_{0.35}As_{0.75}P$
Substrate	GaAs or ZnSe	InP

Active Layer Selection :
Find the band gap E_g of semiconductor that will emit 505nm.

$$h\upsilon = \frac{1.24}{0.505\mu m} = 2.455eV$$

Lasing energy is slightly higher than E_g (gap) of semiconductor. (Bernard – Douraffourg condition $E_{fn} - E_{fp} > h\upsilon > E_g$).

Let E_g = 2.45 eV. Draw a horizontal line (as shown in the figure 20). It gives a composition of ≈ $Zn_{0.8}Cd_{0.2}Se$ [or $Zn_{0.84}Cd_{0.16}Se$ to be very precise] for the circled point on ZnSe -> CdSe line.

Substrate :
Select a material (represented by solid squares) such that it is with 1 – 2% of the lattice parameter of the active layer. In this case ZnSe & GaAs are two potential materials. Either one is good. We select GaAs as it is less expensive and more readily available.

Cladding :
Two properties should be met by cladding layers.
(i)Larger energy gap (0.2 eV – 0.5 eV) than the lasing or active layer. ZnSe can match this requirement.
(ii) Lower index of refraction than ZnCdSe. ZnSe also matches this requirement.

$$n_r\big|_{ZnCdSe} - n_r\big|_{ZnSe} \approx 0.1 - 0.3 \text{ or Higher}$$

Lattice Parameter and Bandgap Data

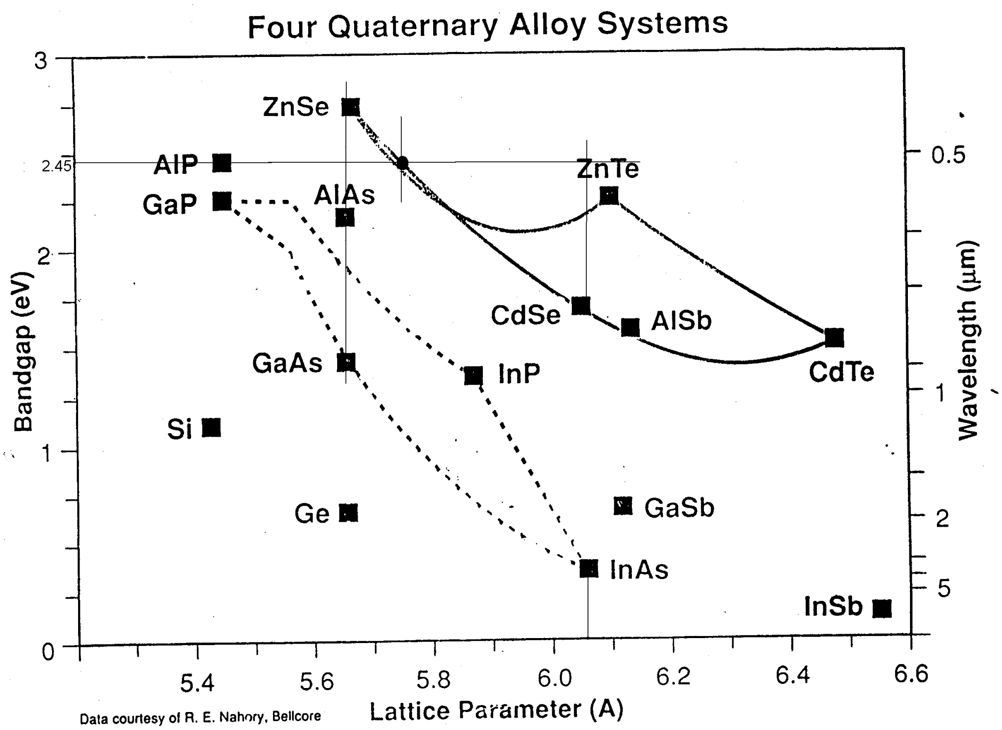

Fig. 22 Lattice constant versus band gap.

7.5 Design of Lasers

The design steps are discussed in two sets I and II. They complement each other. Material details are given in the case of 980 nm lasers. Beam divergence, external quantum efficiency, forward slope, threshold current density etc are provided. Some empirical relations are used for beam divergence. One has to be careful in their usage.

7.5.1. Design of a 1.55μm Laser-*Level I*

Design specifications: Laser emitting at 1.55μm with $J_{TH} < 1000 A/cm^2$, and having single mode output with a power output Pout = 10 mW.

Following steps illustrate the design of an InGaAsP laser. Some empirical relationships (beam divergence) are for AlGaAs-GaAs lasers. They should be modified for InGaAsP laser.

Laser Modes:

Once the light is generated, the intensity distribution in the laser is determined by dielectric boundaries. The intensity distribution in a plane perpendicular to the direction of light propagation determines the modes.

For a single mode laser, not only we need one operating wavelength or frequency but we also want one mode, that is, one spot when we view the emitting face. To obtain a single mode along the transverse direction, we use a three-slab waveguide structure having the thickness of the middle/guide layer to be below a critical value to cutoff higher or TE_1 mode. Only fundamental is permitted (TE_0 and TM_0 in symmetrical waveguides). The single mode along the lateral direction is obtained by creating index changes due to gain guiding and/or index guiding. In both the cases we use a stripe geometry structure. This way the carrier injection maximized the index of refraction where the gain is highest. This type of profile results in gain guiding. Since the index change is quite small, a wider stripe is used (3-5 micron) to obtain a single mode. Index guiding is achieved when ridge waveguides are used. Here the index change under the ridge is quite larger than under the tail regions. (This can be analyzed, see problem set #2, using the effective index method along with three slab waveguide analysis.)

Longitudinal modes are controlled by the method of positive feedback. One uses either a Fabry-Perot type resonator or a distributed feedback (DFB). Fabry-Perot structure could be a cleaved type or distributed Bragg Reflector (DBR) type. Generally, DFB yields larger separation between adjacent modes than cavity type lasers.

The modes of a laser are reflected in near-field and far-field patterns. The beam divergence in the plane of active layer and perpendicular to the plane are two important parameters.

Other parameters are: Forward slope of the laser $\Delta P_{out}/\Delta I$, characteristic temperature T_0 as defined $J_{TH}(T) \sim J_{TH}(0)\exp\{T/T_0\}$, Power output P_o, full width and half maximum (FWHM) or bandwidth at half maximum, Noise (RIN).

Design Steps

A. Selection of active layer, cladding layers, and substrate

Active layer $In_{0.65}Ga_{0.35}As_{0.75}P_{0.25}$

Cladding: Any composition between the Active Layer and InP

Let us go halfway higher.

$$In_{0.65+\frac{0.35}{2}}Ga_{\substack{1-\text{Indium}\\ \text{Comp}}}As_{1-\text{Phosp.}}P_{0.25+\frac{0.75}{2}}$$
$$= In_{0.825}Ga_{0.175}As_{0.375}P_{0.625}$$

Substrate: InP lattice matched to cladding layers

B. Doping Levels

p – cladding, N_A

n – cladding, N_D

Get concentrations in the active layer

n = p = ?

The concentration is obtained from Bernard-Douraffourg condition

$$E_{fn} - E_{fp} \geq h\nu \geq E_g \tag{31}$$

$n_e p_e = n_1^2 e(^{E}{}_{fn}\text{-}E_{fp})/kT$

$$n_e = n_i e^{\left(E_{fn} - E_{fp}\right)/2kT}$$

$$n_e \equiv p_e$$

Once p_e,n_e are known, the doping concentrations are related as:

$$\boxed{\begin{array}{l} N_A > p_e \\ N_D > n_e \end{array}} \tag{58}$$

The computation of p_e requires calculation of n_i in the active layer. $E_g = 0.8eV$

$$\boxed{\begin{array}{l} n_i(E_g = 1.43) = 10^7\, cm^{-3} \\ n_i \propto e^{-E_g/2kT} \end{array}} \tag{59}$$

Since the n_i for InGaAsP is not readily available, we compute it using the following relation. Here we have simplified the calculations making an assumption that effective masses for GaAs and InGaAsP are similar. The value of n_i for GaAs is well known.

$$\frac{e^{-0.8/2kT}}{e^{-1.43/2kT}} = \frac{n_i\,(\text{Active layer at 0.8eV})}{n_i\,(\text{GaAs})} \tag{60}$$

$$n_i\,(\text{InGaAsP Active Layer}) = 10^7 * \frac{e^{\frac{-0.8}{2\times 0.259}}}{e^{\frac{-1.43}{2\times 0.259}}} \tag{61}$$

C. Confinement factor, Γ

By definition, the confinement factor is the ratio of integrated intensity in the active layer to the total emitted intensity. It depends on the thickness, d, of the active layer and the index of refraction difference, Δn_r, between the cladding layer and the active layer. Given below is an empirical relationship generally used for AlGaAs-GaAs lasers.

$$\Gamma = 1 - e^{-C\Delta n_r d}$$, (C & d are given) (62)

$$\Delta n = n_r\big|_{\text{Active layer}} - n_r\big|_{\text{Cladding layer}} \quad (63)$$

For $In_x Ga_{1-x} As_y P_{1-y}$, the index of refraction is given by

$$n(x,y) = 3.52xy + 3.39x(1-y) + 3.60y(1-x) + 3.56(1-x)(1-y) \quad (64)$$

Active Layer $In_{0.65}Ga_{0.35}As_{0.75}P_{0.25}$,

$x = 0.65$

$y = 0.75$

$$= 3.52 \times 0.65 \times 0.75 + 3.39(0.65)0.25 + 3.60 \times 0.75 \times 0.35 + 3.56 \times 0.35 \times 0.25$$
$$= 3.52$$

Clad Layer $In_{0.825}Ga_{0.175}As_{0.375}P_{0.625}$

Show that the composition as noted above.

Qualitatively explain carrier confinement in the active layer due to lower index cladding layers around it.

D. Threshold Current Density

As we can see from the expression of threshold current density, we need to know R_1, R_2, absorption coefficient in the cavity, α, quantum efficiency, η_q, cavity length, L, spontaneous line width, $\Delta\nu_s$, confinement factor, Γ, and Z(T). Fig. 23 shows light out from side walls with R_1, R_2 reflectivity.

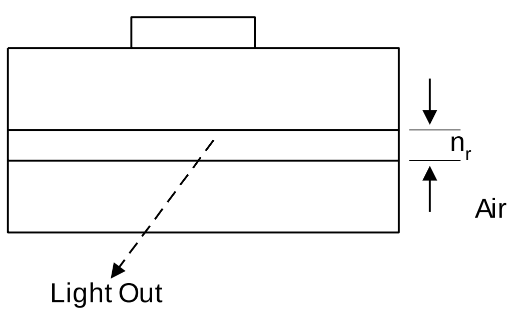

Fig. 23. Light emission from the laser facet at the semiconductor-air interface.

$$R_1 = R_2 = R = \left(\frac{n_r - n_{air}}{n_r + n_{air}} \right)^2 \qquad (65)$$

Thus in this situation, we get

$$= \left(\frac{3.52 - 1}{3.52 + 1} \right)^2 = 0.31$$

$$J_{TH} = \frac{8\pi n_r^2 q d \Delta v_s}{\Gamma \eta_q Z(T)} \left(\frac{v^2}{c^2} \right) \left[\alpha + \frac{1}{2L} \ln \frac{1}{R_1 R_2} \right] \qquad (44B)$$

Assume, $\eta_q \approx 0.9 \rightarrow 1.0$, $Z(T) \approx 0.5 \rightarrow 1.0$

$\Delta\nu_s$ is obtained from the emission spectrum of LEDs (see problem set on lasers), you can use GaAs values. The selection of L determines the power output and also effects the separation between modes. The value of active layer thickness, d, depends whether the structure is a double heterostructure or a quantum well laser.

E. External Differential Efficiency and Power Output
(Ref: A. Yariv: Optical Electronics, publisher HRW)

$$P_{out} = \left(\begin{array}{l} \text{Power emitted by stimulated} \\ \text{emisssion in the cavity} \end{array} \right) * (\text{Fraction lost due to mirrors})$$

$$= \left[\frac{(I - I_{TH})\eta_{\text{int}} h\nu}{q} \right] * \left[\frac{\frac{1}{2L}\ln(1/R_1 R_2)}{\alpha + \frac{1}{2L}\ln(1/R_1 R_2)} \right] \qquad (66)$$

where:

$$\boxed{\eta_{\text{int}} = \eta_{inj} * \eta_q} \quad \textit{Just like LEDs} \qquad (67)$$

Assume $n_{inj} \cong 1, \quad \eta_q = 0.9 \leftrightarrow 1.0$

$$\eta_{ex} = \text{external differential} \rightarrow \text{ quantum efficiency}$$

$$\eta_{ex} = \frac{d\left(P_{out}/h\nu\right)}{d\left[\left(I - I_{TH}\right)/q\right]} \text{= Rate of increase of output power per increase in t} \tag{68}$$

Power conversion efficiency

$$\eta_C = \frac{P_{out}}{V_{app} * I} \tag{69}$$

F. Separation between cavity longitudinal modes

Mode separation $\Delta\lambda = \pm \frac{\lambda^2}{2Ln_r}\left(1 - \frac{\lambda}{n_r}\frac{dn_r}{d\lambda}\right)$ (22)

G. Beam divergence

Lateral Divergence (in the plane of the junction) is shown in Figure below.

$$\theta_{\|} = \frac{\lambda}{W} = \frac{1.55}{15} \cong 0.1 \text{ radian} \approx 6^\circ \tag{70}$$

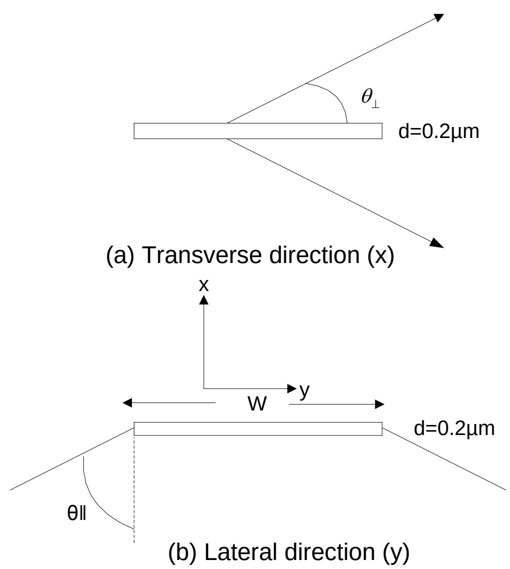

Fig. 23(b). Beam divergence in along transverse axis (x) and lateral axis (y).

Perpendicular to the junction plane divergence (diffraction limited) is shown below in Fig. 14.

$$\theta_{perp.} = \frac{20 * x * d}{\lambda} \tag{71}$$

The above expression Eq. 71 is an empirical simplification for $Al_xGa_{1-x}As$ -GaAs- $Al_xGa_{1-x}As$ double Heterostructure lasers. Here, x is the composition of Aluminum in $Al_xGa_{1-x}As$ and d the thickness of the active layer (i.e. GaAs layer).

In the case of InGaAsP, or other materials, one has to modify this relationship. We believe that for InGaAsP we can modify the above relation as follows. (*x* is the Indium composition in the cladding layer)

$$\theta_{\perp} = \theta_{perp.} = \frac{20x \bullet 0.25 \bullet 0.2\mu m}{1.55\mu m} = 0.52 \text{ radians} \approx 30°$$

An alternate expression for $\theta_{\perp}$ as used in Design Level 3 is: $\theta_{\perp} = \dfrac{4.0(n^2{}_{active} - n^2{}_{clad})d}{\lambda}$ (72)

Laser Design: A device design has several issues. Many times all the parameters are not given. One has to find these parameters. Often the design is an iterative process. You start with some values (e.g. Cavity Length L, Width W, spontaneous line width $\nabla\nu_s$, n_i value etc.). We can refine them through iteration to get the desired specifications. We have followed similar steps in the above example.

7.5.2 Design of an InGaAs-GaAs 980nm Laser-Level 2

Design a double hetero structure laser operation at 980nm (or 0.98μm) using InGaAs-GaAs-AlGaAs material system. Find the operation voltage and current if you need to produce an optical power output of 10mW. Threshold current density should be under 1000 A/cm^2

What would you do to obtain single transverse mode and single lateral mode operation?

a) Outline all the design steps.
b) Show device dimensions (active layer thickness d, cavity length L and width W), doping levels of various layers constituting the diode along with their functionality.
c) Analyze the designed structure and evaluate the various parameters (threshold current density J_{th}, mode separation Δλ and Δυ) and characteristics (beam divergence in the junction plane θ and perpendicular to the junction plane θ, operating current I and voltage $V_{applied}$), required to operate the laser. (Be quantitative where possible).

I. Assume : Active layer thickness d = 0.2μm, Top contact (stripe) width w = 15 μm. (Here d and w are selected to yield single mode operation, show that for your cladding and active layer a d of 0.2μm results in a single transverse mode) Cavity Length L = ? (You select, using optical power output considerations) Confinement factor $\Gamma \approx 1 - \exp(-C\Delta n_r d)$, $\Delta n_r = n_r$(active layer) - n_r(Cladding) and $C = 3x10^6$ cm^{-1}. Determine the index of refraction n_r. $d\, n_r/d\lambda = 2.5\ \mu m^{-1}$, Spontaneous line width $\Delta\upsilon_s = 6x10^{12}$Hz, $Z(T) \approx 1$. Determine the end reflectivities R_1, R_2 and select a value for η_q. Absorption coefficient $\alpha = \alpha_{Diffraction} + \alpha_{Free\ Carrier} + \alpha_{Scattering} = 20$ cm^{-1}.

II. Assume reasonable values of all material related parameter (use GaAs values if you cannot find for the material you are using). Assume D_n, τ_n values from the previous examples.

Design specs: Lasing wavelength 980nm, threshold current density $J_{TH} < 1000 A/cm^2$**,** single mode output power Pout = 10 mW.

Step A: Selection of Active layer, Substrate & Cladding Layers

We have to select proper active layer that would lase at 980nm, cladding layers that would provide adequate carrier and photon confinement.

$$h\upsilon = \frac{1.24}{0.98} = 1.265eV$$

Bernard-Douraffourg condition states that

$$E_{fn} - E_{fp} \geq h\nu \geq E_g$$

Let E_g = 1.26 eV

Find the composition from the following E_g vs lattice constant chart. The active layer is $In_{0.12}Ga_{0.88}As$. (Lattice parameter = 5.7 A˚)

Substrate: GaAs

InGaAs – GaAs lattice mismatch = 5.7 – 5.66 = 0.04 = Δa

$$\frac{0.04}{5.66} = 0.00706 => \frac{\Delta a}{a_{GaAs}}$$

There is a 0.7% of mismatch.

Lattice Parameter and Bandgap Data

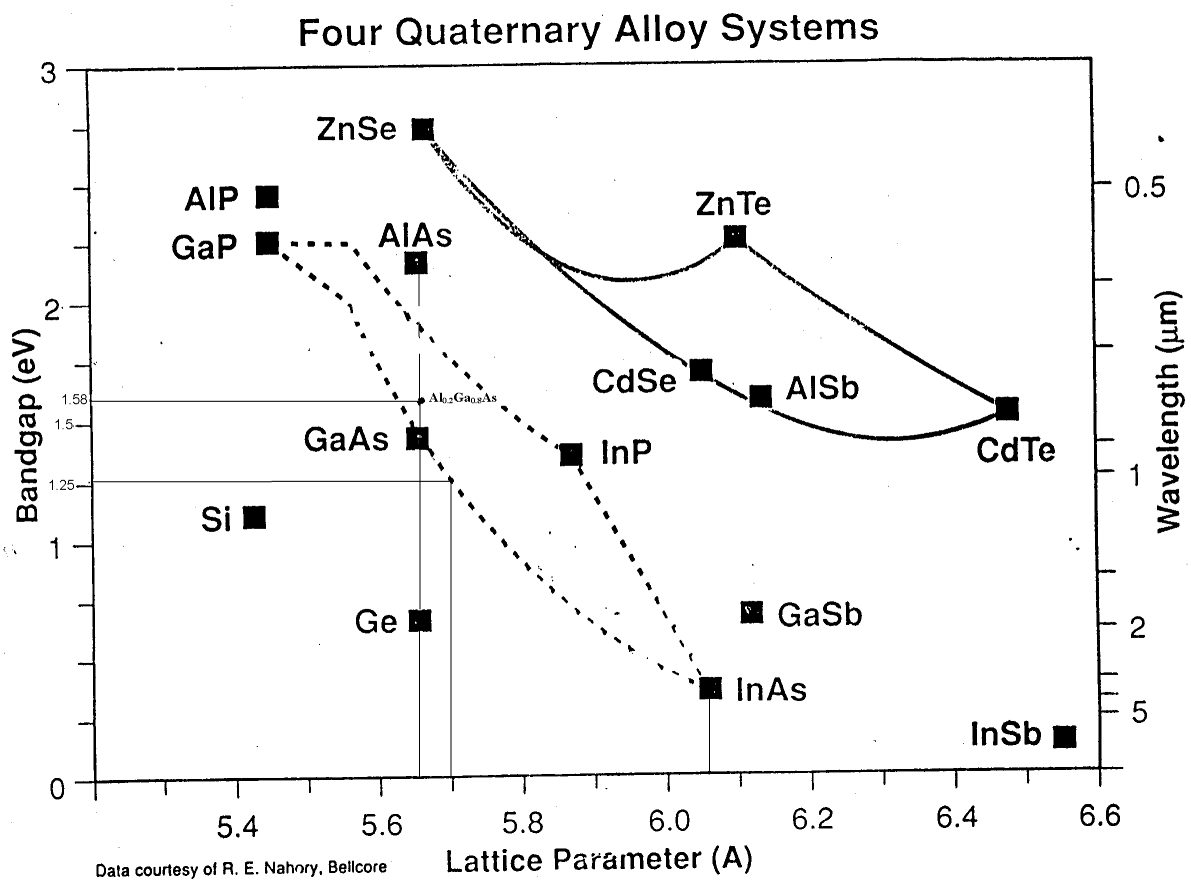

Fig .23(c) Lattice constant versus energy band gap. (Reproduced again)

Cladding layers:

(i) $E_g\big|_{cladding} - E_g\big|_{Active} = 0.2 -> 0.5eV$

(ii) $n_r\big|_{Active} - n_r\big|_{cladding} = \Delta n_r \approx 0.01$

Index of refraction of $In_{0.12}Ga_{0.88}As$ using the index relation is given by,

$In_xGa_{1-x}As_yP_{1-y}$ => $In_{0.12}Ga_{1-0.12}As$

y = 1 ; x = 0.12

$n_r = 3.52xy + 3.39\,(1-y) + 3.6y\,(1-x) + 3.56\,(1-x)\,(1-y)$

= 3.52*0.12 + 0 + 3.6 (1-0.12)
= 3.5904

$n_r\big|_{clad} \leq 3.49$

Cladding material:

Select GaAs or $Al_xGa_{1-x}As$. Let x=0.2, $Al_{0.2}Ga_{0.8}As$ => $E_g\big| = 1.58eV$

$n_r\big|_{AlGaAs} = 3.59 - 0.71x + 0.091x^2$

x = 0.2
n_r = 3.452

So $Al_{0.2}Ga_{0.8}As$ satisfies the index condition. The energy gap is 1.58 eV.

$$E_g\big|_{clad,Al_{0.2}Ga_{0.8}As} - E_g\big|_{Active,In_{0.12}Ga_{0.88}As} = 1.58 - 1.26 = 0.32eV$$

Step B: Doping Level of Active / Cladding Layers

The doping levels in cladding are crucial as they should be higher doping than the injection levels n_e in the active layer that would satisfy the Bernard-Douraffourg condition.

$$p = n = n_i$$

The concentration is obtained from Bernard-Douraffourg condition

$$E_{fn} - E_{fp} \geq h\nu \geq E_g$$

$$n_e = n_i e^{(E_{fn} - E_{fp})/2kT}$$

$$n_e \equiv p_e$$

$$n = n_1 e^{(E_c - E_i)/kT}$$

$$p = n_1 e^{(E_c - Ev)/kT}$$

$$np = n_1^2,\ e^{(E_c - Ev)/kT}$$

$$n = n_e,\ p = p_e$$

$$n_e = p_e$$

$$n_e > n_i\, e^{(Eg/2kT)}$$

$$n_e > n_i\ e^{(Eg/2kT)}$$

Once p_e,n_e are known, the doping concentrations are related as:

$$\boxed{\begin{array}{l} N_A > p_e \\ N_D > n_e \end{array}}$$

$$n_e = n_i e^{\frac{E_{fn}-E_{fp}}{2kT}} = n_i e^{\frac{E_g}{2kT}}$$
$$= n_i\big|_{Active} e^{\frac{1.26}{2kT}}$$
$$= 2.66\text{x}10^8\text{x}3.66\text{x}10^{10} = 9.7\text{x}10^{18}\ \text{cm}^{-3}$$

$$\frac{e^{-1.26/2kT}}{e^{-1.43/2kT}} = \frac{n_i(\text{In}_{0.12}\text{Ga}_{0.88}\text{As})}{n_i(\text{GaAs})}$$

$$n_i(GaAs) = 10^7\ cm^{-3}$$
$$n_i(\text{In}_{0.12}\text{Ga}_{0.88}\text{As}) = 10^7\, e^{\frac{1.43-1.26}{2*0.0259}} = 2.66x10^8\ cm^{-3}$$

Step C: Active layer thickness d for a Single Transverse Mode and Stripe width W for a single lateral mode

a) Active layer thickness d ≈ 0.2μm

For single transverse mode, condition for single transverse mode (m = 1) is
Gain coefficient high then the carrier concentration is low and index is high. This is shown in Figs. 24 and 25.

$$d < \frac{m\lambda}{2\sqrt{n_r^2\big|_{active} - n_r^2\big|_{clad}}} \qquad (73)$$
$$< \frac{0.98\,\mu m}{2*0.9857} \quad \text{where m=1,2,3} \qquad < 0.5\,\mu m$$

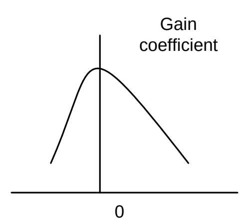

Fig .24. Gain coefficient in active layer along lateral axis y.

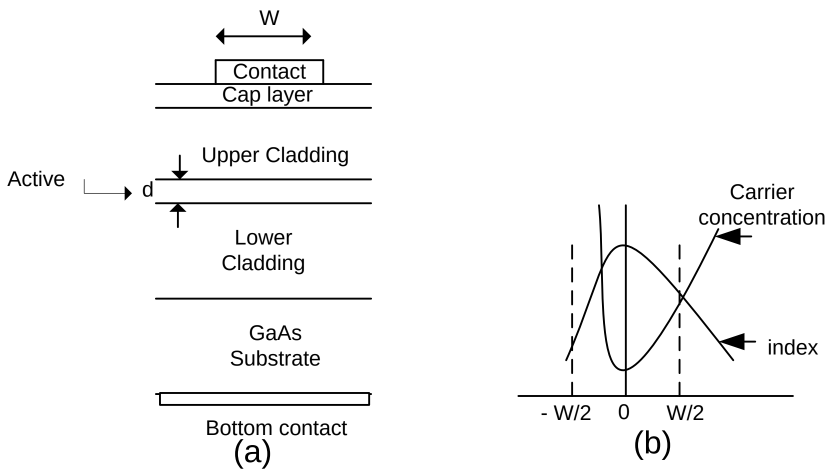

Fig. 25 (a) structure, (b) carrier concentration and index of refraction in the active layer.

b) Given for a single lateral mode W = 15μm

$$W < \frac{m\lambda}{2\sqrt{n_r^2\Big|_{MiddleOfGainRegionInActiveLayer} - n_r^2\Big|_{CornerOfActiveLayerAwayFromWhereGainIsSmall}}} \qquad (74)$$

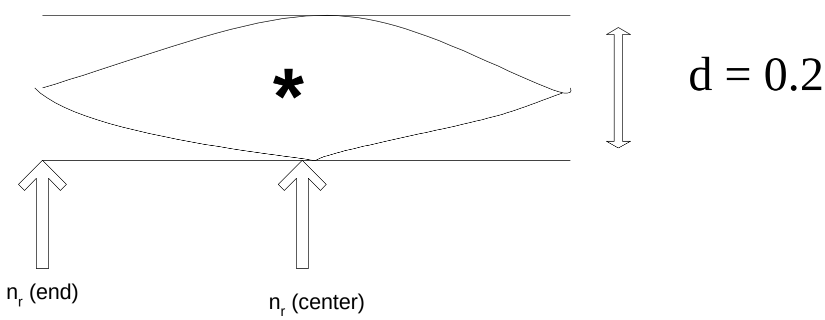

Fig .26. Lateral confinement due to index variation in the center and end regions of the active layer.

n_r (center) – n_r (end) ≈ 0.005

Index increases if carrier concentration decreases. This is know as Gain Guiding and is responsible for lateral confinement.

$$W \le \frac{0.98\mu m}{2x0.005x2x3.59} \le 13.8\mu m$$

Confinement Factor Γ

The simplest empirical expression for AlGaAs-GaAs heterostructure laser is

Transverse Confinement Factor = Γ_x = 1 - exp (-C Δn_r d), here C= $3x10^6$

$= 1 - \exp(-3x10^6 x0.138x0.2x10^{-4})$

$= 1 - 2.5x10^{-4} \approx 1$

Or, use the general relation

Step D: Calculation of threshold current density J_{th}

$$R_1 = R_2 = \left(\frac{n_r|_{active} - n_{air}}{n_r|_{active} + n_{air}} \right)^2$$

$$= \left(\frac{3.59 - 1}{3.59 + 1} \right)^2 = 0.318$$

We need the cavity length L. It determines the optical power output. We will assume a L value and see if P_{out} > 10mW, if it is not we will increase L.

Let L = 500μm.

$$J_{th} = \frac{8\pi n_r^2 q d \Delta\upsilon_s}{\Gamma \eta_q Z(T)} \left(\frac{1}{\lambda^2} \right) \left(\alpha + \frac{1}{2L} \ln\left(\frac{1}{R_1 R_2} \right) \right) \qquad \therefore \left(\frac{\upsilon}{c} \right)^2 = \frac{1}{\lambda^2}$$

α = 20 cm^{-1}

$$\frac{1}{2L} \ln\left(\frac{1}{R_1 R_2} \right) = \frac{1}{2x500x10^{-4}} \ln \frac{1}{0.318^2} = 22.9 cm^{-1}$$

Substituting for $\Delta\upsilon_s$ and other parameters.

$$J_{th} = \frac{8\pi * 3.59^2 * 1.6 * 10^{-19} * 0.2 * 10^{-4} * 6 * 10^{12}}{1 * 0.9 * 0.5} \frac{1}{(0.98 * 10^{-4})^2} (20 + 22.9) = 61.7 A/cm^2$$

$$I_{th} = w * L * J_{th} = 15 * 10^{-4} * 500 * 10^{-4} * 61.7 = 4.62 mA$$

Step E: Finding the Operating Current and Voltage that would provide desired laser output

In this step, we will calculate the operating current and voltage that would provide 10mW optical power. We will also calculate power conversion efficiency η_c and external differential efficiency $\eta_{ex.}$

Optical power output = 10mW

$$\eta_{int} = \eta_q * \eta_{inj} \approx 0.9$$

Stimulated photons generated in the cavity per second * fraction of light exiting mirrors due to R_1 and R_2. Stimulated photons are related to current above threshold.

$$PowerOutput = \frac{(I - I_{th}) \eta_{int} h\upsilon}{q} \frac{\frac{1}{2L} \ln\left(\frac{1}{R_1 R_2} \right)}{\alpha + \frac{1}{2L} \ln\left(\frac{1}{R_1 R_2} \right)}$$

$$10mW = (I - 4.62*10^{-3})*0.9*1.26*Volts\,\frac{22.9}{42.9}$$

$$I = 4.62*10^{-3} + \frac{42.9}{22.9}*\frac{10^{-2}}{0.9*1.26} = 21.12x10^{-3}\,A$$

Operating voltage is related by the I-V equation

$$I = I_s\left(e^{\frac{qv_{applied}}{kT}} - 1\right)$$

Junction Area = wL = 15 * 10^{-4} * 500 * 10^{-4} cm^{-2} = $0.75x10^{-4}$ cm^{-2}

$$I_s \cong \frac{qAD_n n_{p0}}{L_n} + \frac{qAD_p p_{n0}}{L_p} \cong \frac{qAD_n n_{p0}}{L_n}$$

In the active layer $n_{p0} = \frac{n_i^2(InGaAs)}{N_A(InGaAs)} = \frac{(2.66*10^8)^2}{10^{16}} = 7.07cm^{-3}$

Assume D_n = 50 cm^2 / s ; $\tau_n = 10^{-8}$

$$L_n = \sqrt{50*10^{-8}} = 7.07x10^{-4}\,cm$$

$$I_s = \frac{1.6*10^{-19}*0.75*10^{-4}*50*7.07}{7.07*10^{-4}} = 6x10^{-8}\,A$$

From $I = I_s\left(e^{\frac{qv_{applied}}{kT}} - 1\right)$, $V_{applied} = \frac{kT}{q}\ln\left(\frac{I + I_s}{I_s}\right)$

$$V_{applied} = 0.0259*\ln\left(\frac{21.12*10^{-3} + 6*10^{-18}}{6*10^{-18}}\right) = 0.927volts$$

Conversion Efficiency :

$$\eta_c = \frac{10mW}{21.12*10^{-3}*0.927} = 0.51 = 51\%$$

External Differential Efficiency:

$$\eta_{ext} = \frac{d(P_{out}/h\upsilon)}{d((I - I_{th})/q)}$$

Rewriting the P_{out} expression gives,

$$\left(P_{out}/h\upsilon\right) = \frac{(I - I_{th})}{q} * \eta_{\text{int}} * \frac{\frac{1}{2L}\ln\left(\frac{1}{R_1 R_2}\right)}{\alpha + \frac{1}{2L}\ln\left(\frac{1}{R_1 R_2}\right)}$$

$$\frac{\partial\left(P_{out}/h\upsilon\right)}{\partial\left((I - I_{th})/q\right)} = \eta_{\text{int}} * \frac{\frac{1}{2L}\ln\left(\frac{1}{R_1 R_2}\right)}{\alpha + \frac{1}{2L}\ln\left(\frac{1}{R_1 R_2}\right)}$$

$$\eta_{ext} = 0.9 * \frac{22.9}{42.9} = 0.48 = 48\%$$

Step F: Computation of Mode Separation Δλ, frequency separation Δυ, beam divergence in the junction plane $\theta_{\parallel}$ and perpendicular to the junction plane $\theta_{\perp}$.

$$\Delta\lambda = \pm\frac{\lambda^2}{2Ln_r}\left(1 - \frac{\lambda}{n_r}\frac{dn_r}{d\lambda}\right)^{-1}$$

.98µm =.98*10^{-4} cm

(.98)L/(2*500*3.59) µm

=8.42*10^{-4} µm

$$= \frac{(0.98*10^{-4})^2}{2*500*10^{-4}*3.59}\left(1 - \frac{0.98\mu m}{3.59}*2.5\mu m^{-1}\right)$$

= 8.42x10^{-8} cm = 8.42 A°

$$\Delta\upsilon = \frac{c\Delta\lambda}{\lambda^2} = \frac{3*10^{10}*8.42*10^{-8}}{(0.98*10^{-4})^2} = 2.6x10^{11}Hz = 260GHz \quad \left(\because \lambda_1\lambda_2 \approx \lambda^2;; \lambda_1 = \lambda_2 + \Delta\lambda\right)$$

Beam Divergence:

$$\theta_{\parallel} = \frac{\lambda}{w} = \frac{0.98*10^{-4}}{15*10^{-4}} = 0.0653 radians = 3.74^{\circ}$$

$$\theta_{\perp} = \frac{20xd}{\lambda} = \frac{20*0.2*0.2*10^{-4}}{0.98*10^{-4}} = 0.888 radians = 50.9^{\circ} \quad \left(\therefore x = 0.2\ for Al_{0.2}Ga_{0.8}As\right)$$

Where $\frac{20xd}{\lambda}$ =AlGaAs

Alternate expression $\theta_{\perp}$ = (4.0(n$^2_{\text{acitiv-}}$ n$^2_{\text{clad}}$)d)/λ

Figures 27 and 28 show the gain guided and index guided laser structures.

Figure 29 shows the high index change in an index guided ridge waveguide laser.

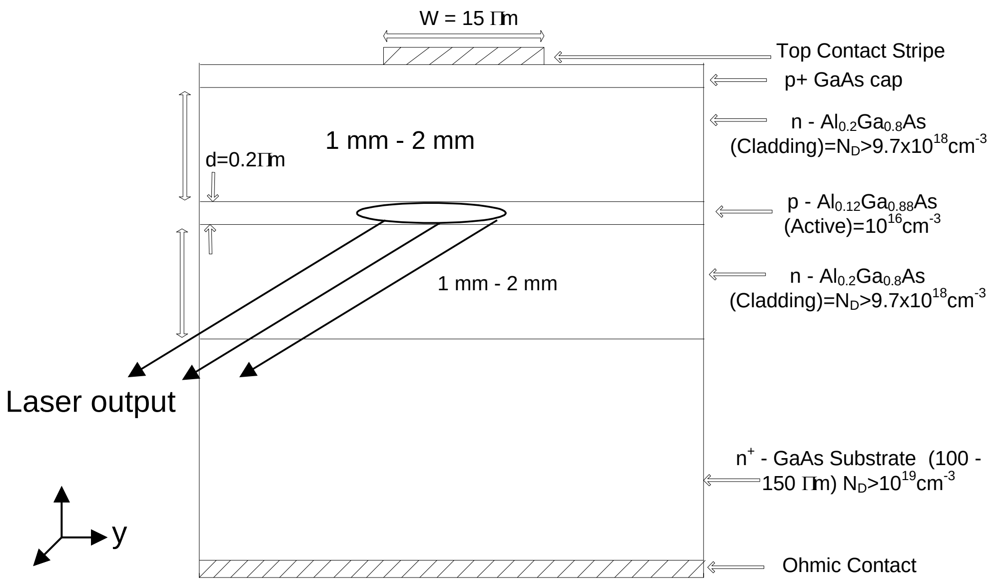

Fig. 27 Cross-section of gain guided stripe geometry 980 nm single-mode laser.

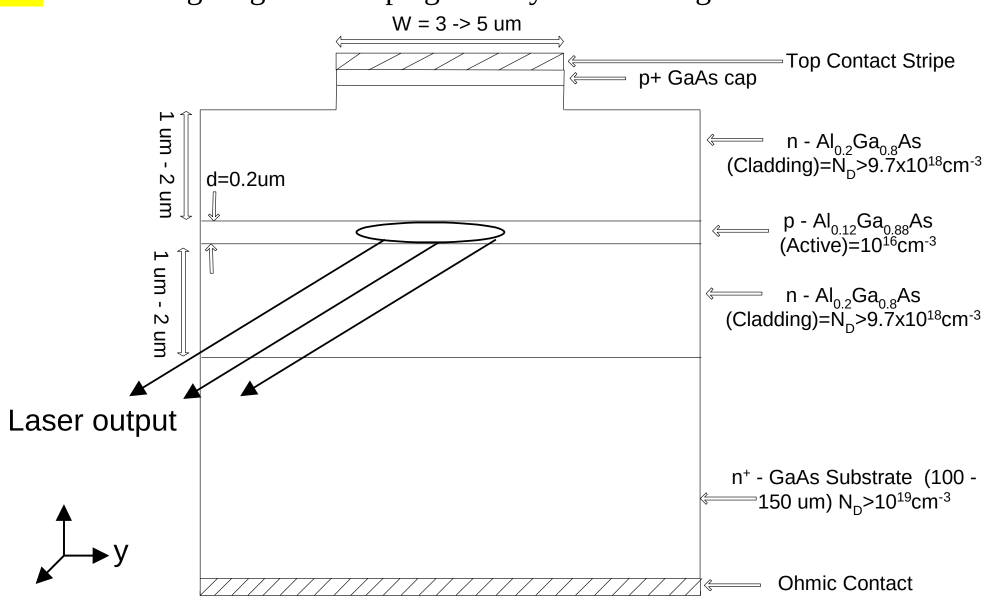

Fig. 28 Cross-section of an index guided ridge waveguide 980 nm single-mode laser.

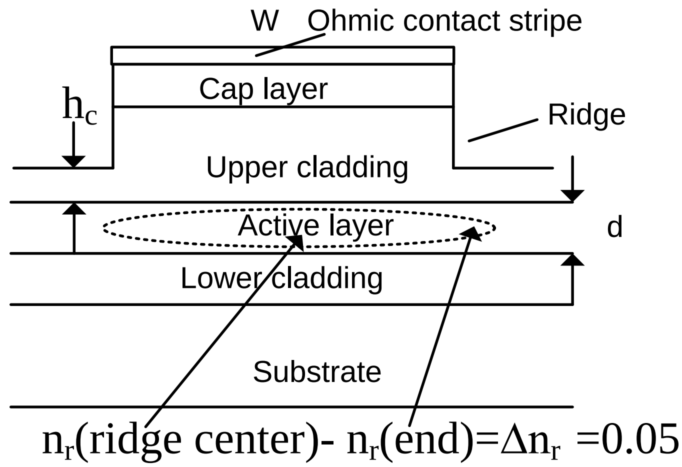

Fig. 29. Schematic cross-section of a ridge waveguide laser.

7.6. Quantum well and quantum dot lasers

Excess carriers can be produced either by injection using a p-n junction or by excitation using e-beam or optical beams. In the case of p-n junctions or heterojunctions, the active layer in which majority of injected carriers recombine and produce photons can be one the following:

a. 3-d layer (relatively thick epitaxial layer where dimensions are greater than the electron and hole wavelength in x, y, and z directions) no quantum confinement.
b. 2-d layer or quantum well (thickness comparable to carrier wavelength) resulting one-degree of quantum confinement.
c. 1-d layer consisting of quantum wires which are confined along the transverse and one lateral direction. Two degree of confinement.
d. 0-d layer consisting of quantum dots which are confined along transverse and lateral and longitudinal directions. Three dimensional confinement.

Using a lower dimensional active layer yields higher optical gain coefficient and lower threshold current density. Since lower dimensionality requires use of etching etc. in terms of fabrication, the quantum efficiency is lower and if not rectified results in higher threshold current density.

7.6.1 Optical transitions in quantum confined systems.

In lasers we use downward transitions which are either due to free carriers or due to excitons. The upward transitions are related with absorption.

Absorption (Upward transitions)

Transitions with exciton formation,
Transitions involving free carriers.

Applications where photon absorption is used.

MOS/CCD Camera Imaging
Solar Cells
Photodetectors
Modulators, Optical Switches

Emission (Downward transitions):

Transitions with exciton formation,
Transitions involving free carriers.

Applications where photon emission is used.

LEDs
Lasers
Bioluminescence

7.6.2 Effect of Strain on Energy Band E-k Diagram:

The energy vs k diagram gets modified when a strain is present, particularly in an epitaxial layer sandwiched between two layers or one layer and the substrate.

This is shown below in Fig. 30 for a direct gap semiconductor. Here, the valence band is shown with three sub-bands: (a) heavy hole band, light hole band, and sub-band due to spin orbit coupling.

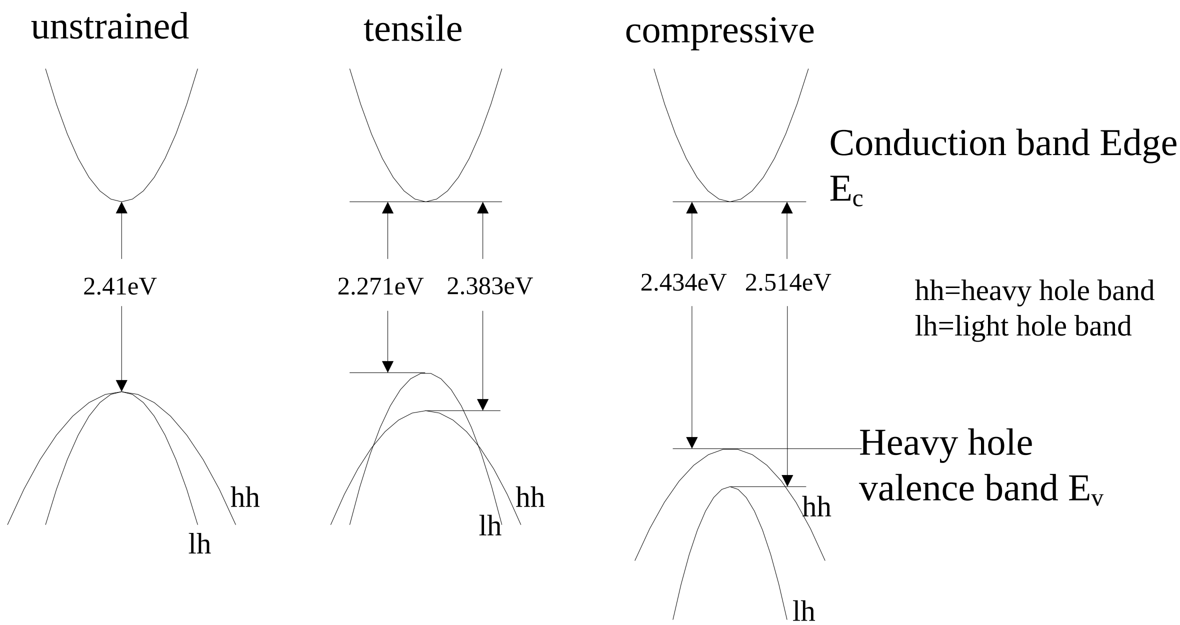

Figure 30.Energy gap changes due to lattice strain. [Ref: W. Huang, 1995, UConn Ph.D. Thesis]

1. Under the tensile strain, the light hole band is lifted above the heavy hole, resulting in a smaller band gap.
2. Under a compressive strain the light hole is pushed away from heavy. As a result the effective band gap as well as light and heavy hole m asses are a function of lattice strain. Generally, the strain is +/- 0.5-1.5%. "+" for tensile and "-" for compressive.
3. Strain does not change the nature of the band gap. That is, direct band gap materials remain direct gap and the indirect gap remain indirect.

7.6.3 Gain due to Free Carrier and Excitonic Transitions in Quantum Well, Wire/ Dots:
The probability of transition P_{mo} from an energy state "0" to an energy state in the conduction band "m" is given by an expression (see Moss et al.). This is related to the absorption coefficient α. It depends on the nature of the transition.

The gain coefficient g depends on the absorption coefficient α in the following way:

$$g = -\alpha_0 \square\square\square\square\square\, f_e - f_h). \tag{33}$$

$$f_e = \frac{1}{1+e^{\frac{E_c - E_{fn}}{kT}}}$$

$$f_n = 1 - \frac{1}{1+e^{\frac{E_v - E_{fp}}{kT}}}$$

The gain coefficient g can be expressed in terms of absorption coefficient α_0 and Fermi-Dirac distribution functions f_e and f_h for electrons and holes, respectively. Here, f_e is the probability of finding an electron at the upper level and f_h is the probability of finding a hole at the lower level.

Free carrier transitions: A typical expression for g in semiconducting quantum wires, involving free electrons and free holes, is given by:

$$g_{free}(\omega) = \frac{2\pi e^2}{\varepsilon_0 n_{rm_0} c\omega L_x} \sum_{l,h} [\frac{(2m_{eh})^{1/2}}{\pi\hbar L_y L_z} |M_b|^2 \bullet |\int \Psi_e(y)\Psi_h(y)dy|^2$$
$$\bullet \int \Psi_e(z)\Psi_h(z)dz|^2 \bullet \int (E - E_e - E_h)^{-1/2} \rho(E) \bullet L(E)dE(f_e + f_h - 1)] \qquad (75)$$

Excitonic Transitions: Another form of transitions is due to excitons. That is, injected electrons in the conduction band (higher energy states) of a semiconductor region (primarily hosting holes or holes may be introduced from the other side of this region), form electron-hole pairs which are bound via the Coulombic attraction. The collapse of excitons results in the emission of photons. Generally, exciton binding energy is small (4-6 meV) in GaAs, Si, InP and Ge. However, it is higher in ZnSe, GaN and other low dielectric constant semiconductors. Similar is the situation in polymer and organic semiconductors, which are known to exhibit higher binding energy. Exciton binding energy is reduced with increased electron and hole concentrations, which causes screening to counter the coulomb attraction. The binding energy of excitons can be increased by confining the constituent electrons and holes in quantum wells, wires, and dots.

In the case of excitonic transitions, the gain coefficient is:

$$g_{ex}(\omega) = \frac{2\pi e^2}{\varepsilon_o n_r m_o c\omega L_y L_z} \sum_{l,h} [|M_b|^2 \bullet 2\pi^{1/2} |\phi_{ex}(0)|^2$$
$$\bullet (|\Psi_e(y)\Psi_h(y)dy|^2 |\Psi_e(z)\Psi_h(z)dz|^2) \bullet \rho_{ex} \bullet \mathrm{L}(E_{ex}) \bullet (f_c + f_v - 1)] \qquad (76)$$

Similarly, we can calculate the absorption and gain coefficient in quantum wells and quantum dots.

In the case of lasers, we need to find the gain coefficient and its relationship with f_e and f_h, which in turn are dependent on the current density (injection laser) or excitation level of the optical pump (optically pumped lasers).

The gain coefficient depends on the current density as well as losses in the cavity or distributed feedback structure.

$$J_{th} = \frac{8\pi n_r^2 \nu^2 q d \Delta\nu_s}{\Gamma \eta c^2 z(T)} \bullet \left[\alpha + \frac{1}{2L} \ln \frac{1}{R_1 R_2}\right] \qquad (44B)$$

$$g = \frac{1}{2L} \ln(\frac{1}{R_1 R_2}) + \alpha_f + \alpha_c + \alpha_d$$ (Using Eqs. 15 and45)

Threshold current density is obtained once we substitute g from the lower equation.

For modulators, we need to know:

1. Absorption and its dependence on electric field (for electroabsorptive modulators)
2. Index of refraction n_r and its variation Δn as a function of electric field (electrorefractive modulators)
3. Change of the direction of polarization, in the case of birefringent modulators.

In the presence of absorption, the dielectric constant ε (ε_1-jε_2) and index of refraction n (n_r –j κ) are complex. However, their real and imaginary parts are related via Kramer Kronig's relation. See more in the write-up for Stark Effect Modulators.

7.6.4 Threshold current density

An important objective in laser design is to reduce the threshold current density to as small a value as possible. This means reducing spontaneous line width $\Delta\nu_s$, active layer width d, losses in the cavity (α's), and increasing quantum efficiency η_q.

Parameters influencing threshold current density:

(1) Spontaneous Line width, $\Delta\nu'_s$

It is determined by the active layer material and the degree of freedom the carriers enjoy in it. For a given material, it reduces as the carriers become more confined. That is, $\Delta\nu's$ in Quantum dots < Quantum wires < Quantum wells < 3D epitaxial layer.

In general, the stimulated line with is smaller than spontaneous line width.

(2) Critical Temperature, T_0

Quantum dot lasers are theoretically predicted to be insensitive to temperature variations.

$$J_{TH}(T) \sim J_{TH}(0)\exp\{T/T_0\}.$$

(3) Active layer thickness, d

Active layer thickness d is reduced in quantum well lasers. A quantum well is 5-10nm thick. Two or more quantum wells can be used. However, quantum wells are separated by energy barriers. If two wells are used we have three barriers (one between the wells and two above and lower the wells). The total thickness may be 60-80nm. Similar thickness is used in quantum wire and dot lasers. In the case of quantum wires and dots, there is additional barriers along other axies.

The quantum well/dot active layer is sandwiched using a double heterojunction (DH). This provides the carrier confinement as well as photon confinement. This is reproduced below. The carrier confinement in a pAlGaAs/n^-GaAs well/nAlGaAs structure takes place in following way.

Carrier confinement: Holes are injected from the pAlGaAs layer into the nGaAs layer. Because of nAlGaAs layer, these holes are now confined to be in the nGaAs layer as it acts as a barrier to them. So they are forced to recombine with electrons in the n^-GaAs quantum well. In addition unlike p-n homojunctions, the electrons cannot be injected from the n-GaAs layer into the p-AlGaAs layer even it is doped lighter than nGaAs. This results in an injection efficiency of unity. It is a consequence of energy band discontinuity in the conduction band at the pAlGaAs-nGaAs heterointerface which prevents this injection.

Photon confinement: Photons generated in the active layer, which is a quantum well confining injected carriers, do not remain confined in this layer. The AlGaAs layers sandwiching the QW have lower index of refraction and act as cladding layers. A waveguide region (~0.1 micron or so) is used to provide optical gain in the quantum well. This is achieved by dividing the AlGaAs layer into two parts-- one forming the waveguide region and the other forming the cladding layers.

(4) Absorption coefficients, α's

The absorption coefficient in the active layer as well as in the waveguide regions should be as small as possible at the lasing wavelength. This is accomplished by reducing the doping levels in these layers which cause lowering of the free carrier absorption. Note that heavy injection of carrier causes quasi Fermi levels to be in the conduction and valence bands. Any emission below this energy ($h\nu < E_{fn} - E_{fp}$; also known as the Bernard-Dourafforg condition) will yield lower absorption, generally referred to as the transparency condition.

When the Gain coefficient g (depending on the injection current density) equals or exceeds all the losses α_T (including output or leakage from mirrors), we get lasing.

Gain coefficients are generally higher as we use quantum wells, wires, and dots. This is explained next.

Including the effect of confinement, we get J in terms of confinement factor Γ

$$J = \frac{8\pi n_r^2 \nu^2 e L_x \Delta\nu_s}{\Gamma \eta_q c^2 [1 - e^{\frac{h\nu - \Delta\zeta}{kT}}]} .g \qquad (41)$$

Threshold current density in Quantum wire/dot Structures

The threshold occurs when the gain becomes equal to all the losses at the operating wavelength λ.

The threshold current density is related to the excitonic gain coefficient [Huang and Jain]

The threshold current density J_{th} is obtained by setting the gain equal to the sum of various loss coefficients (free carrier α_f, scattering α_c and diffraction loss α_d) as expressed by Eq. (11).

$$g = \frac{1}{2L} \ln\left(\frac{1}{R_1 R_2}\right) + \alpha_f + \alpha_c + \alpha_d \qquad (15)$$

If we account for the losses in active layer as well as in the cladding layer, we get

g= $[\Gamma\alpha_{FC,AL} + (1-\Gamma)\,\alpha_{FC,CL} + \Gamma\alpha_{DIFF,AL} + (1-\Gamma)\,\alpha_{DIFF,CL} + (1/2L)\ln(1/R_1R_2)]$.Here, we have used $\square_{FC,CL}$ for the losses in the core due to free carrier as well as other scattering losses. $\square_{DIFF,CL}$ is the loss

due to diffraction in the cladding.
Substituting in for J, we get

$$J_{TH} = [\{q\ d\ \Delta\nu_s\ 8\ \pi\ \nu^2\ n_r^2\}/\{\eta_q\ c^2\}]$$

$$[\Gamma\alpha_{FC,AL}+(1-\Gamma)\alpha_{FC,CL}+\Gamma\alpha_{DIFF,AL}+(1-\Gamma)\alpha_{DIFF,CL}+(1/2L)\ln(1/R_1R_2)]\ [1-\exp\{h\nu-\Delta\zeta\}/kT]^{-1}$$

Here, L is the length of the cavity and R_1 and R_2 are the mirror reflectivities.

5. Quasi Fermi Levels E_{fn}, E_{fp}, and $\Delta\zeta$

Quasi Fermi levels are evaluated using charge neutrality condition. In the case of quantum wells and wires and dots, it is given below.

<u>*Quantum Wells*</u>

$$\frac{m_e}{\pi\hbar^2 L_x}\int_{E}^{\infty}\frac{dE}{1+e^{(E-E_{Fn})/kT}} = \frac{m_{hh}}{\pi\hbar^2 L_x}\int_{E_{hh}}^{\infty}\frac{dE}{1+e^{(E-E_{Fn})/kT}} + \frac{m_{lh}}{\pi\hbar^2 L_x}\int_{E_{lh}}^{\infty}\frac{dE}{1+e^{(E-E_{Fn})/kT}} --(77)$$

<u>*Quantum Wires*</u>

$$\frac{(2m_e)^{1/2}}{\pi\hbar L_x L_y}\int_{E_e}^{\infty}\frac{(E-E_e)^{-1/2}dE}{1+e^{(E-E_{Fn})/kT}} = \frac{(2m_{hh})^{1/2}}{\pi\hbar L_x L_y}\int_{E_{hh}}^{\infty}\frac{(E-E_{hh})^{-1/2}dE}{1+e^{(E-E_{Fn})/kT}} + \frac{(2m_{lh})^{1/2}}{\pi\hbar L_x L_y}\int_{E_{lh}}^{\infty}\frac{(E-E_{lh})^{-1/2}dE}{1+e^{(E-E_{Fn})/kT}} --(78)$$

<u>*Quantum Dots*</u>
The charge neutrality condition for quantum dots is:

$$\frac{1}{L_x L_y L_z}\int_{E_{e(l,m,n)}}^{\infty}\frac{\delta(E-E_{e(l,m,n)})\ dE}{1+e^{(E-E_{Fn})/kT}} = \frac{1}{L_x L_y L_z}\int_{E_{hh(l,m,n)}}^{\infty}\frac{\delta(E-E_{hh(l,m,n)})dE}{1+e^{(E-E_{Fn})/kT}}$$

$$\underrightarrow{or} = \frac{1}{L_x L_y L_z}\int_{E_{lh(l,m,n)}}^{\infty}\frac{\delta(E-E_{lh(l,m,n)})\ dE}{1+e^{(E-E_{Fn})/kT}} --(79)$$

In the case of quantum dots, we take either heavy or light holes.
6. Operating Wavelength λ:

The operating wavelength of the laser is determined by resonance condition

$$L=m\lambda/2n_r$$

Since many modes generally satisfy this condition, the wavelength for the dominant mode is obtained by determining which gives the maximum value of the value of the gain. In addition, the index of refraction, n_r, of the active layer is dependent on the carrier concentration, and knowing its dependence on the current density or gain is important. For this we need to write the continuity equation.

7.6.5 Time dependent continuity equation for carrier (n) and photon (N_{ph}) concentrations

Dependence of index of refraction on injected carrier concentration
The rate of increase in the carrier concentration in the active layer due to forward current density J can be expressed as:

$$\frac{dn}{dt} = \frac{J\eta_{\text{int}}}{qd} - \frac{(n - n_{po})}{\tau_n} - \frac{\Gamma g_m}{E}(\beta I_{sp} + I_{av}) \qquad (80A)$$

here, n_{po} is the equilibrium minority carrier concentration, τ_n is the carrier lifetime, β is the spontaneous emission coefficient which gives coupling of spontaneous power/intensity I_{sp} into a guided laser mode in the active layer, g_m is the material gain [$g_m = a\,(n - n_o) - a_2\,(\lambda - \lambda_p) \sim a\,(n - n_o)$; here a is known (as differential gain = dg/dn) and n_0 is the carrier concentration at the transparency]. $\eta_{int} = \eta_q\,\eta_{inj}$ where internal efficiency η_{int} is a product of quantum efficiency η_q and injection efficiency η_{inj}.
Eq. 80A can be simplified as

$$\frac{dn}{dt} = \frac{\eta_{\text{int}} J}{qd} - \frac{n}{\tau_n} - v_g g N_{Ph} \qquad (80B)$$

Equation 80B neglects equilibrium minority concentration n_{po}. We can neglect I_{av} which is the intensity from an external light signal (as in the case of a laser amplifier). $\beta I_{sp} g_m / E = v_g\, g\, N_{ph}$

β_{sp} is the spontaneous emission factor (or fraction of total emission coupled to the lasing mode). It is reciprocal of number of available optical modes in the band width of the spontaneous emission.

Rate equation for photon density N_{ph} is expressed in terms of rate of estimated emission R_{st}, fraction coupled to a lasing mode from spontaneous emissions $\beta_{sp} R_{sp}$. Here N_{ph}/τ_{ph} is the rate of decay of photons in the cavity via stimulated carrier recombination.

$$\frac{dN_{ph}}{dt} = \Gamma\left(R_{st} + \beta_{sp} R_{sp}\right) - \frac{N_{Ph}}{\tau_{Ph}} = \Gamma\left(v_g g N_{Ph} + \beta_{sp} R_{sp}\right) - \frac{N_{Ph}}{\tau_{Ph}} \qquad (81)$$

As can be seen that the Eqs. 80 and 81 are coupled equations and need to be solved simultaneously.

The phase condition is modified as n_r is a function of the carrier concentration n.

$L = m\,\lambda \square 2\, n_r$

Similarly the gain coefficient is a funciton of cavity index of refraction n_r.

7.6.6 Direct computation of gain dependence on photon energy

Gain coefficient can be calculated directly from the absorption coefficient and Fermi-Dirac distribution functions. However, it depends on the nature of transitions. We are considering free electron-hole and excitonic transitions. Of these the excitonic transitions are relevant in the case of wide energy semiconductors such as GaN, ZnSe, related ternary and quaternary compounds, and other low dielectric constant and wide energy gap semiconductors including organic semiconductors.

Free Carrier Transitions

A. Optical Gain in Quantum Wires

The gain coefficient due to free carrier band-to-band transitions in quantum wire lasers can be expressed by substituting for α □as:

$$g_{free}(\omega) = \frac{2\pi e^2}{\varepsilon_0 n_{rm_0} c\omega L_x} \sum_{l,h} [\frac{(2m_{eh})^{1/2}}{\pi\hbar L_y L_z} |M_b|^2 \bullet |\int \Psi_e(y)\Psi_h(y)dy|^2 \quad (82)$$
$$\bullet \int \Psi_e(z)\Psi_h(z)dz|^2 \bullet \int (E - E_e - E_h)^{-1/2} \rho(E) \bullet L(E)dE(f_e + f_h - 1)]$$

where the polarization factor ρ(E) for free carrier transition in quantum wire is taken from the literature [5]. E_e and E_h are the ground state energies for electron and hole inside the quantum wire. The summation is over the heavy hole and light hole.

B. Optical Gain in Quantum Dots

The gain coefficient in a quantum dot for free electron-hole transitions can be expressed by

$$g_{free}(\omega) = \frac{2\pi e^2}{\varepsilon_o n_r m_o c\omega} \sum_{l,h} [(\frac{2}{L_x L_y L_z}) |M_b|^2 \bullet |\int \psi_e(x)\psi_h(x)dx|^2$$
$$\bullet |\int \psi_e(y)\psi_h(y)dy|^2 \bullet |\int \psi_e(z)\psi_h(z)dz|^2 \rho(E)$$
$$\bullet \frac{1}{\sqrt{\pi}\delta} e^{[(\hbar\omega - \hbar\omega)^2/\delta^2]}] \quad \bullet (f_c + f_v - 1) \qquad (83)$$

modifying Eq. 4 (b).

Here, the polarization factor ρ(E) is for free carrier transitions and is taken from the literature [5]. The summation is over the heavy and light holes.

A. Excitonic Transitions

Optical Gain in Quantum Wire Structures

In case of quantum wires, the exciton density of states N_{ex}(wire) equals to

$2\,\pi^{1/2}\,|\phi_{ex}(0)|^2/L_yL_z$,

and the overlap function is $|\Psi_e(y)\Psi_h\ (\psi)\ \delta\psi|^2 \bullet |\ \Psi_\varepsilon(\zeta)\Psi_\eta\ (\zeta)\ \delta\zeta|^2$.Substituting the exciton density and overlap function in Eq. 3, we get

$$g_{ex}(\omega) = \frac{2\pi e^2}{\varepsilon_o n_r m_o c\omega L_y L_z} \sum_{l,h} [|M_b|^2 \bullet 2\pi^{1/2} |\phi_{ex}(0)|^2$$

$$\bullet (|\Psi_e(y)\Psi_h(y)dy|^2 |\Psi_e(z)\Psi_h(z)dz|^2) \bullet \rho_{ex} \bullet L(E_{ex}) \bullet (f_c + f_v - 1)] \tag{84}$$

Here, $|\phi_{ex}(0)|^2$ is related to a, the variational parameter or exciton radius, as $(2/\Box a^2)^{1/2}$. The details are given in our paper [3].

Optical Gain in Quantum dot Structures

In case of quantum dots, the exciton density N_{ex}(dot) is expressed as
$N_{ex}(dot) = 1/(L_x L_y L_z) = 1/[4\pi a^3{}_{Bex}]$,

and the overlap function is $|\Psi_e(x)\Psi_h(x)\,dx|^2 \bullet |\Psi_e(y)\Psi_h(y)\,dy|^2 \bullet |\Psi_e(z)\Psi_h(z)\,dz|^2$. Substituting these in Eq. 3, the excitonic gain coefficient for quantum dots is expressed by

$$g_{ex}(\omega) = \frac{2\pi e^2}{\varepsilon_o n_r m_o c\omega} \sum_{l,h} [(\frac{2}{(4\pi/3)a^3_{B,ex}}) |M_b|^2 \bullet |\int \psi_e(x)\psi_h(x)dx|^2$$

$$\bullet |\int \psi_e(y)\psi_h(y)dy|^2 \bullet |\int \psi_e(z)\psi_h(z)dz|^2 \rho_{ex}$$

$$\bullet \frac{1}{\sqrt{\pi}\delta} e^{[(\hbar\omega_{ex} - \hbar\omega)^2/\delta^2]}] \bullet (f_c + f_v - 1) \tag{85}$$

In quantum wires, we add both free and excitonic contributions. However, in the case of quantum dots, we need to consider excitonic part only.

8. Comments

i) The absorption coefficient, α_{FC} and α_{DIFF} which appear in the threshold condition represents the free carrier absorption and diffraction loss (they vary 20-40 cm^{-1} in value and do not represent interband transitions).

ii) The confinement factor depends on the waveguide construction. It's value is 2-2.5% in quantum well, wire and dot lasers.

iii) Spontaneous line width $\Delta\nu_s$ does depend on well, wire, and dots.

iv) L_x is the active layer thickness (i.e. the thickness of well in quantum well, thickness in the transverse direction in quantum wire and dots); L_y is the wire dimension along the lateral direction; and L_z refers to the dot dimension along the length of the cavity. ***Note: I have changed L_z by L_x in the threshold equation (2). It is the same as d.***

v) The quasi Fermi levels are different in three cases.

vi) For a given operational wavelength the value of material composition will be different due to shift in the energy levels.

vii) The Gain coefficient variation with λ at a given current will be different for well, wire, and dots.

viii) The quantum efficiency η_q is somewhat different. The difference is significant in heavily dislocated materials and in which exciton transitions are dominant.

Table I. Comparison of Double Heterostructure, Quantum Well, Quantum Wire, and Quantum Dot Laser Parameters

(see also Chapter 1)

<table>
<tr><td>Laser Type</td><td>Heterostructure</td><td>Quantum Well</td><td>Quantum Wire</td><td>Quantum Dot</td></tr>
<tr><td>Quantum System</td><td>3D</td><td>2D</td><td>1D</td><td>0D</td></tr>
<tr><td>Degrees of Confinement</td><td>0D</td><td>1D</td><td>2D</td><td>3D</td></tr>
<tr><td>Parameters</td><td></td><td>Strained
Unstrained</td><td>Strained
Unstrained</td><td></td></tr>
<tr><td>$\Delta\nu_s$</td><td>High</td><td colspan="3">Decreases (Good)</td></tr>
<tr><td>Γ</td><td>High</td><td>Low</td><td>Low</td><td>Low</td></tr>
<tr><td>d
Active Layer Thickness</td><td>High</td><td>Low
Good</td><td>Low
Good</td><td>Low
Good</td></tr>
<tr><td>J_{TH}</td><td>High</td><td>Low
Good</td><td>Low
Good</td><td>Low
Good</td></tr>
<tr><td>Temperature</td><td colspan="3">Reduces</td><td>No or Little</td></tr>
<tr><td>Density of State
$\int_{E_1}^{E_2} N(E)dE$</td><td>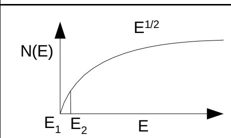

Low
$N(E)_{3D}$<</td><td>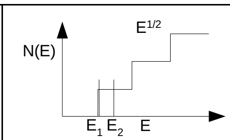

High
$N(E)_{2D}$<</td><td>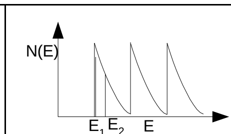

Higher
$N(E)_{1D}$<</td><td>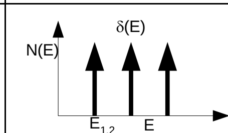

Highest
$N(E)_{0D}$</td></tr>
<tr><td>α, g</td><td>Low</td><td>High</td><td>Higher</td><td>Highest</td></tr>
</table>

The density of states values are very high in Quantum Dots.

$$N(E)_{3D} < N(E)_{2D} < N(E)_{1D} < N(E)_{0D}$$

Modeling QD Modulators and Lasers: Theoretical Approach

Calculate elastic strain in the superlattice according to lattice mismatch and obtain strain modified band gap and band offset

↓

Establish system Hamiltonian, solve Schrodinger equation and obtain electron, hole, and exciton wave functions and their energies

↓

Compute imaginary part of the dielectric constant, including excitonic transition

↓

Compute the real part of the dielectric constant using Kramers-Kronig relations

↓

Calculate index of refraction and absorption coefficient from the imaginary and real part of the dielectric constant

↓

Compute gain coefficient and threshold current density for laser structures

Source: Wenli Huang PhD Thesis, UConn, 1995

Modeling QD Lasers and Modulators: Procedure

- Modify values in *Input* files
- Run specified programs in sequence
  - **Laser gain**: *runall.c*, *well-width.c*, *exhh0.c*, *exlh0.c*, *gain.c*
  - **Modulator**: *scan.c, well-width.c, field.c, overlap.c, auto0lh.c, autolh.c, auto0hh.c, autohh.c, abs-del.c.*
- Last program requires input
- Open output data file in Excel
- Plot data in Excel

QD Laser Gain Input Parameters for ZnSe-CdSe

Electron Mass	$0.11m_0$
Light Hole Mass	$0.14m_0$
Heavy Hole Mass	$0.75m_0$
Conduction Band Offset	0.541 eV
Light Valence Band Offset	0.232 eV
Heavy Valence Band Offset	0.058 eV
Conduction to Light Hole Bandgap	1.692 eV
Conduction to Heavy Hole Bandgap	1.692 eV
Dielectric Constant	9.6

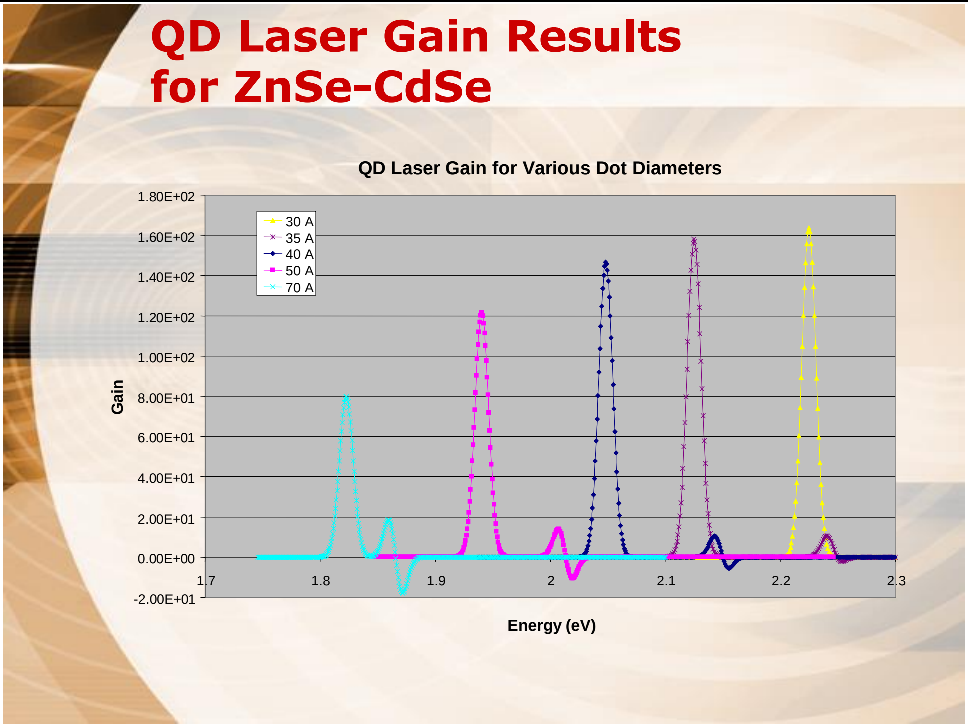

Fig. 31 Gain as a function of photon energy

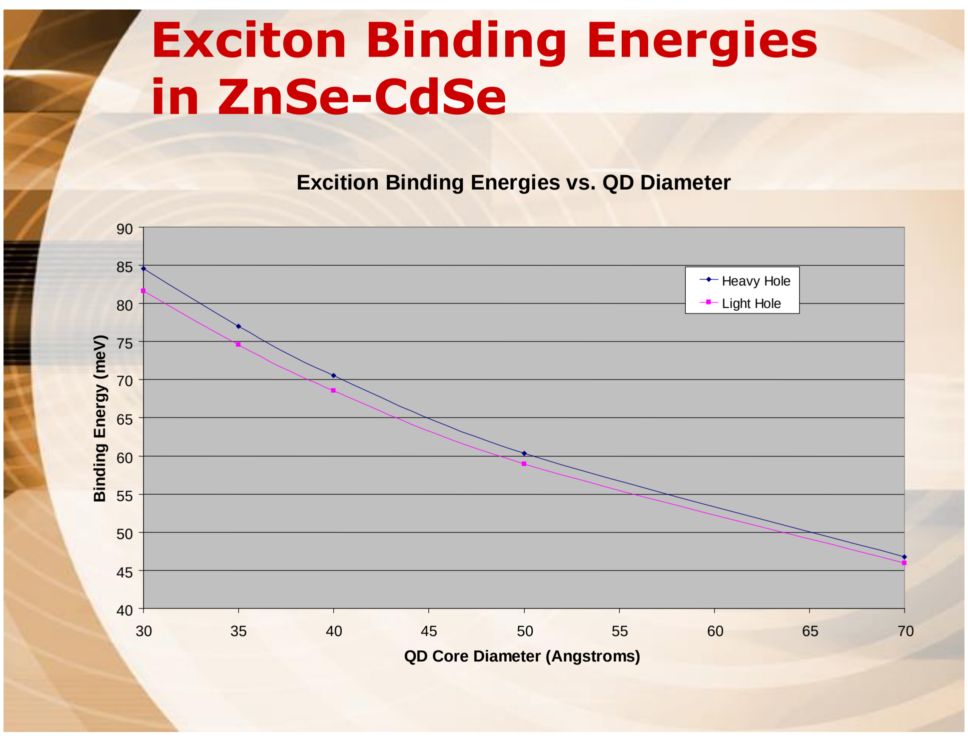

Fig. 32 Exciton binding enrgy

QD Gain Input Parameters for ZnCDSe-ZnMgSSe (No Strain)

Electron Mass	$0.16m_0$
Light Hole Mass	$0.14m_0$
Heavy Hole Mass	$0.54m_0$
Conduction Band Offset	0.576 eV
Light Valence Band Offset	0.384 eV
Heavy Valence Band Offset	0.384 eV
Conduction to Light Hole Bandgap	2.41 eV
Conduction to Heavy Hole Bandgap	2.41 eV
Dielectric Constant	9.6

QD Laser Gain Results for ZnCdSe-ZnMgSSe

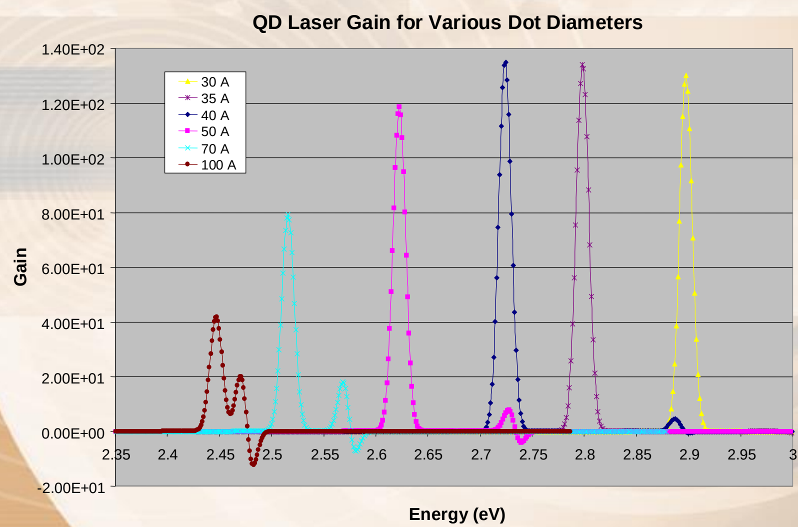

Fig. 33 Gain in ZnCdSe QWell with ZnMgSSe barrier as a function of photon energy

Exciton Binding Energies in ZnCDSe-ZnMgSSe

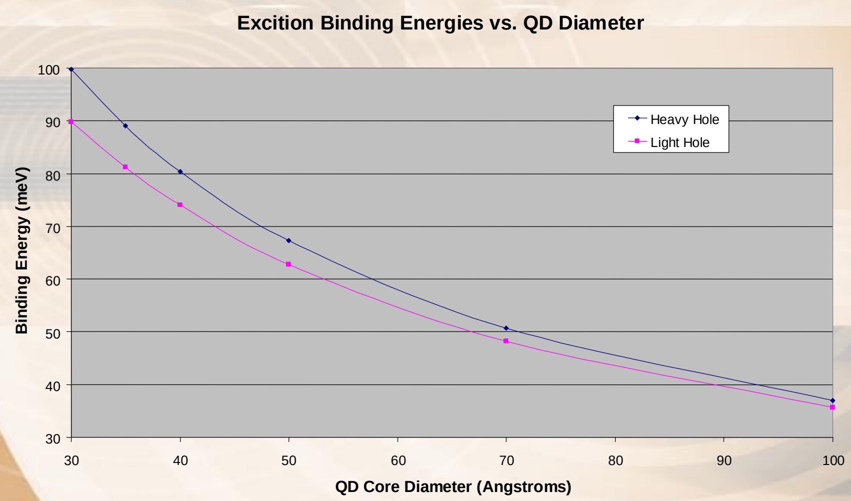

Fig. 34 Exciton binding energy as a funciton of quantum dot diameter.

Adjusting the Valence Band Fermi Level

- For each of the QD core diameters, the Fermi level of the valence band was adapted so as to produce a single gain peak.
  - This became progressively more difficult to accomplish as the core diameter was increased.

QD Diameter (Å)	30	35	40	50	70	100
ZnSe-CdSe Fermi Level (eV)	0.16	0.13	0.105	0.07	0.03	-
ZnCdSe-ZnMgSSe Fermi Level (eV)	0.23	0.20	0.17	0.11	0.03	0.011

QD Modulator: Input Parameters

Electron Mass	$0.19m_0$
Light Hole Mass	$0.17m_0$
Heavy Hole Mass	$0.78m_0$
Conduction Band Offset	0.443 eV
Light Valence Band Offset	0.286 eV
Heavy Valence Band Offset	0.296 eV
Conduction to Light Hole Bandgap	2.935 eV
Conduction to Heavy Hole Bandgap	2.935 eV
Intervalley Relaxation Time	3.6×10^{-13} s
Orbit-spin Splitting Delta	0.34 eV
Dielectric Constant	7.84

QD Modulator Results: Absorption for 30Å QDs

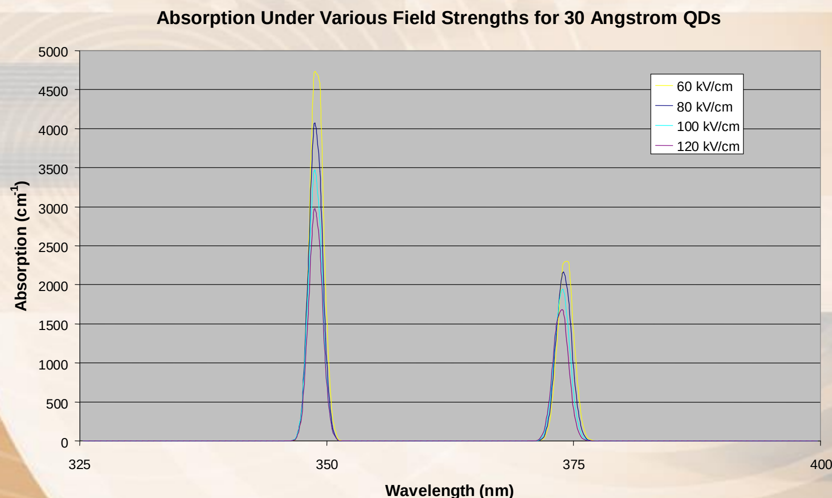

Fig. 35 Absorption coefficient in a layer of Quantum dots as a funciton of photon energy.

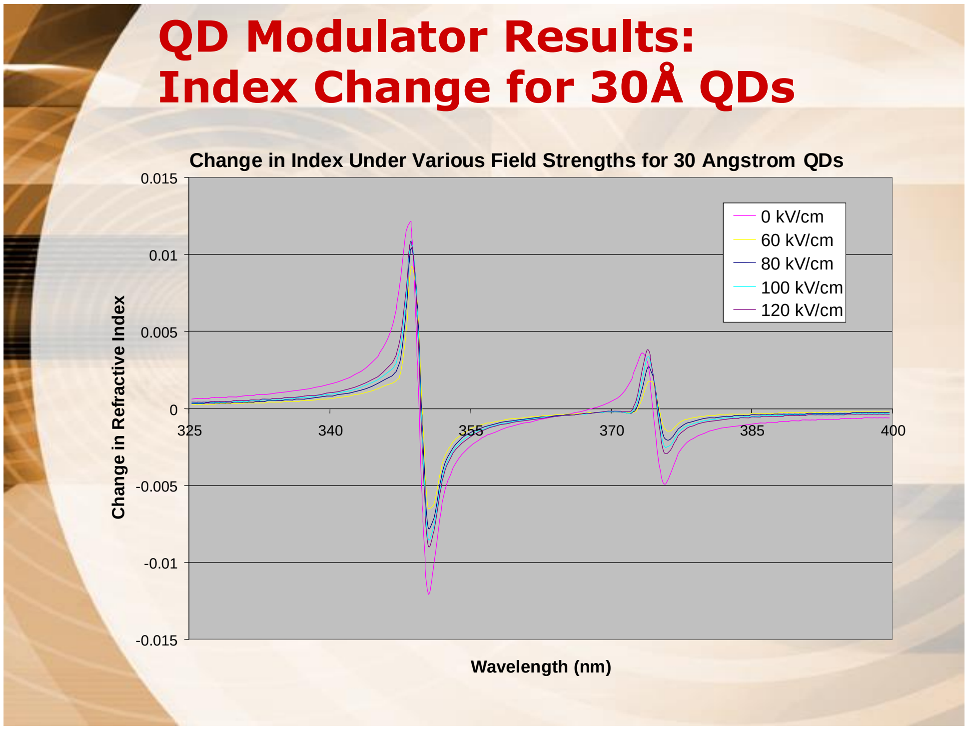

Fig. 36 Change in index of refraction in an optical modulator as a function of wavelength.

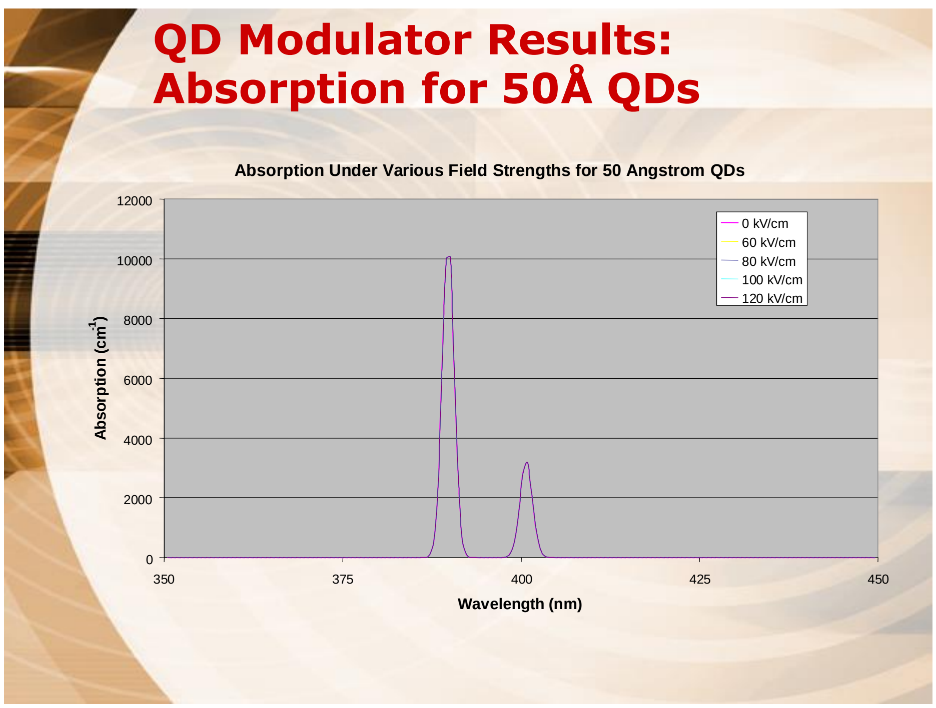

Fig. 37 Absorption coefficient in quantum dot layer as a function of photon energy.

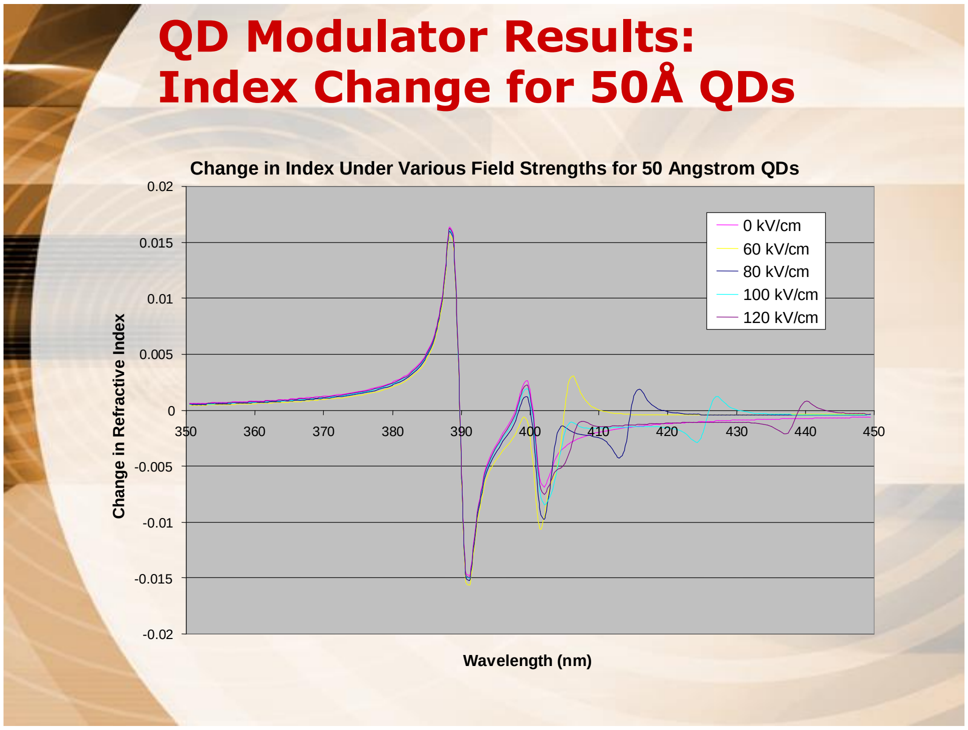

Fig. 38 Index of refraction change (at different electric field) as a function of photon energy.

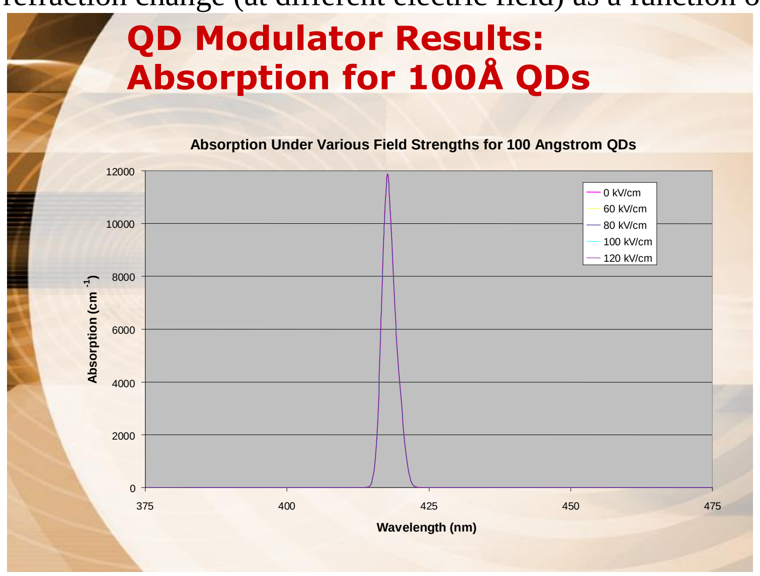

Fig. 39 Absorption coefficient in 100 A quantum dot layer as a function of photon energy.

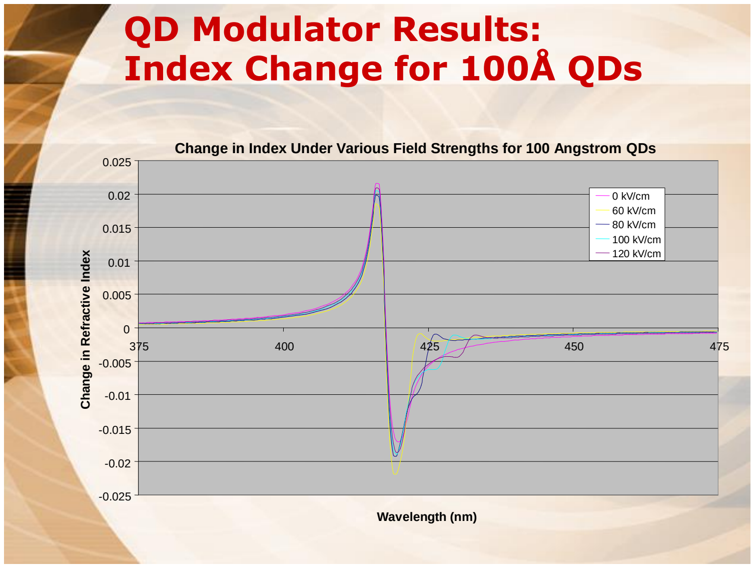

Fig. 40 Index of refraction change (at different electric field) in a 100 angstrom dia QD layer.

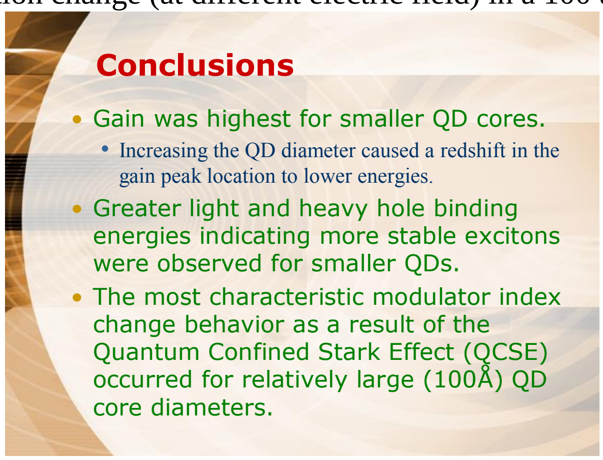

7.7 Design of Quantum Well/Dot LASERS-Level 3

Design a single mode Double Heterostructure laser operating at 1.35 micron using InGaAsP-InP material system. A 1 mW optical power output is needed.

Q.1. Find the composition f the active layer for the 1.35 micron laser configured as a Quantum dot laser using InGaAsP-InP system. Given: Use of following equation to find E_g:
$h\nu = >1.24/1.35\mu m = E_g + E_{e1} + E_{hh1} + 0.0006$ (in eV)
Table I and II give the value of energy levels in a Dot of 50A: E_{e1} =0.174 and E_{hh1}=0.042 eV

E_g= < 0.919 – 0.174 – 0.042 – 0.0006 = 0.7024eV

Active layer composition is obtained by intersection of a line at 0.70eV on y-axis and InP square on the x-axis. The point is B. Its composition is $In_{0.53}\ Ga_{0.47}As$.

Barrier composition: Barrier composition is obtained by adding 0.5eV to the active layer band gap. This is point C. Its composition is ***$In_{0.9235}\ Ga_{0.0765}As_{0.163}P_{0.837}$***

Use two or three layers of dots separated by InGaAsP barriers of 100Angstroms on either side. The active layer thickness is 50x3 + 2x 100(inter-dot barrier + 2x150 Outer barriers) =650 Angstrom = 0.065 microns.

Barrier index of refraction should be smaller by at least 0.01 – 0.005 than dot material.

Cladding composition: Energy gap should be higher than barrier and index should be smaller. If we add 0.5eV to the barrier energy gap, we obtain 1.2 + 0.5 =1.7eV. Now the material gets out of InGaAsP material system. So we go to a lattice matched ZnSeTe cladding layer. One can also use InP. The cladding composition is about $ZnSe_{0.5}\ Te_{0.5}$.

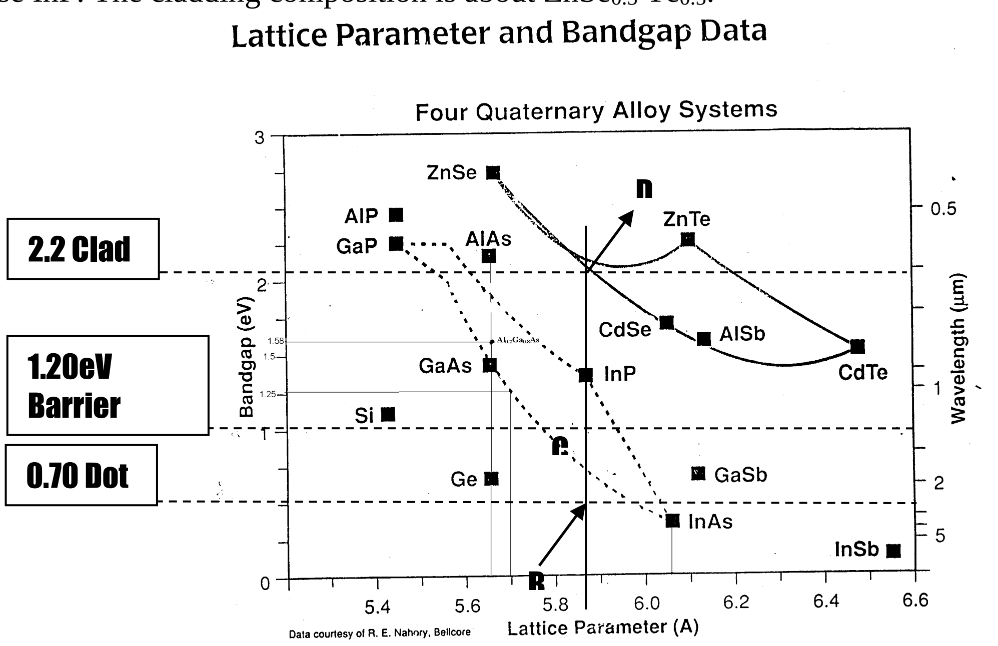

Fig .41 Band gap as a function of material composition and lattice parameter.

Be quantitative where possible.

⇒a. Outline all the design steps

⇒What would you do to obtain single transverse mode and single lateral mode operation?

⇒b. Show device dimensions (active layer thickness d, cavity length L and width W), doping levels of various layers constituting the laser diode (shown below in Fig. 1).

HINT: Active layer thickness d **to yield single transverse mode d < m λ/[2(n_r^2-n_{r1}^2)$^{1/2}$], m=1, 2, 3,**

Top contact (stripe) width W for single mode:[**W < m λ/[2($n_{r,center}^2$-$n_{r,corner}^2$)$^{1/2}$], m=1, 2; if you cannot find it use W=5 μm]; Use $n_{r,center}$ –$n_{r,corner}$ ~0.005 in gain guided lasers.**

Cavity length L=? (You select L such that it will result in the desired J_{TH} and optical power output).

⇒Find the confinement factor Γ. Use for Γ:

$\Gamma = 2\pi^2 d^2 (n^2{}_{active} - n^2_{clad})/\lambda^2$. **(λ is the free space wavelength.)**

⇒Find threshold current density and show that it is under **200 A/cm²**; explain if it is not.

⇒c. Analyze the designed structure and evaluate various parameters such as mode separation Δλ and Δv.□□□

⇒d. Find the beam divergence in the junction plane $\theta_{\|}$ and perpendicular to the junction plane $\theta_{\perp}$ □□$[= 4.0(n^2{}_{active} - n^2_{clad})d/\lambda]$,

⇒e. Find operating current I_{op} and voltage V_{op} required to obtain 10mW laser output power.

The index of refraction equation $In_xGa_{1-x}As_yP_{1-y}$ is

$n(x,y) = 3.52xy + 3.39x(1-y) + 3.60y(1-x) + 3.56(1-x)(1-y)$.

Select d and W for single transverse mode and lateral mode, respectively.

Assume: $\frac{dn_r}{d\lambda}$ =1.5 μm^{-1}, Spontaneous line width Δ□$_s$ = 6x10^{12} Hz and Z (T) ≈0.5.

Internal Quantum efficiency = η_q = 0.9

Absorption coefficient $\alpha=\alpha_{Diffraction} + \alpha_{Free\ carrier} + \alpha_{scattering}$ =20 cm^{-1}

Electron effective masses m_n = 0.067m_o, heavy hole mass m_p = 0.62m_o,

Determine the end reflectivity R_1, R_2. (If you cannot find them, use R_1=R_2=0.3)

Minority hole lifetime □$_p$ =5x10^{-9} sec Minority electron lifetime □$_n$ =1x10^{-8} sec

Hole diffusion coefficient D_p=10 cm²/s Electron diffusion coefficient D_n=50 cm²/s

Find n_i in the active layer from the energy gap of the active layer.

Table Needed for Quantum Well/Dot laser design only.

Electron_Mass (m_n) well/dot	0.067
Heavy_Hole_Mass (m_{HH}) well/dot	0.62
Conduction_Band_Offset_(delta_Ec)	0.3 eV (Calculate)
Light_Hole_Valence_Band_Offset_(delta_Ev)	0.2 eV(Calculate)
Heavy_Hole_Valence_Band_Offset_(delta_Ev)	0.05805 eV
Width_of_the_Quantum Dot/Quantum Box	50Å
Dielectric_Constant calculate	12.32 F/m
Conduction_to_light_hole_gap	Eg_{hh}+ 0.2 eV
Conduction_to_heavy_hole_gap	Eg

Quantum Well/DOT: The quantum well levels are given below for two different barrier layer energy gaps, that is when ΔE_g (between well and barrier) is 0.2eV and when □E_g = 0.5eV. Assume ΔE_c=0.6 * ΔE_g.

The quantum dot levels are also listed (simply well levels multiplied by 3). The cladding layer should have a higher energy gap then the barrier adjacent to the quantum dots. Use ZnSeTe for cladding layers with a band gap E_g = 2.31eV and a dielectric constant of 8.5.

Table I: Well/Dot Energy Levels

Well-Barrier Difference	Electron Level in well (50A°)	Heavy hole Level in well (50A°)	Electron Level in Dot (50A°)	Heavy hole Level in Dot (50A°)
ΔE_g=0.22eV	Ee_1=.058eV	E_{h1}=.014eV	Ee_1=.174eV	E_{h1}=.042eV
ΔEg=0.5eV	Ee_1=.085eV	E_{h1}=.016eV	Ee_1=.255eV	E_{h1}=.048eV

Table II: Well Barrier Parameters

Elecron Mass in barrier(m_{nb})	0.08
Hole Mass in barrier(m_{hb})	0.58
Electron_Mass (m_n) in well	0.067
Heavy_Hole_Mass (m_{HH}) in well	0.62
Conduction_Band_Offset_(delta_Ec) for ΔEg=0.22eV	0.13 eV
Heavy_Hole_Valence_Band_Offset_(delta_Ev) for ΔEg=0.22eV	0.088 eV
Dimension of_the_Dot	50Åx50Åx50Å
Conduction_Band_Offset_(delta_Ec) for ΔEg=0.5eV	0.3 eV
Heavy_Hole_Valence_Band_Offset_(delta_Ev) for ΔEg=0.5eV	0.2 eV

HW 9S **LASER Design-I Supplementary Information for regular DH laser (no quantum well etc.)** F. Jain

⇒(a) Find active layer composition (doping is given), cladding layers doping (thickness is given). Use hv= E_g + kT/3.

⇒(b). Find active layer thickness d and stripe width W to obtain single transverse mode and single lateral mode, respectively. **Show these values (part a and b) using Fig. 1.**

⇒

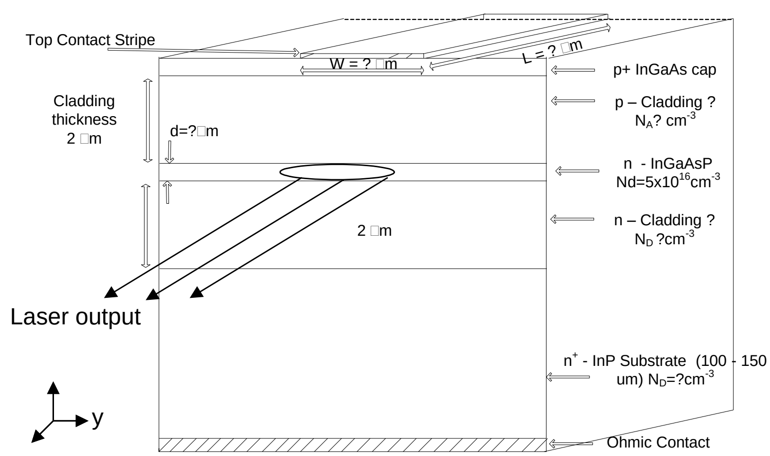

Fig. 42. Laser structure (fill in values)

⇒(c). Find the transverse confinement factor Γ. Use one of the two relations for Γ:

(1) $\Gamma = 2\pi^2 d^2 (n^2{}_{active} - n^2_{clad}) / \lambda^2$. **(λ is the free space wavelength.)**

(2) (3) $\Gamma = \dfrac{V^2}{2+V^2} = \dfrac{0.10726}{2.10726}$

$$V^2 = \frac{4\pi(d^2)(n^2_{active} - n^2_{cladding})}{\lambda^2}$$

⇒(d). Select of cavity length L and find the threshold current density J_{TH} and show that it is under **200 A/cm^2**; explain if it is not.

⇒(e). Evaluate mode separation $\Delta\lambda$ and $\Delta\nu$.

⇒(f) Find the beam divergence in the junction plane $\theta_{\parallel}$ and perpendicular to the junction plane $\theta_{\perp}$ □□[$= 4.0(n^2_{active} - n^2_{clad})d / \lambda$],

⇒(g). Find operating current I_{op} and voltage V_{op} required for obtaining 1mW laser output power.

HINT: Active layer thickness d **to yield single transverse mode d < m $\lambda/[2(n_r^2 - n_{r1}^2)^{1/2}]$, m=1, 2, 3,**

Top contact (stripe) width W for single mode:[**W < m $\lambda/[2(n_{r,center}^2 - n_{r,corner}^2)^{1/2}]$, m=1, 2; if you cannot find it use W=5 μm]; Use $n_{r,center} - n_{r,corner}$ ~0.005 in gain guided lasers.**

Select d and W for single transverse mode and lateral mode, respectively.

Cavity length L=? (You select L such that it will result in the desired J_{TH} and optical power output.

Given: InGaAsP energy band (see Fig. 2). The index of refraction equation $In_xGa_{1-x}As_yP_{1-y}$ is
$n(x,y) = 3.52xy + 3.39x(1-y) + 3.60y(1-x) + 3.56(1-x)(1-y)$.

$\frac{dn_r}{d\lambda}$ =1.5 μm^{-1}, Spontaneous line width $\Delta\nu_s = 6\text{x}10^{12}$ Hz, Z (T) ≈0.5, Internal Quantum efficiency = η_q = 0.9; Absorption coefficient $\alpha = \alpha_{Diffraction} + \alpha_{Free\ carrier} + \alpha_{scattering}$ =20 cm^{-1}

Electron effective masses $m_n = 0.067m_o$, heavy hole mass $m_p = 0.62m_o$,

N-Active layer	**P-Cladding layer**
Doping n-type 5x1016cm-3	Find N_A based on Bernard-Duraffourg condition
Minority hole lifetime τ_p =5x10^{-9} sec	Minority electron lifetime τ_n =1x10^{-8} sec
Hole diffusion coefficient D_p=10 cm^2/s	Electron diffusion coefficient D_n=50 cm^2/s

Find n_i in the active layer from the energy gap of the active layer.

N-type bottom cladding layer: Find N_D based on Bernard-Duraffourg condition.**Substrate n+ InP doping ~10^{19}cm^{-3}. Determine** the end reflectivity R_1, R_2. (If you cannot find them, use $R_1=R_2=0.3$).

Finding the energy levels in a quantum well: Once we know the well, we can find QDot levels

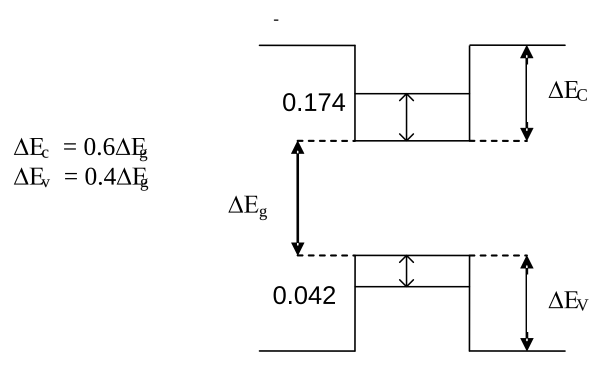

Fig. 43. Energy levels in a finite quantum well.

$E_{gBarrier} - E_{g\ cladding} = \Delta E_g = 0.5$

$\Delta E_c = 0.6\Delta E_g = 0.3eV$, and $\Delta E_v = 0.4\Delta E_g = 0.2eV$

$$h\upsilon > E_g + 3Ee_1 + 3E_{hh1}$$

$$0.919eV > E_g + 0.174 + 0.042$$

$$0.919 - 0.174 - 0.042 > E_g$$

Active Layer $E_g < 0.703$

$$E_{fn} - E_{fp} > 0.703eV > E_g$$

$$E_g \approx 0.7$$

From band gap-lattice constant plot, 0.7eV corresponds to

$In_xGa_{1-x}AsP_{1-y}$;Y=1 X=0.53

$$In_{0.53}Ga_{0.47}As$$

Barrier Layer $E_{g\ Barrier}$ =0.7+0.5=1.2eV and the material is InGaAsP

This corresponds to the point 'C' which is 19 division above point B (while InP is above 27 division) $In_{0.86}Ga_{0.14}As_{0.3}P_{0.7}$

Refractive Index of dot layer (x=0.53; y=1)

n_r = 3.52xy + 3.39 (1-y) + 3.6y (1-x) + 3.56 (1-x) (1-y)

$n_{r(dot)=}$ 3.52*0.53*1+3.39*0.53*0+3.6*1*(1-0.53) = 1.8656+1.692 = 3.5576

Refractive Index of Barrier (x=0.86;y=0.30)

n_r = 3.52xy + 3.39 (1-y) + 3.6y (1-x) + 3.56 (1-x) (1-y)

$n_{r(Barrier)}$=3.52*0.86*0.30+3.39*0.86*(1-0.30)+3.6*0.30*(1-0.86)+3.56(1-0.86)(1-0.30) = 3.448

Effective refractive index of composite active layer =3.49

[(index of dot + 2x index of barrier)/3]. Barrier is taken to tbe twice as thick. This can be modified depending on the approximation.

Upper and lower cladding layers:

The cladding has a lower index of refraction than active layer. Also it needs to have a higher band gap for carrier injection and confinement as well as lower index of refraction for the confinement of photons.

The cladding energy gap E_g(Clad) = E_g(barrier) + 0.5eV=1.2 + 0.5 = 1.7eV.

This energy gap is more than the InGaAsP ternary material system.

For lattice matching, we select ZnSeTe cladding.

$$n_{clad} = \sqrt{8.5} = 2.915,\ E_g = 2.20eV,\ E_{gClad} - E_{gBarrier} = 2.20 - 1.2 = 1.0eV$$

ΔE_c = 0.6*1.0 =0.6 eV and ΔE_v = 0.4*1.0 =0.4 eV

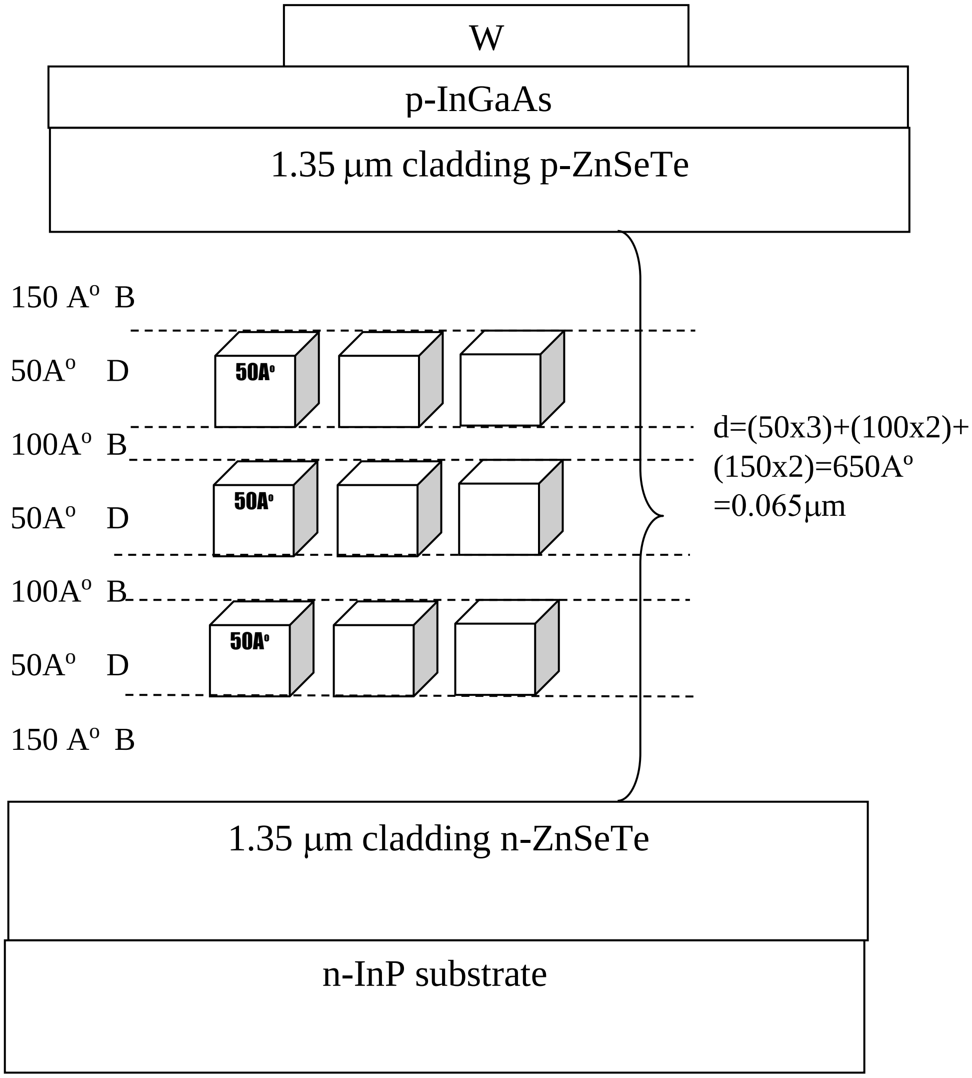

Fig. 44 Active layer thickness: d = (50x3) + (100x2)+(150x2) =650A°=0.065μm. D for dot and B for barrier.

Active layer index of refraction; Average of barrier and dot core.

Intrinsic carrier concentration in the active layer:

$$n_i(active) = 10^7 * \frac{e^{-(0.7/2kT)}}{e^{-(1.43/2kT)}}$$

$$= 10^7 * e^{(1.43-0.7)/2kT} = 10^7 * e^{(0.73)/2*0.0259}$$

$$= 1.319 * 10^{13} \text{ cm}^{-3}$$

From Bernard-Durafourg condition

$$n_e = n_i e^{(E_{fn} - E_{fp})/2kT}$$

$$=1.319 * 10^{13} * e^{(0.702)/2*0.0259}$$

$$=1.12*10^{19} \text{ cm}^{-3}$$

Cladding doping > $1.12*10^{19}$ cm $^{-3}$

Single Traverse mode

$$d < \frac{m\lambda}{2\sqrt{n_r^2\big|_{active} - n_r^2\big|_{clad}}}$$

$$d < \frac{m \times 1.35\mu m}{2\sqrt{(3.490)^2 - (2.915)^2}}$$

$$d < \frac{1.35\mu m}{2\sqrt{12.18 - 8.5}}$$

$$d < \frac{1.35\mu m}{2 \times 1.918} = 0.351$$

The value of d=0.065μm meets this requirement. **Single lateral mode:**

$$W < \frac{m\lambda}{2\sqrt{n_r^2\big|_{MiddleOfGainRegionInActiveLayer} - n_r^2\big|_{CornerOfActiveLayerAwayFromWhereGainIsSmall}}}$$

$$W < \frac{1.35\mu m}{2\sqrt{(3.490)^2 - (3.485)^2}}$$

$$W < \frac{1.35\mu m}{2\sqrt{0.005 \times (3.490 + 3.485)}}$$

$$W < \frac{1.35\mu m}{2\sqrt{.034878}}$$

$$W < 3.61$$

So we take W= 3 μm

$$J_{th} = \frac{8\pi n_r^2 q d \Delta\upsilon_s}{\Gamma \eta_q Z(T)} \left(\frac{1}{\lambda^2}\right)\left(\alpha + \frac{1}{2L}\ln\left(\frac{1}{R_1 R_2}\right)\right)$$

d=0.065μm

W=3μm

L=500μm

n_q=0.9

Z(T)=0.5

$\Delta\nu_s = 6 \times 10^{12}$ Hz

$n_{ractive}$=3.4903

Γ =0.05 See calculations on the next page.

α=20 cm^{-1}

$$R = R_1 = R_2 = \left(\frac{n_r\big|_{active} - n_{air}}{n_r\big|_{active} + n_{air}} \right)^2$$

$$= \left(\frac{3.490 - 1}{3.490 + 1} \right)^2 = \left(\frac{6.20}{20.16} \right)$$

R=0.307=0.31

$$\frac{1}{2L} \ln\left(\frac{1}{R_1 R_2} \right) = \frac{1}{2x500x10^{-4}} \ln \frac{1}{0.318^2} = 23.4cm^{-1}$$

$$\alpha + \frac{1}{2L} \ln\left(\frac{1}{R_1 R_2} \right) = 20 + \frac{1}{2x500x10^{-4}} \ln \frac{1}{0.318^2} = 43.4cm^{-1}$$

The confinement factor is given by:

$$\Gamma = \frac{V^2}{2 + V^2} = \frac{0.1072}{2.1072} = 0.05$$

Here,

$$V^2 = \frac{4\pi (d^2)(n_{active}^2 - n_{cladding}^2)}{\lambda^2}$$

$$V^2 = \frac{4\pi (.065\mu m)^2 (3.490^2 - 8.5)}{(1.35\mu m)^2}$$

$$V^2 = 0.1072$$

The threshold current density is

$$J_{th} = \frac{8\pi * 12.82 * 1.6 * 10^{-19} * 0.065\mu m * 6 * 10^{12}}{0.05 * 0.9 * 0.5 * (1.35\mu m)^2} * 43.4 = 212.79 A/cm^2$$

This current density is greater than 200 A/cm^2. So we want to reduce it. One way is to increase the cavity length to 600microns. This now results in

$$\alpha + \frac{1}{2L} \ln\left(\frac{1}{R_1 R_2} \right) = 20 + \frac{1}{2x600x10^{-4}} \ln \frac{1}{0.318^2} = 39.5cm^{-1}$$

This gives a new J_{th} = old J_{th} x (39.5/43.4) = 174 A/cm^2.

$$I_{th} = W * L * J_{th} = 3 * 10^{-4} * 600 * 10^{-4} * 174 = 3.13mA$$

Operating Current I_{op} for 1.0mW power output

$$PowerOutput = \frac{(I - I_{th})\eta_{\text{int}} h\upsilon}{q} \frac{\frac{1}{2L} \ln\left(\frac{1}{R_1 R_2} \right)}{\alpha + \frac{1}{2L} \ln\left(\frac{1}{R_1 R_2} \right)}$$

$\eta_{int} = \eta_q * \eta_{inj} \approx 0.9$

$$1.0mW = \frac{(I - 3.13mA) \times 0.9}{1.6 \times 10^{-19}} \times \frac{19.5}{39.5} \times .919eV$$

$$I = 3.13mA + \frac{1.0\times10^{-3}\times1.6\times10^{-19}\times39.5}{0.9\times19.5\times0.919\times1.6\times10^{-19}}$$
$$= 3.13mA + 2.449mA$$
$$I_{0p} = 5.579mA.$$

V_{op} is 0.371V to be calculated below:

$$I = I_s\left(e^{\frac{qv_{applied}}{kT}} - 1\right)$$

$$I_s \cong \frac{qAD_n n_{p0}}{L_n} + \frac{qAD_p p_{n0}}{L_p} \cong \frac{qAD_n n_{p0}}{L_n}$$

L_n=7.07*10^{-4}cm; D_n=50cm^2/s;s $\tau_n = 10^{-8}S$; A=W*L=1500*10^{-8}cm^2 ;

$n_p = \frac{(1.3\times10^{13})^2}{10^{16}} = 1.93\times10^{10}$, here the active layer background doping is 10^{16}cm-3.

$$I_s = \frac{1.6*10^{-19}*1500*10^{-8}*50*1.93*10^{10}}{7.07*10^{-4}} = 3.2758*10^{-9}\,Amp$$

The operating voltage V_{op} to obtain 1mW output laser power is:

$$V_{applied} = \frac{kT}{q}\ln\left(\frac{I+I_s}{I_s}\right) = 0.0259\ln\left(\frac{5.579\times10^{-3}}{3.27\times10^{-9}}\right) = 0.371V$$

Mode separation and beam divergence $\Delta\lambda, \Delta v, \theta_\perp, \theta_{11}$

$$\Delta\lambda = \pm\frac{\lambda^2}{2Ln_r}\left(1 - \frac{\lambda}{n_r}\frac{dn_r}{d\lambda}\right)^{-1}$$
$$= \frac{(1.35*\mu m)^2}{2*600*\mu m*3.490}\left(1 - \frac{1.35\mu m}{3.490}*1.5\mu m^{-1}\right)^{-1} = \frac{(1.35)^2*10^{-8}}{1200*10^{-4}*3.490}\left(1 - \frac{1.35\times1.5}{3.490}\right)^{-1}$$
$$= 0.0435x10^{-6}(1-0.582)^{-1}$$
$$= 1.0366*10^{-7}\,\text{cm}$$
$$= 10.366\,\text{Å}$$
$$\Delta\upsilon = v_1 - v_2$$
$$= \frac{c}{\lambda_1} - \frac{c}{\lambda_2}$$
$$= 3*10^{10}*\left(\frac{1}{\lambda_1} - \frac{1}{\lambda_2}\right)$$
$$\Delta\upsilon = \frac{c\Delta\lambda}{\lambda^2} = \frac{3*10^{10}*10.366*10^{-8}}{(1.35*10^{-4})^2} = 170.6GHz$$
$$\theta_\parallel = \frac{\lambda}{w} = \frac{1.35\mu m}{3.0\mu m} = 0.45*\frac{180}{\pi} = 25.78^\circ$$
$$\theta_\perp = \frac{4.0(n^2{}_{active} - n^2{}_{clad})d}{\lambda} = \frac{4.0*4.0576*0.065\mu m}{1.35\mu m} = 0.781radians = 44.7^\circ$$

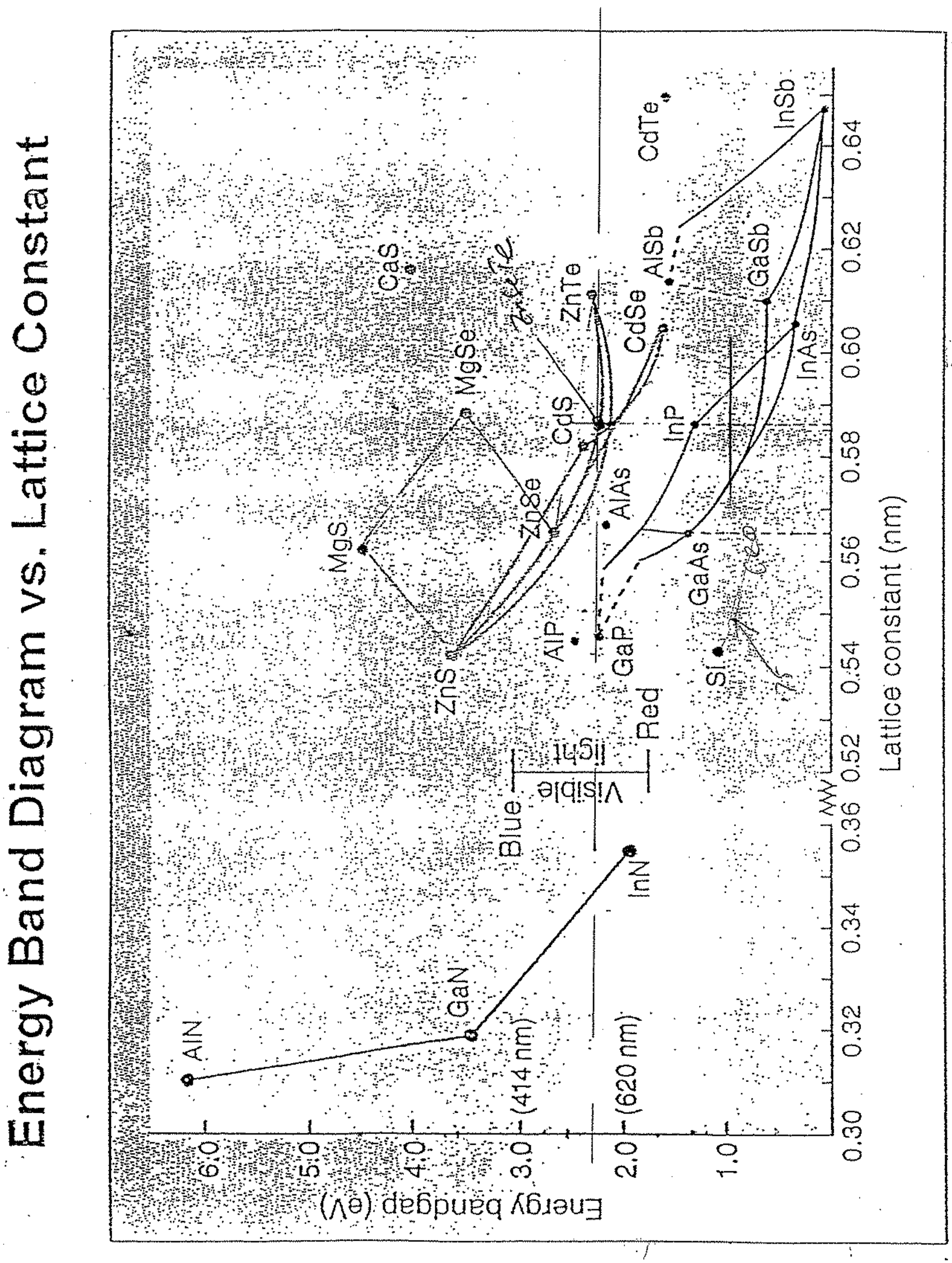

Fig. 45 Energy band diagram showing AlN-GaN-InN system.

How to Find Electron and Hole Energy Level

$E_c = 0.6\ E_g$
$E_v = 0.4\ E_g$

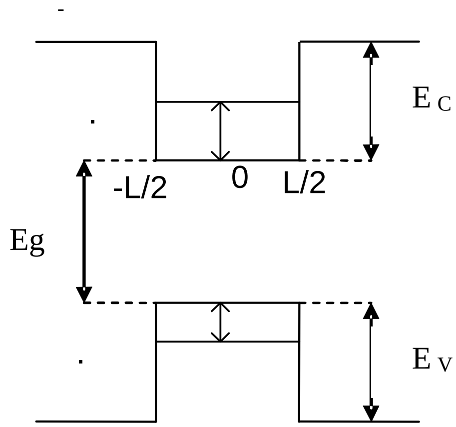

Schrödinger equation:

$$\left[-\frac{\hbar^2}{2m}\nabla^2 + V(z)\right]\psi(x,y,z) = E\phi(x,y,z) \qquad \textbf{(1)}$$

The Schrödinger equation in a system with multiple layers. (the m_e values are different in the well (m_{ew}) and barrier (m_{eb})):

$$\left[-\frac{\partial}{\partial z}\frac{1}{m}\frac{\partial}{\partial z} + V(z)\right]\phi(z) = E\phi(z) \qquad \textbf{(2)}$$

Schrodinger equation in a well:

$$-\frac{\hbar^2}{2m_{ew}}\frac{\partial^2\varphi(z)}{\partial z^2} = E\phi(z)$$

$$\frac{\partial^2\varphi(z)}{\partial z^2} = -\frac{2m_{ew}}{\hbar^2}E\phi(z)$$

$$= -k^2\phi(z) \qquad \textbf{(3)}$$

$$k^2 = \frac{2m_{ew}E}{\hbar^2} \qquad \textbf{(4)}$$

Boundary Conditions (BC)

$$\text{BC\#1.}\quad \phi\left(z = \frac{L^+}{2}\right) = \phi\left(z = \frac{L^-}{2}\right) \qquad \textbf{(5)}$$

$$\text{BC\#2.}\quad \frac{1}{m_{eb}}\frac{d}{dz}\phi\left(z=\frac{L^{+}}{2}\right)=\frac{1}{m_{ew}}\frac{d}{dz}\left(z=\frac{L^{-}}{2}\right) \quad \textbf{(6)}$$

$$-\frac{L}{2}<z<\frac{L}{2}$$

In the well the solution of Equation (3) is:

$$\phi(z)=C_2\cos kz+C_2^{'}\sin kz \quad \textbf{(7)}$$

Even Wavefunction: $\phi(z)=C_2\cos kz$ **(7a)**

Odd Wavefunction: $\phi(z)=C_2^{'}\sin kz$ **(7b)**

In the barrier $\left(|z|>\frac{L}{2}\right)$, Equation (2) reduces to:

$$\left[-\frac{\hbar^2}{2m_{eb}}\frac{\partial^2\phi(z)}{\partial z^2}+V_0\phi(z)\right]=E\phi(z)$$

$$-\frac{\hbar^2}{2m_{eb}}\frac{\partial^2\phi(z)}{\partial z^2}+(V_0-E)\phi(z)=0,\ \text{where}\ V_0=\Delta E_C$$

$$\frac{\partial^2\phi}{\partial z^2}=+\frac{2m_{eb}}{\hbar^2}(V_0-E)\phi(z) \quad \textbf{(8)}$$

$$\alpha^2=\frac{2m_{eb}(V_0-E)}{\hbar^2} \quad \textbf{(9)}$$

For $z>\frac{L}{2}$, the solution is: $\phi(z)=C_1e^{-\alpha\left(z-L/2\right)}+C_1^{'}e^{+\alpha\left(z-L/2\right)}$

At $z=\infty$, the second term becomes infinite. For a physical solution $C_1^{'}=0$, therefore:

$$\phi(z)=C_1e^{-\alpha\left(z-L/2\right)}\ \text{for}\ z>\frac{L}{2}$$

$$\text{or}\ \phi(z)=C_1e^{+\alpha\left(z+L/2\right)}\ \text{for}\ z<\frac{-L}{2}$$

Evaluation of C_2, C_1 for even wave function

First boundary condition, Equation (5):

$$\phi\left(z=\frac{L^+}{2}\right)=\phi\left(z=\frac{L^-}{2}\right)$$

$$C_1 e^{-\alpha\left(\frac{L}{2}-\frac{L}{2}\right)}=C_2\cos kz$$

$$C_1=C_2\cos k\frac{L}{2} \qquad \textbf{(10)}$$

Using the second boundary condition,

$$\left.\frac{1}{m_{eb}}\frac{d}{dz}C_1 e^{-\alpha\left(z-L/2\right)}\right]_{z=\frac{L}{2}}=\left.\frac{1}{m_{ew}}\frac{d}{dz}C_2\cos kz\right]_{z=\frac{L}{2}}$$

$$\frac{1}{m_{eb}}C_1(-\alpha)=-\frac{1}{m_{ew}}C_2 k\sin k\frac{L}{2}$$

$$C_1=C_2\frac{m_{eb}}{m_{ew}}\frac{k}{\alpha}\sin k\frac{L}{2} \qquad \textbf{(11)}$$

Dividing (11) by (10), we get the Eigen value equation:

$$1=\frac{m_{eb}}{m_{ew}}\frac{k}{\alpha}\tan\frac{kL}{2}$$

Eigen value equation: $$\tan\frac{kL}{2}=\frac{m_{ew}}{m_{eb}}\frac{\alpha\frac{L}{2}}{k\frac{L}{2}} \qquad \textbf{(12)}$$

Odd wave function Eigen equation is:

$$\cot k\frac{L}{2}=-\frac{m_{ew}}{m_{eb}}\left(\frac{\alpha L/2}{k L/2}\right) \qquad \textbf{(13)}$$

From equation (12)

$$\alpha = \frac{m_{eb}}{m_{ew}}\sqrt{\frac{2*m_{ew}E}{h^2}}*\tan\sqrt{\frac{2*m_{ew}E}{h^2}}*\frac{L}{2} \qquad \textbf{(14)}$$

By ploting equation (9) and (12) we will get the energy levels.

The points of intersection are obtained by using Matlab program:

```
%CONSTANTS
h=6.626e-34/(2*3.14);
q = 1.6e-19;
l=50e-10;
m0=9.109e-31;


%For electrons

V0=0.132*q;
mb=0.08*m0;
mw=0.067*m0;

%e1=0:0.001:1
%e2=0:0.001:1

e1=0:0.001:0.0925
e2=0:0.001:0.0925

alpha1=(mb/mw)*sqrt((2.*mw.*e1.*q)/h^2).*tan(sqrt((2.*mw.*e1.*q)./h^2)*(l/2));
alpha2=sqrt(2*mb*(V0-(e2*q))/h^2);
plot(e1,alpha1,e2,alpha2)
xlabel('EV (eV)');
ylabel('Alpha');
title('Alpha Vs Ev (eV) For Electrons');
```

I. For Well-Barrier Difference (ΔEg=0.22eV)

Figs. 46a shows electron energy level in well (50A°):- Ee_1=.058eV.

Figs. 46b shows hole energy level in well (50A°):- Ehh_1=.014eV.

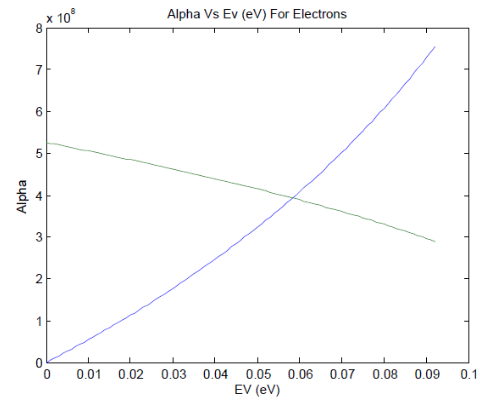

Fig.46a : Electron Level in well (50A°):- Ee_1=.058eV

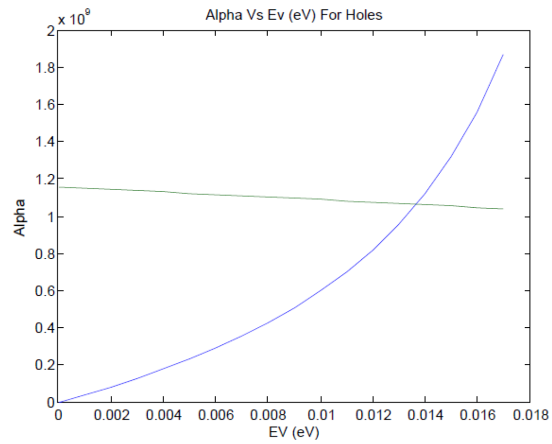

Fig. 46b Heavy hole Level in well (50A°):- E_{h1}=.014eV

II. Well-Barrier Difference ΔE_g=0.5eV

The energy levels are different if the barrier height is different as shown below in fig. 47.

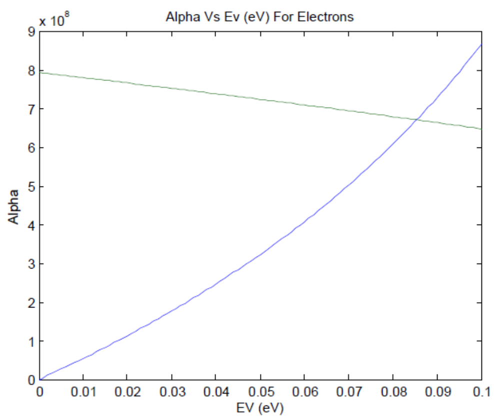

Fig .47a Electron Level in Dot (50A°) Ee_1=0.085x3=0.255eV

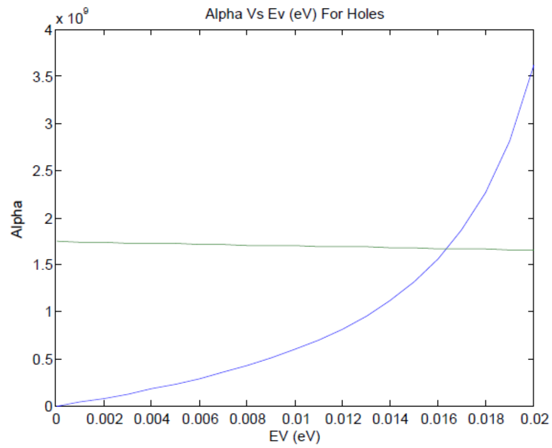

Fig. 47b Heavy hole Level in Dot (50A°):- E_{h1}=0.016x3=0.048eV

Energy level Table

Well-Barrier Difference	Electron Level in well (50A°)	Heavy hole Level in well (50A°)	Electron Level in Dot (50A°)	Heavy hole Level in Dot (50A°)
ΔE_g=0.22eV	Ee_1=.058eV	E_{h1}=.014eV	Ee_1=.174eV	E_{h1}=.042eV
ΔE_g=0.5eV	Ee_1=.085eV	E_{h1}=.016eV	Ee_1=.255eV	E_{h1}=.048eV

How to obtain J_{th} using laser parameters via Wenli Huang's program

Step 1:

Input parameters in *input file*

Elecron Mass in barrier(m_{nb})	0.08
Hole Mass in barrier(m_{hb})	0.58
Electron_Mass (m_n) in well	0.067
Heavy_Hole_Mass (m_{HH}) in well	0.62
Conduction_Band_Offset_(delta_Ec) for ΔEg=0.22eV	0.13 eV
Heavy_Hole_Valence_Band_Offset_(delta_Ev) for ΔEg=0.22eV	0.088 eV
Dimension of_the_Dot	50Åx50Åx50Å
Conduction_Band_Offset_(delta_Ec) for ΔEg=0.5eV	0.3 eV
Heavy_Hole_Valence_Band_Offset_(delta_Ev) for ΔEg=0.5eV	0.2 eV
Dielectric_Constant	12.32
Conduction_to_light_hole_gap	0.802 eV
Conduction_to_heavy_hole_gap	0.702 eV
Spontaneous line width	1.6×10^{12}

Step 2:
Run *run_all.c*
Converts input into what we can use; calculates well width of QD

Step 3:
Compile, run *well-width.c*. Build workspace.

Step 4:
Run *exhh0.c.* (Build and close each time.)
Calculates exciton HH binding energy; zero binding energy offset.

Step 5:
Run *exlh0.c.*
Calculates exciton LH binding energy.

Step 6:
Compile and build *gain.c*. Run.
"Intervalley relaxation time" = 4
"Input the Fermi level of valence band Efp" = -0.05 – 0.5

- Open output data file in Excel
- Plot data in Excel

7.8 Distributed Feedback Lasers (DFB)

(Ref. A. Yariv's Book on Optical Electronics)

Distributed feedback lasers are distinct from cavity type lasers. Here a grating is created in one of the cladding layers. This is achieved by selective etching and re-growth. Figure below shows the structure.

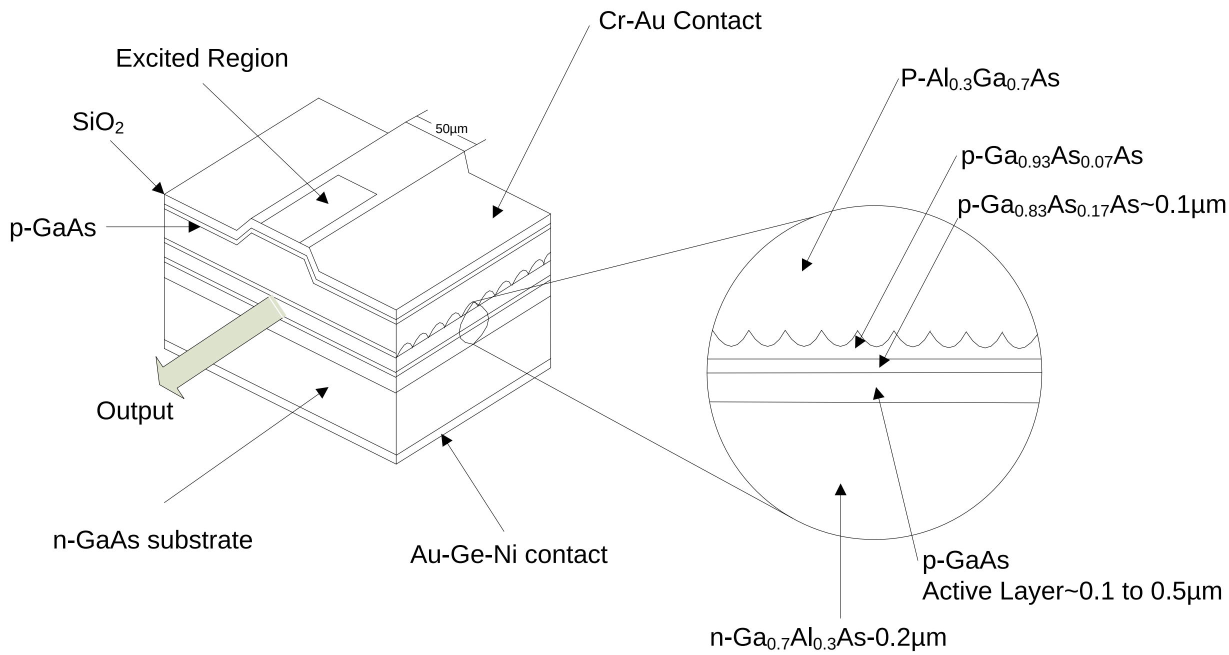

Fig .48 3-D view of a distributed feedback laser. The inset shows the details of cladding.

Emission spectrum of a distributed feedback laser (double heterojunction type). Ref. Nakamura et al, APL <u>25</u>, 487(1974). Note the absence of the axial cavity modes normally seen in heterojunction lasers with cleared reflectors. (This is not meant to imply that the other modes are not present.)

Coupling of modes in a DFB laser is much more involved and is complicated by the periodic variation of the index of refraction.

The solution of the coupled wave equation in a waveguide with positive feedback gives a relationship for Eleectric filed as funciton of distance along the propagation axis z. The incident wave at z divided by its amplitude at z=0 is:

$$\frac{E_i(z)}{E_i(0)} = \frac{e^{-j\beta z}\left\{(\gamma - j\Delta\beta)\sinh\left[s\left(L-Z\right)\right] - s\cosh\left[s\left(L-Z\right)\right]\right\}}{\left[\left(\gamma - j\Delta\beta\right)\sinh sL - s\cosh sL\right]}$$

<u>Condition of oscillation in a DFB laser:</u>

1) $(\gamma - j\Delta\beta)\sinh sL = s\cosh sL$

This condition can also be written as:

$$2)\qquad \frac{s-(\gamma - j\Delta\beta)}{s+(\gamma - j\Delta\beta)}e^{2sL} = -1$$

$$j=\sqrt{-1};\quad \Delta\beta = \beta - \beta_0;\quad \beta = \frac{\pi}{\Lambda}$$

Λ = Period of variation of the dielectric constant

$$\beta = \frac{\omega}{\nu} = \frac{\omega}{c/n};\qquad \overline{n}_r = \text{index of refraction}$$

$$3)\qquad s^2 \equiv k^2 + (\gamma - j\Delta\beta)^2$$

In equations 1 and 2, γ is the exponential gain coefficient of the medium.

s is defined:

where,

$$k = \frac{\pi n_1}{\lambda} + j\frac{\gamma_1}{2}$$

λ = wavelength in free space

n_1 = amplitude of index of refraction change

$$n(z) = n_0 + n_1 \cos 2\beta_0 z$$

$$\gamma(z) = \gamma_0 + \gamma_1 \cos 2\beta_0 z$$

γ_0 and n_0 are mean values

$$\text{Bragg Frequency}\quad \omega_0 = \beta_0\nu = \frac{\pi}{\Lambda} * \frac{c}{n}$$

where z is the direction of propagation and

Equation 2 reduced (under $\gamma >> k$ or high gain condition) to:

$$\frac{4(\gamma - j\Delta\beta)^2}{k^2} e^{2sL} = -1 = e^{j(2m+1)\pi}$$

By equating the phases on both sides, we get (for a mode *m*)

$$-2(\Delta\beta)_m L + 2\tan^{-1}\frac{(\Delta\beta)_m}{\gamma_m} + \frac{(\Delta\beta)_m Lk^2}{\gamma_m^2 + (\Delta\beta)_m^2} = (2m+1)\pi$$

for $m = \{0, \pm 1, \pm 2, \ldots\}$

If $r_m >> (\Delta\beta)_m$:

$$(\Delta\beta)_m L \cong -(m + \tfrac{1}{2})\pi$$

$$(\Delta\beta)_m \equiv (\beta - \beta_0)_m \cong -(\omega - \omega_0)\frac{n_{eff}}{c}$$

$$\omega_m = \omega_0 - (m + \tfrac{1}{2})\frac{\pi c}{n_{eff} L}$$

Mode separation

$$\omega_{m-1} - \omega_m \cong \frac{\pi c}{n_{eff} L}$$

Equating the amplitude

$$\frac{e^{2\gamma_m L}}{\gamma_m^2 + (\Delta\beta)_m^2} = \frac{4}{k^2}$$

Fig. 49 (a) shows the dielectric waveguide with corrugated layer serving as grating..

Fig. 49 (b) shows the incident and reflected electric field profile in the waveguide having a gain γ. [Reference: A. Yariv “Optical Electronics”, Holt, Rinehart and Winston (1976).]

As we have seen in a Fabry-Perot cavity, the ratio of incident wave to the reflected wave gives the gain.

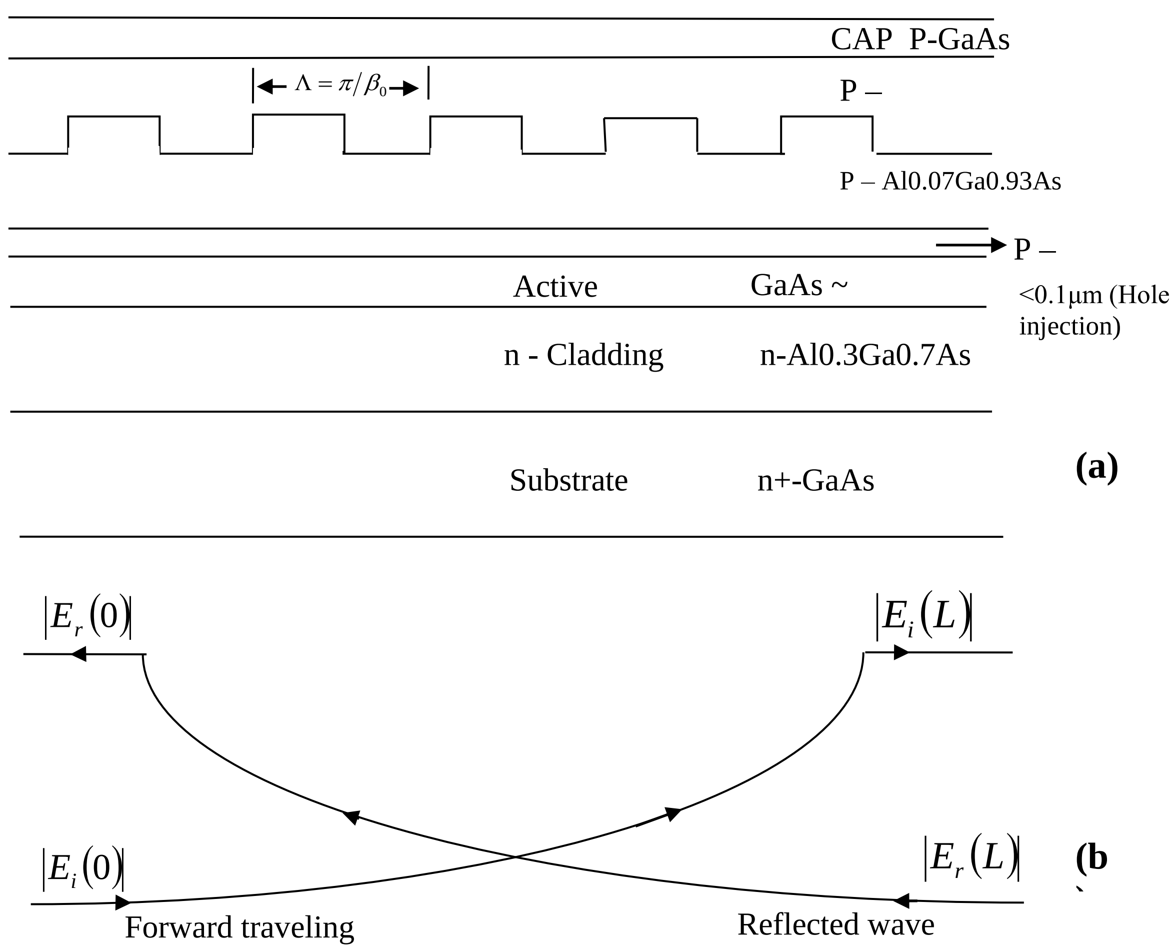

Fig .49 (a) Schematic of a distributed feedback Laser (b) E-field profile for forward and backward traveling wave

DFB Lasing

$$(\gamma - i\beta)\frac{e^{SL} - e^{-SL}}{2} = S\,\frac{e^{SL} + e^{-SL}}{2}$$

$$(\gamma - i\Delta\beta)\frac{e^{SL}}{2} \; - \; (\gamma - i\Delta\beta)\frac{e^{-SL}}{2} = \frac{Se^{SL}}{2} + \frac{Se^{SL}}{2}$$

$$[-S + (\gamma - i\Delta\beta)]\frac{e^{SL}}{2} = [S + (\gamma - i\Delta\beta)]\frac{e^{-SL}}{2}$$

$$\frac{-[S-(\gamma-i\Delta\beta)]}{[S+(\gamma-i\Delta\beta)]}e^{2SL}=1 \tag{1}$$

$S^2 = k^2 + (\gamma - i\Delta\beta)^2$; Where k is defined as a coupling co-efficient

$$S^2=\left(\gamma-i\Delta\beta\right)^2\left[1+\frac{k^2}{\left(\gamma-i\Delta\beta\right)^2}\right]$$

$$S=\pm\left(\gamma-i\Delta\beta\right)\left[1+\frac{k^2}{\left(\gamma-i\Delta\beta\right)^2}\right]^{1/2}$$

By making an approximation,

$$S=\pm\left(\gamma-i\Delta\beta\right)\left[1+\frac{k^2}{2\left(\gamma-i\Delta\beta\right)^2}\right] \tag{2}$$

Taking '-' Sign $S+\left(\gamma-i\Delta\beta\right)=-\frac{k^2}{2\left(\gamma-i\Delta\beta\right)^2}$ (3)	Taking '-' Sign $S=-\left(\gamma-i\Delta\beta\right)-\frac{k^2}{2\left(\gamma-i\Delta\beta\right)^2}$ $S-\left(\gamma-i\Delta\beta\right)=-2\left(\gamma-i\Delta\beta\right)-\frac{k^2}{2\left(\gamma-i\Delta\beta\right)^2}$ (4) $\approx -2\left(\gamma-i\Delta\beta\right)$

Now from the equations (1) and (3)&(4) we get

$$\begin{aligned}\frac{[S-(\gamma-i\Delta\beta)]}{[S+(\gamma-i\Delta\beta)]}e^{2SL}&=-1=\frac{-2(\gamma-i\Delta\beta)}{k^2}(-2((\gamma-i\Delta\beta)e^{2SL})\\ -1&=\frac{4(\gamma-i\Delta\beta)^2}{k^2}e^{2SL}\end{aligned} \tag{7}$$

Equating the phases on both sides

$$2\tan^{-1}\left(\frac{(\Delta\beta)_m}{\gamma_m}\right)-2(\Delta\beta)_m L+\frac{(\Delta\beta)_m L k^2}{\gamma_m^2+(\Delta\beta)_m^2}=(2m+1)\pi$$

assuming $\gamma_m >> (\Delta\beta)_m k$

$(\Delta\beta)_m L = -(m+\frac{1}{2})\pi$ is the oscillating frequency

$$(\Delta\beta) = \beta - \beta_0 \ ; \ \frac{(\omega\text{-}\omega_0)n_{eff}}{C}$$

$$\omega_m = \omega_0 - \left(m + \frac{1}{2} \right) \frac{\pi C}{n_{eff} L}$$

7.9 Introduction to Distributed Bragg Reflectors and Photonic Band Gap Structures

I. Distributed Bragg Reflectors (DBRs)

Distributed Bragg reflectors (DBRs) comprise multiple periodic layers consisting of (usually two) different semiconductor materials, with a significant but not necessarily large Δn (where the Δn is the refractive index difference semiconductors). The thickness of the layers is a function of their respective refractive indexes, usually given by

$$t = \lambda / 4n_r \ \text{(quarter wavelength)} \tag{1}$$

where t is the layer thickness, □ is the wavelength of intended operation, and n_r is the layer refractive index.

Light that is indent on the surface of the DBR will be partially reflected from each of the layer interfaces. As a result of the quarter wavelength thickness of the layers, the reflected components of the electromagnetic wave at each of the layer interfaces will arrive in phase with each other and superpose. Thus, the DBR functions as a highly reflective mirror, the reflectivity of which increases as the number of reflective layers in the DBR increases. For a DBR in air, the reflectivity R for light at normal incidence is given by

$$R = \left[\frac{1 - n_s \left(\frac{n_1}{n_2} \right)^{2m}}{1 + n_s \left(\frac{n_1}{n_2} \right)^{2m}} \right]^2 \tag{2}$$

where n_s is the substrate index, n_1 and n_2 are the contrasting semiconductor indexes, and m is the number of periods of layers in the DBR.

As indicated by the above equation, in addition to a large number of periods it is desirable to have a large Δn, since this will produce the greatest reflectivity for a given m. When fabricating a DBR structure, one must chose two materials that are lattice matched. One notable application for DBR structures is a vertical cavity surface emitting laser (VCSEL). This device consists of two DBRs with a cavity between them, known as a Fabry-Perot cavity. Photons supplied to the cavity are reflected back and forth between the two DBR mirrors. If the gain is great enough, stimulated emission will eventually occur out of the top layer.

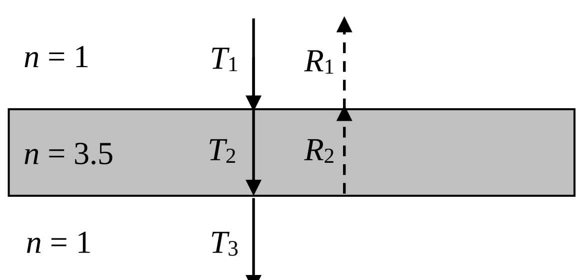

Figure 50: **Reflection and transmission of light incident on a single layer in air**

To understand how light is reflected from the many contrasting layers of a DBR, we will first consider the case of a light incident normally on a single layer of dielectric material in air, as shown in Fig. 1. Here the light is partially reflected at the two dielectric-air interfaces. The reflectivity R at each interface is given by

$$R = \left(\frac{n_2 - n_1}{n_2 + n_1} \right)^2 \quad (3)$$

where n_1 and n_2 are the two contrasting refractive indexes. If we let n_1 equal the refractive index of the surround air (1) and n_2 the index of the slab (3.5), we find using Eq. (3) that the reflectivity at the first interface is R_1 = 0.309. Thus, approximately 31% of the incident light is reflected, and the rest is transmitted through the first interface. At the second interface percentage of light reflected will be the same as at the first interface, but since 69.1% of the light is transmitted to the second interface, the percentage of the original light reflected is (0.309)(0.691) = 0.213 = 21.3%. The total percentage of the incident light reflected from the slab is therefore

$$R = R_1 + R_2 = 0.309 + 0.213 = 0.522 = 52.2\%$$

and the total light transmitted through the slab is

$$T_3 = 1 - R = 1 - 0.511 = 0.478 = 47.8\%$$

We now consider a DBR comprising InGaAsP (n_1 = 3.47) and InP (n_2 = 3.16) layers, with an InP substrate (n_s = 3.16). We will first assign five periods (m = 5) to this DBR. Using Eq. (2), while is similar to Eq. (3) but takes into account the multiple alternating layers in a DBR, the reflectivity is calculated to be R = 60.7%. The reason the reflectivity is not any larger for this number of periods is because the index contrast is relatively small (Δn = 0.31 compared with Δn = 2.5 for the previous case of the single slab). We now increase the number of periods to 10, calculating R = 82.3%. If we aging double the number of periods and set m = 20, we find that R = 97.0%. Finally, for m = 30, R = 99.5%, which is near total transmission. Thus, we see that R becomes very close to unity when the number of layers is large.

It is fairly easy to simulate a DBR or Fabry-Perot structure using computer software programs. In such simulations the reflectivity can be calculated for a range of wavelengths in order to show how the reflectivity changes as we move away from the intended operational wavelength of the DBR. Fig. 2(a) shows a common type of DBR modulator structure. It consists of a Fabry-Perot cavity containing a multi-quantum well (MQW) located between two InGaAsP/InP DBRs, designed for operation at λ = 1.55 μm. These DBRs contain a relatively large number of layers. In Fig. 2(b), the corresponding reflectivity as a function of wavelength is shown. We see reflectivities on the order of 0.96 with a sharp dip at 1.55 μm, which is a result of the MQW cavity. The average reflectivity decreases as the distance from the target wavelength increases. As was demonstrated above, by increasing the number of DBR periods, the reflectivity can me made to approximate unity.

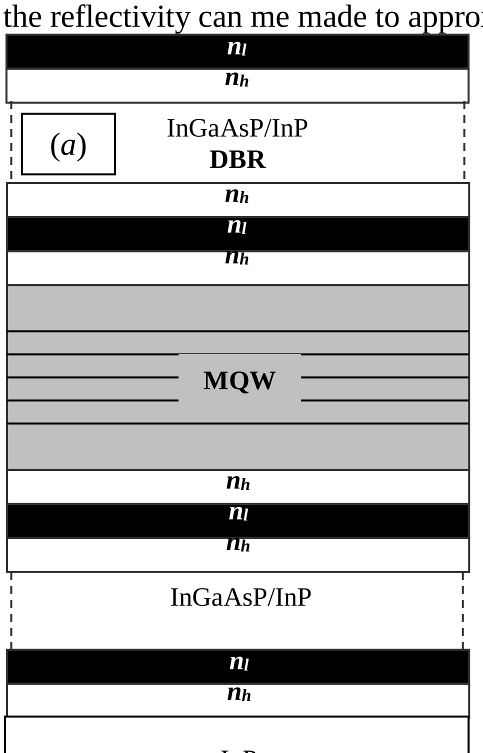

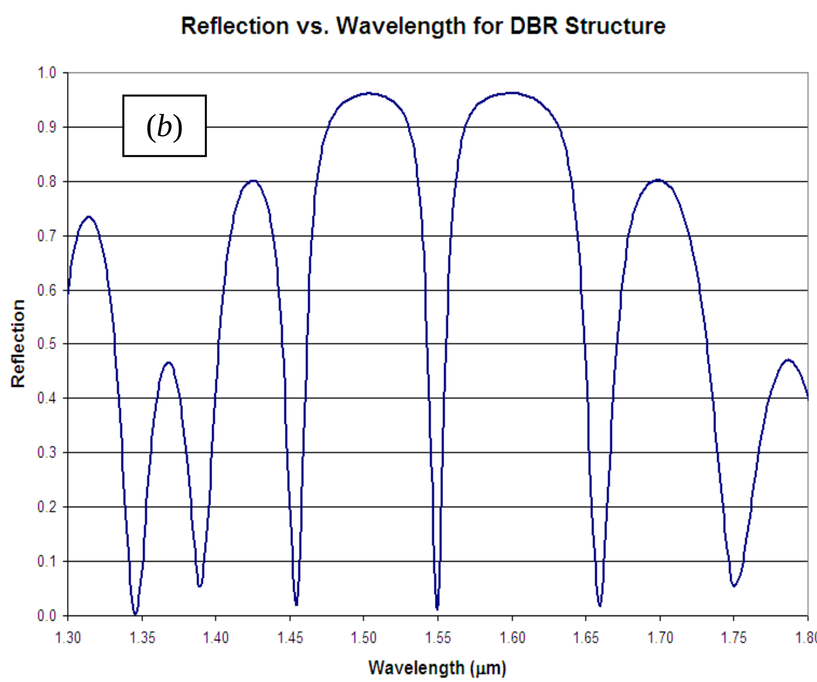

Figure 51: Modulator with Fabry-Perot cavity situated between

II. PBG Structures

Basically, any physical device that possesses a *photonic band gap* (PBG) can be classified as a PBG structure. A photonic band gap is similar to the band gap of a semiconductor material, except that instead of comprising a range of energies, a PBG consists of a range of optical frequencies that cannot exist in the structure. PBGs arise because of the symmetry of a structure. For example, for a DBR (refer to previous write up on DBRs), a basic type of PGB structure, the PBG exists only for light normal to the plane of incidence. If the wavelength of light incident on the DBR is close enough to the wavelength for which it was designed, the light will be reflected at each layer interface. The light penetrating into the DBR is evanescent, i.e. decaying exponentially. Thus, modes within a frequency range centered at a frequency corresponding to this wavelength cannot exist within the DBR. We designate this range of frequencies the PBG of this particular DBR structure (it is possible for a structure to have multiple PBGs).

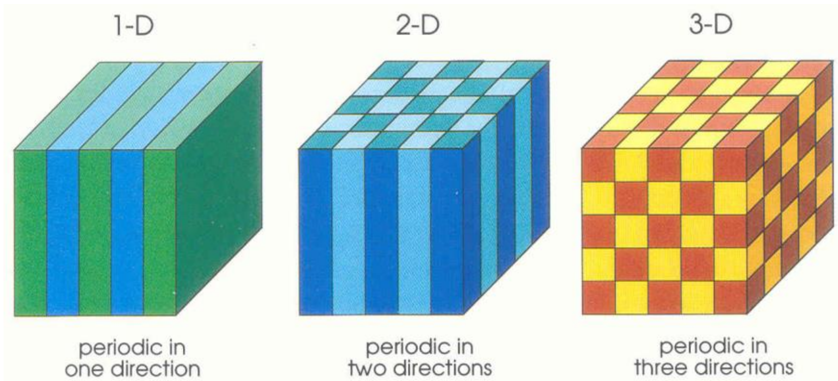

Figure 52: Simple examples of 1D, 2D, and 3D photonic crystals. The different colors represent materials with different refractive indexes.
Ref: *Photonc Crystals: Molding the Flow of* ***Light*, by J. D. Joannopoulos**

A type of structure that has become analogous to PBG structures is what is known as a photonic crystal (PC). PCs, which rely on distributed Bragg reflection, are characterized by regions of periodically alternating refractive indexes. PCs may be one-dimensional (1D), two-dimensional (2D), or three dimensional (3D), as shown in Fig. 52. One-dimensional PCs are basically DBRs, which have been discussed. In 2D PCs, a PBG exists for light traveling *in a plane*, while in 3D PCs, the PGB apples to light traveling in any direction. Two-dimensional PCs are easier to design simpler to fabricate than 3D PCs, and can be combined with cladding to confine light in three-dimensions. In the following paragraphs we will be dealing with 2D PCs.

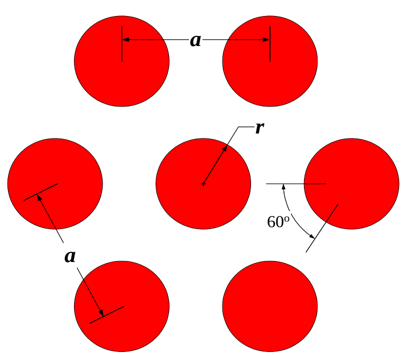

Figure 53: **Side view of silicon 2D PC (*a*) with air columns and air cladding, and top view of a triangular lattice PC (*b*) showing lattice constant *a* and radius *r***

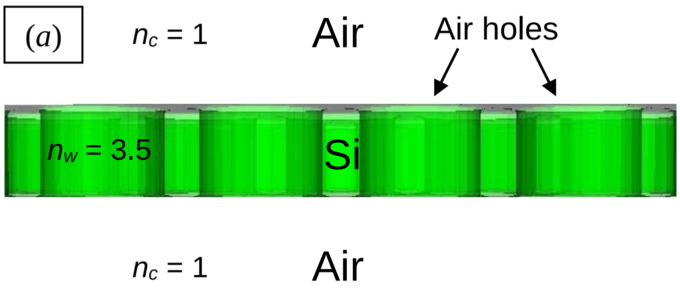

(b)

Most 2D PCs consist either of a lattice of cylindrical dielectric columns in air, or air columns in a dielectric material. The former type of structure has a PBG for transverse magnetic (TM) polarized electromagnetic waves, while the latter PC variety, which we have been simulating, has a PBG for transverse electric (TE) waves [Fig. 53(*a*)]. In addition, the air columns may be arranged in either a square lattice or a triangular (a.k.a. hexagonal) lattice [Fig. 53(*b*)]. Triangular lattice PCs generally produce much larger PBGs, and are consequently more useful for most applications. To provide light confinement at any angle, cladding layers may be added on the top and bottom of a 2D PC. The light is then confined by the air columns in the lateral direction, and by the cladding layers in the transverse direction via total internal reflection.

The primary utility of PCs is based on their inherent ability to confine light. Although no forbidden frequencies are allowed inside the regular PC lattice, if the symmetry of the lattice is broken by creating a defect state, modes that were prohibited from internal propagation can be confined within the defect. For example, by removing a single column in a 2D PC, a point defect, or cavity, is created. If modes with frequencies that belong to the PBG are present in this cavity, they will be reflected by the cavity walls (which act as near-perfect mirrors) and thus will be tightly confined in the cavity. Similarly, by removing a row of columns, a line-defect waveguide is formed [Fig. 54(*a*)], where light is confined by the PC lattice walls on the two sides of the waveguide and made to propagate along a single axis.

A third type of defect PC structure is known as a coupled-cavity waveguide (CCW), shown in Fig. 54(*b*). A CCW consists of a row of neighboring defect cavities separated by a finite-length PC lattice. Most of the light traveling though the waveguide is localized in the defects. Because of weak modal interactions between the defects, light will “hop” or couple between defect cavities. This type of waveguide can be used to guide light in almost any direction, and incorporates a delay factor that has applications for energy storage.

We have seen that PCs are a type of PBG structure that provide PBGs in one, two, and three dimensions. Two-dimensional PCs can be made to confine light in many different ways though the introduction of defects to their symmetrical lattices. PCs are still a relatively new development, and are the focus of much ongoing research that is yielding new types of PC devices such as low threshold lasers.

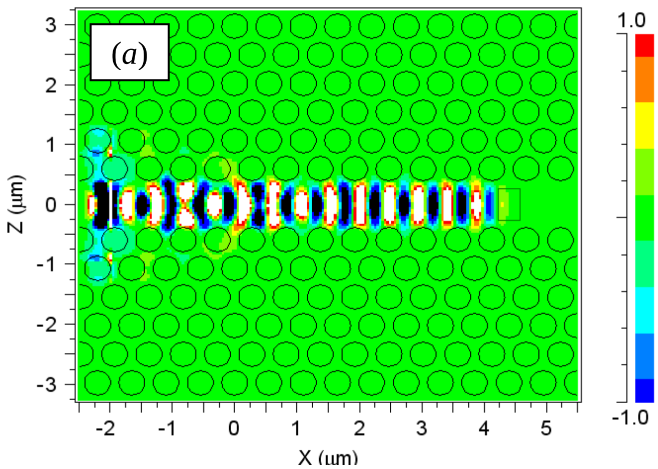

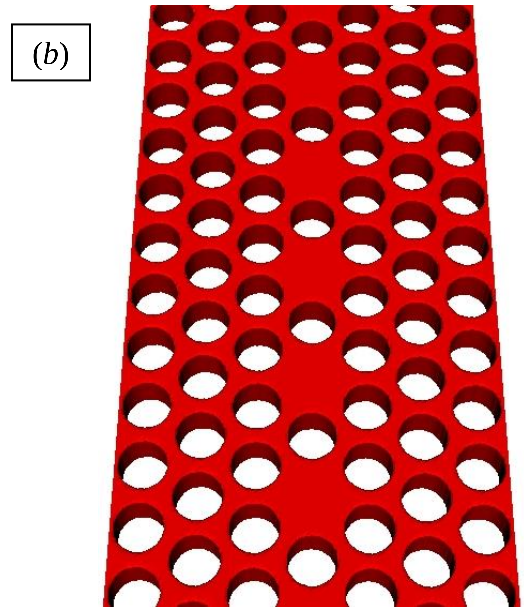

Figure 54: **Light propagating through a line-defect PC waveguide (*a*), and a PC CCW showing neighboring defect cavities (*b*).**

7.10 DBR Laser and Vertical Cavity Surface Emitting Lasers (VCSELs)

DBR Laser: Figure 55 shows a cavity laser with one mirror on the right being the distributed Bragg mirror (DBR) and the other is a conventional mirror [Coldern et al. 2012). Here L_a represents the gain region, L_p the phase region (for tuning if needed), and L_g the DBR region. Leff is the effective length of the DBR as seen by the lasing beam. The total cavity length is shown by Leff. Here distributed Bragg grating, serving as reflector, is realized in one of the cladding layers by adjusting the index of refraction like in DFB lasers. DBR lasers produce very narrow line widths for a given mode.

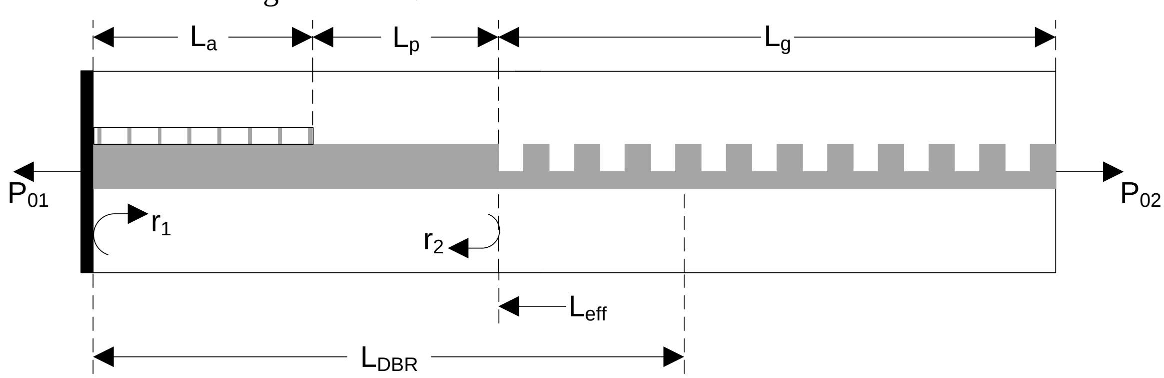

Fig. 55 Cross-sectional schematic of a DBR laser along the cavity axis.

VCSEL: Fig. 56 shows cross-sectional schematic of a vertical cavity surface emitting laser (VCSEL).

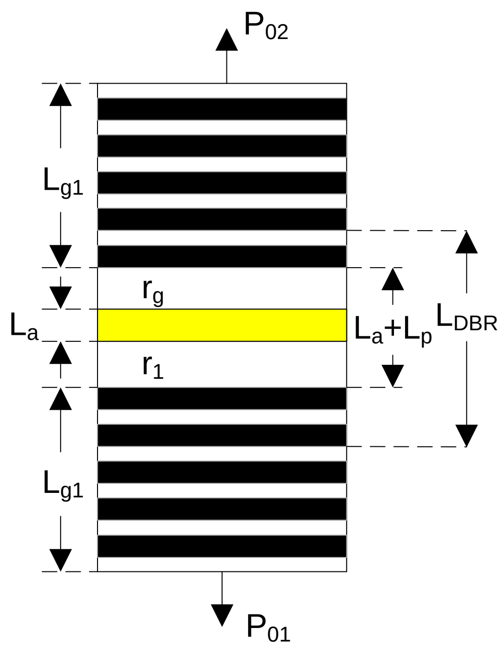

Fig. 56 shows cross-sectional schematic of a vertical cavity surface emitting laser (VCSEL).

Here L_a represents the gain region which is sandwiched in a waveguide region designated as L_p. The magnitude of L_p is multiple of integral half wavelength in the lasing medium. The index of gain region L_a is generally higher than L_p. The two DBR mirrors are made of low and high index of refraction layers each quarter wavelength in thickness. Fig. 57 shows a commercial JDSU VCSEL at 850nm. The laser output comes out of the hole which is surrounded by top circular electrode. The big pad is used to probe for wire bond. The bottom electrode is on the other side of the wafer. The total die is about 0.5 mm x 0.5mm and the emitting area is in 10 micron diameter or so.

	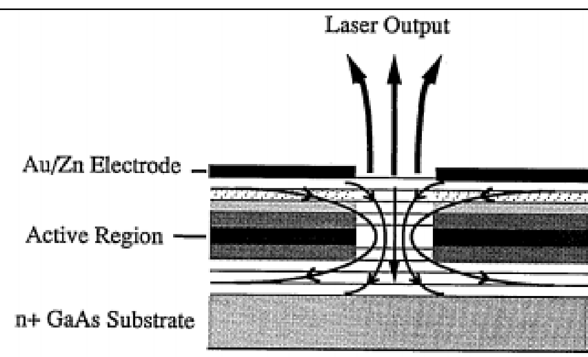
Fig . 57 Photograph of a 850nm GaAs VCSEL.	Fig . 58 Surface-emitting laser [Ref. J. Jahns et al, Applied Optics, 31, pp. 592-596, 1992].

Fig. 58 shows schematic of a surface emitting laser with vertical cavity formed by DBR mirrors. The light is emitted as the current flows from the bottom contact to the annular top contact.

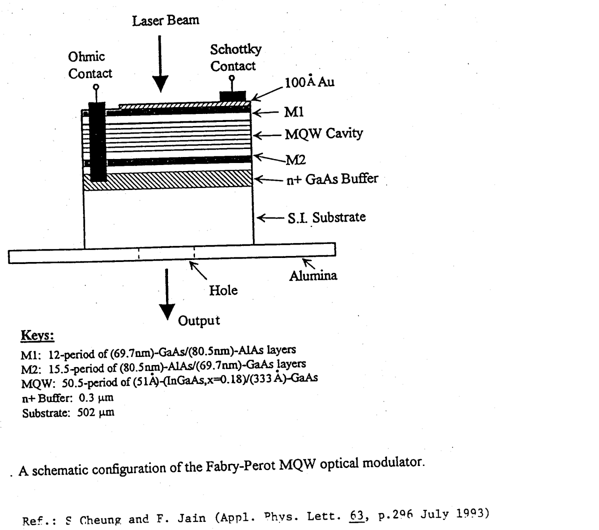

Fig. 59A. Cross-sectional schematic of a MQW modulator with 12 periods of GaAs-AlAs layers in top mirror M1, a MQW cavity and having 13.5 periods of GaAs-AlAs in bottom mirror M2.

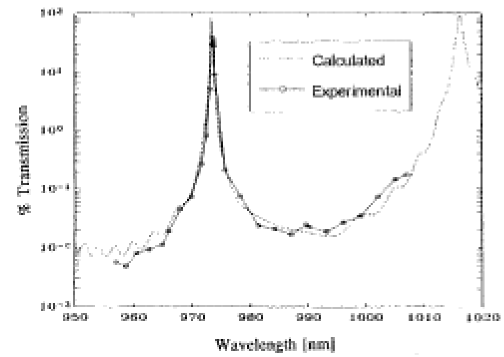

Fig. 59B. Transmittance peak in a Fabry-Perot modulator; note the narrow peak (Ref. S. Cheung, F. Jain, R. Sacks, D. Cullen, G. Ball, and T. Grudkowski, Appl. Phys. Lett., 63, July 19, 1993.

Fig. 59B shows the % transmission in a modulator fabricated in our lab using a cavity with DBRs. The laser is quite similar to this Multiple Quantum Well (MQW) surface normal modulator. In laser the MQWs are replaced by one or two InGaAs quantum wells and a waveguide region forming the cavity, similar to Fig. 58.

7.11 Tandem Multiple Beam Output and Transistor Lasers

7.11.1 Tandem Lasers characteristic and fabrication steps

A tandem laser is shown in Fig. 60. Here, there are two active layers comprising of a single AlGaAs quantum well (sandwiched between two barrier layers), and each active layer producing an output. The active layers are separated by a $n1^{+}/p2^{++}$ GaAs tunnel junction. (Ref., Jain et al, 1997).

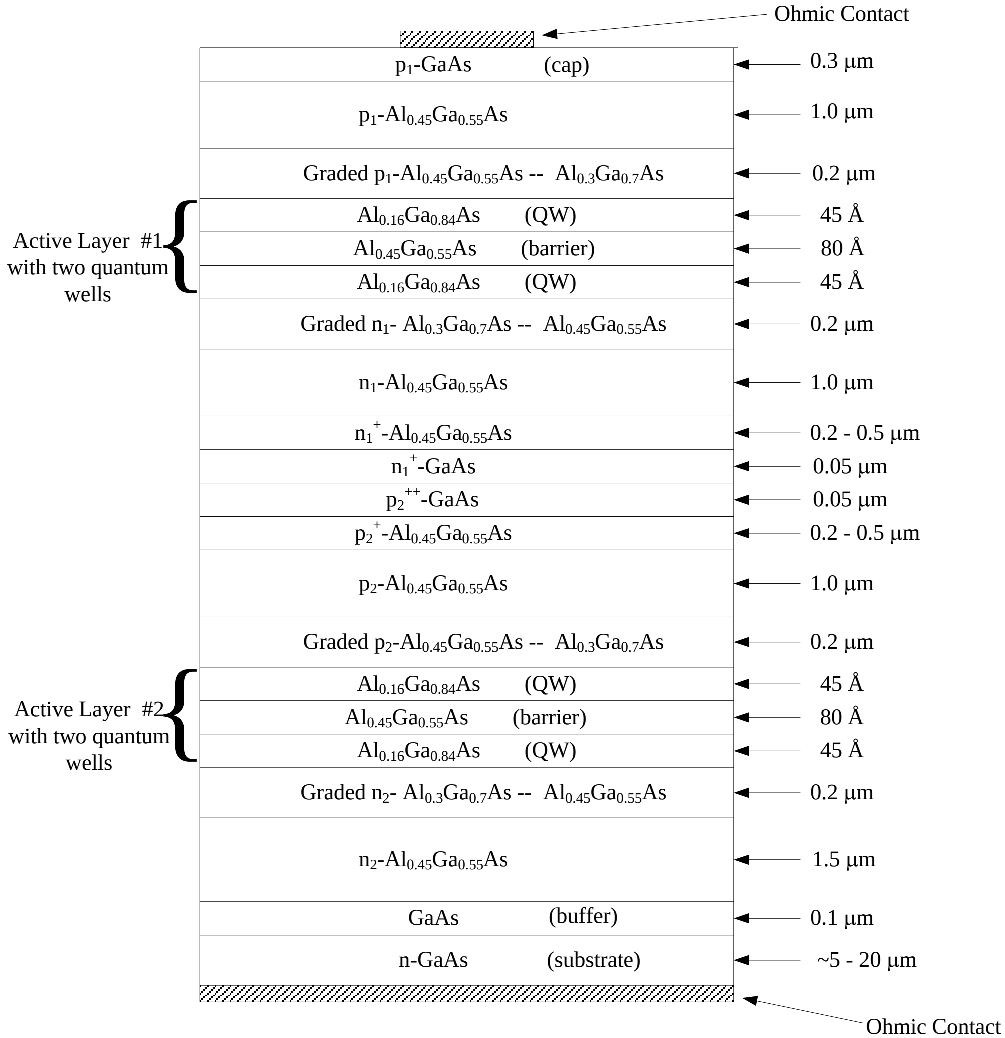

Fig. 60. Beam output AlGaAs Quantum Well Tandem Laser emitting at 719 nm is **shown.**

The near-field pattern is shown in Fig. 61 reproduced below.

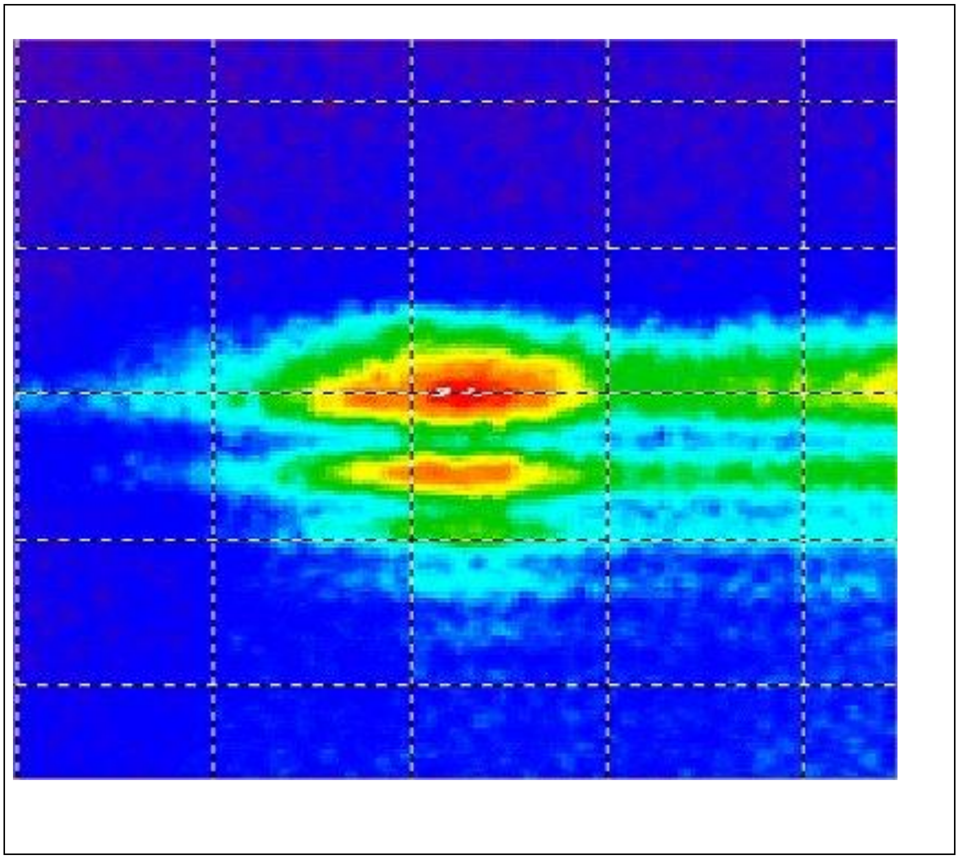

Fig. 61 Near Field Pattern showing 2-lasing spots (red) from upper and bottom active layers.

Fabrication of Tandem Laser (Ref. W.Zappone, MS thesis, Chapter 3, UConn, 2004)

1 Processing Steps: The flowchart for the process steps is shown in Fig. 62.1.

2 Mask Design: A 3x3-inch mask was designed using the L-Edit software to pattern the oxide with three different stripe widths: 25 μm, 50 μm, and 100 μm on 500 μm centers (Fig. 62.2).

3 Oxide Deposition: A layer of SiO_2 was deposited using the IPE Model 1000 Plasma Enhanced Chemical Vapor Deposition System (PECVD) machine at Cornell's CNF facility. A temperature of 300° C was used to deposit 1500 Å of SiO_2. The SiO_2 layer isolates laser top contact stripes.

4 Photolithography: The photolithographic process is used to define the openings for the top (P-metal) metallization. The first step in the photolithography process is the application of photoresist. The type of positive photoresist used was AZ1518. It was applied using a photoresist spinner for 30 seconds at 5000 revolutions per minute. Then a pre-bake was done on the sample, using a hot plate for 2 minutes at 90° C. Pre-baking drives excess solvents from the

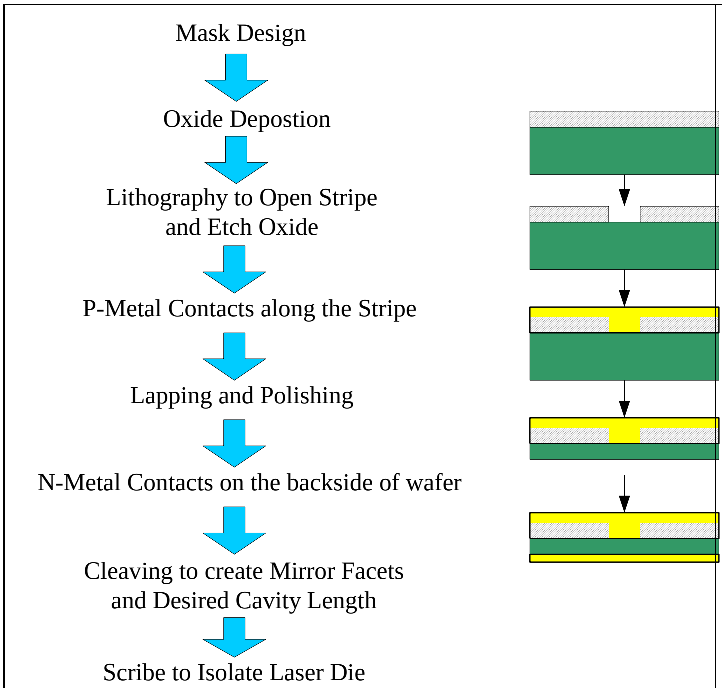

Fig. 62.1: Flowchart for making a broad-area laser.

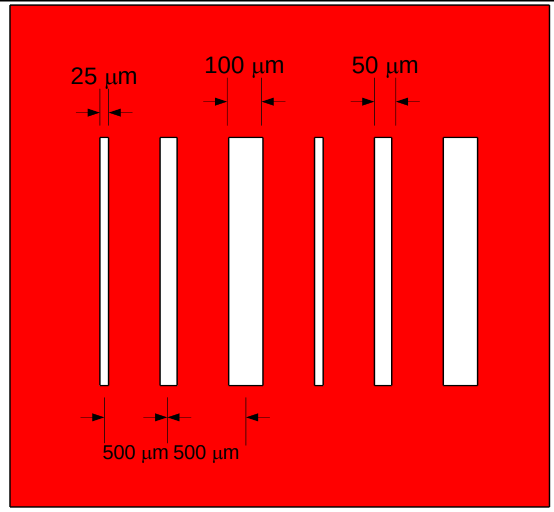

Fig. 62.2: Mask design used to produce stripe pattern for broad-area laser.

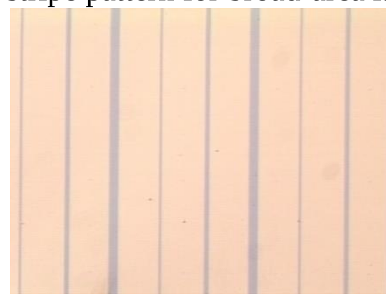

Figure 62.3: Developed photoresist exposing underlying oxide (blue).

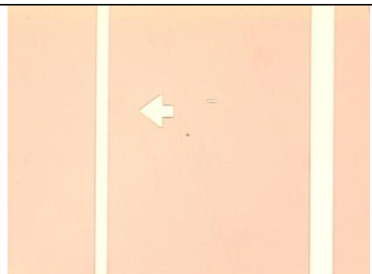

Fig. 62.4: Removal of oxide in the stripe avenues.

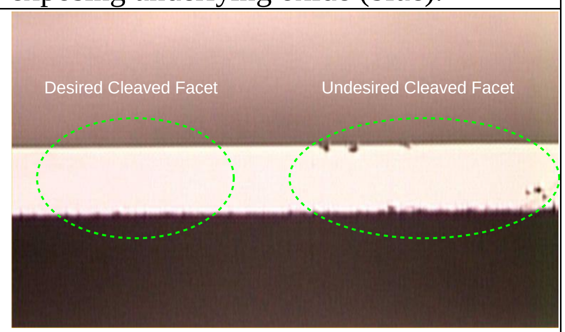

Fig 62.5: Cleaved facets of the tandem laser bar.

resist and promotes better adhesion. A HTG Model ILS84-2 optical UV mask aligner was used to transfer the pattern to the wafer. The stripes of the mask were aligned parallel to a cleaved edge on the wafer, and then the photoresist was exposed to the UV radiation for 30 seconds. The exposed areas of photoresist have been softened by the UV radiation and can now be washed away with a solvent (identified as Developer). AZ351 Developer was used in a 3:1 solution with de-ionized water (3 parts de-ionized water to 1 part Developer solution) to wash away the exposed photoresist. The sample was placed in the Developer and gently agitated for 45 seconds, and then immediately submerged in a larger beaker of de-ionized (DI) water. After the Developer was washed off, the sample was dried using a Nitrogen jet. The final step in the photolithographic process is post-bake. The function of this step is to harden the resist so it can better withstand the harsh environment of the etching process needed to remove the oxide in the stripe avenues. The post-bake also promotes adhesion and helps prevent undercutting. The conditions of the post-bake step were the same as the pre-bake step, bake on a hot plate for 2 minutes at 90° C. Figure 62.3 shows the developed photoresist.

5 Oxide Etch: Typically, there are two methods used to remove SiO_2, wet chemical etching (using Buffered HF) and dry chemical etching (reactive ion etching, RIE). For this particular process, a wet chemical process was used to remove the SiO_2, specifically; a 10:1 Buffered Oxide Etch (BOE) and DI water (10 parts DI water to 1 part of hydrofluoric acid). After the 6 seconds, an optical inspection was performed to observe if the oxide had been completely etched away. An additional 3 seconds of etching was performed followed by another optical inspection. The resulting inspection revealed the stripe avenues were free of oxide (Fig. 62.4).

6 P-Metal Ohmic Contact: A good Ohmic metal-semiconductor interface should exhibit several characteristics including Good mechanical strength, Strong adhesion (no peeling), and Does not add excessive stress to the semiconductor.

A multilayer contact scheme was used to create a good ohmic contact to the p-type GaAs cap layer of the structure (figure 62.5). The metal contact was deposited using a CVC SC4500 combination thermal/E-gun evaporation system at Cornell's CNF laboratory. The cryopumped evaporator contains 4 electron gun sources and 3 thermal evaporation sources. The combination of e-gun and thermal sources allows a one-pump-down evaporation of layered materials such as Ti-Pt-Au. In fact, the p-metal multilayer contact used for the tandem laser was Ti-Pt-Au, and the thicknesses deposited were as follows: Ti -500 Å, Pt-200 Å, and Au-1000 Å.

7 Lapping and Polishing: Back lapping is the thinning of the semiconductor wafer by mechanically removing material from the unpolished (or unprocessed) side of the wafer. Reducing the thickness of the substrate makes cleaving laser bars easier and more repeatable. The lapping and polishing was performed using a Logitech LP30 at the University of Connecticut Micro/Optoelectronics Laboratory. The sample was mounted on a glass substrate/carrier using bee's wax. The starting wafer thickness was measured to be 520 μm. The lapping grit size used was 0.5 μm, which produced a lapping rate of 30 μm per minute. The lapping process consisted of lapping for 3 minutes, stopping to measure the thickness, then continuing to lap until the desired thickness of 125 μm (5mils) was obtained. After reaching the desired thickness, an inspection of the surface revealed a very rough surface with many scratches. For optimal cleaving, a smooth, mirror-like surface is desired. In order to obtain this smooth, mirror-like surface, mechanical polishing was performed. A specific polishing grit size is used (0.05 μm) in congruence with a polishing pad. A similar process of polishing and stopping to inspect the wafer was used until the desired mirror-like finish was obtained.

8 N-Metal Ohmic Contacts: The n-metal contact was deposited using a CVC SC4500 combination thermal/E-gun evaporation system at Cornell's CNF laboratory (the same machine used to deposit the p-metals). The n-metal multilayer contact used for the tandem laser was Ni-Ge-Au, and the thicknesses were as follows: Ni-100 Å, Ge-500 Å, and Au-1200 Å. Both the top and bottom contacts have been deposited on the sample. The final step to complete the metallization process is to alloy the metal layers into the cap layer and substrate by using a technique called Rapid Thermal Annealing (RTA). A RTA oven is a device that is able to quickly, and with great control, ramp the temperature to a programmed level, maintain that level for a programmed time, and then quickly ramp down the temperature. The RTA conditions used to anneal the ohmic contacts of the tandem laser sample were an initial ramp to 400° C for 20 seconds, and then further ramp up to 450° C and maintaining that temperature for 10 seconds, followed by a ramp down of the temperature.

9 Cleaving Facet Mirrors: Having a clean mirror-like facet is essential for a diode laser. Cracking and striations can lead to catastrophic failures or high thresholds (see figure 3.5). The tandem laser was cleaved using a Kulicke and Soffa Model752D wafer cleaver. The sample was mounted on sticky tape and placed on the vacuum chuck of the cleaving instrument. The sample was aligned with the stripes oriented perpendicular to the cleaving needle. Starting from the edge, the sample was stepped by 500 μm increments; this step size determines the cavity length for the laser diode. At each increment, the needle at the top of the sample makes a small scribe mark. After stepping through the entire sample, it is removed from the vacuum chuck, and a piece of lens paper is placed over the sample. A small cylindrical rod is rolled over the scribed regions in order to propagate the scribe mark down the length of the sample. Once all cleaves have propagated, the laser bars are removed from the sticky tape.

10 Scribing into Laser Die: Each laser bar contains several stripes (500 μm in length) on 500 μm centers with 2 cleaved facets on either side. The next step is to isolate each stripe to form a single laser diode using a process called scribing. Once again, we place the lasers bars on sticky tape and mount on the vacuum chuck of the cleaving instrument. This time the stripes are placed parallel to the scribing needle. Starting from the edge of the bar, a scribe mark is made across the entire width of the laser bar. Then the sample is stepped in increments of 500 μm, each time making a scribe mark in-between adjacent stripes. A small cylindrical rod is used to roll over the scribed regions and snap the device from the laser bar. Once all devices have been isolated, the laser dies are removed from the sticky tape.

5.12.2 Heterojunction Bipolar Transistor (HBT) and Resonant Tunneling Transistor (RTT) Lasers: Heterojunction bipolar transistors have been proposed by Jain et al (1991 ISDRS Proc., and US Patent 1993) and demonstrated by N. Holonyak and M. Feng (IEEE Spectrum, February 2006). Resonant tunneling transistor lasers have also been investigated (see journal article R. LaComb, and F. Jain, "A Self-Consistent Model to Simulate Large-Signal Electrical Characteristics Of Resonant Tunneling Bipolar Transistors", Solid-State Electronics Vol. 39, pp. 1621-1627, November 1996).

7.12 Summary Equations:

Propagation coefficient γ in laser gain medium

<table>
<tr>
<td>

$$\bar{E} = Ee^{-j\gamma z} \cdot e^{j\omega t} = Ee^{-j(\gamma z - \omega t)}$$

where $\gamma = (n_r - j\kappa)k_0$

</td>
<td>

$\kappa = \dfrac{\alpha\lambda}{4\pi}$ (7c)

$\gamma = n_r k_o - j\dfrac{\alpha\lambda}{4\pi}k_o$ (8a)

$\gamma = n_r\dfrac{2\pi}{\lambda} + j\dfrac{(g-\alpha)}{2}$ (8c)

Eq. 8c is applicable when optical gain is there.

</td>
</tr>
</table>

Lasing conditions in semiconductor active layer

$$g = \alpha + \frac{1}{2L}\ln\left(\frac{1}{R_1 R_2}\right) \qquad (15)$$

$$L = \frac{m\lambda}{2n_r} \qquad (17)$$

Separation of successive cavity longitudinal modes

$$\Delta\lambda = \pm\frac{\lambda^2}{2Ln_r}\left(1 - \frac{\lambda}{n_r}\frac{dn_r}{d\lambda}\right)^{-1} \qquad (22)$$

Frequency separation is related to mode separation as

$$\Delta\upsilon = \frac{c\Delta\lambda}{\lambda^2} = \frac{3*10^{10}*8.42*10^{-8}}{(0.98*10^{-4})^2} = 2.6x10^{11}Hz = 260GHz$$

Bernard-Duraffourg condition: Transparency condition

$$E_{fn} - E_{fp} > h\nu > E_g \qquad (31)$$

Also gain coefficient g is given by

$$g = -\alpha_o\,[1-f_e-f_h] \qquad (33)$$

Which can also be expressed

$$g = \frac{J\eta}{qd\,v_g\,\Delta\nu_s}\,\frac{c^2 v_g}{8\pi n_r^2\nu^2}\left[1 - e^{\frac{h\nu-\Delta\zeta}{kT}}\right] \qquad (41)$$

Equating Eq. 15 with Eq. 41 we get threshold current density $J=J_{TH}$

$$J_{th} = \frac{8\pi n_r^2\nu^2 qd\Delta\nu_s}{\Gamma\eta c^2 z(T)} \bullet \left[\alpha + \frac{1}{2L}\ln\frac{1}{R_1 R_2}\right], \text{ here } z(T) = \left[1 - e^{\frac{h\nu-\Delta\zeta}{kT}}\right]. \qquad (44B)$$

The gain in the active layer is less because of confinement factor Γ. Various approximations:
(1) $\Gamma = 1 - \exp(-C\Delta n_r d) = 1 - \exp(-3x10^6 x0.138x0.2x10^{-4}) = 1 - 2.5x10^{-4} \approx 1$
(2) Use $\Gamma = 2\pi^2 d^2 (n^2_{active} - n^2_{clad})/\lambda^2$. **(λ is the free space wavelength.)**

(3) $\Gamma = \dfrac{V^2}{2+V^2} = \dfrac{0.10726}{2.10726}$ = 0.05. Here,

$$V^2 = \frac{4\pi (d^2)(n_{active}^2 - n_{cladding}^2)}{\lambda^2}$$

The threshold current density is a function of T. To is the characteristic temperature. To is higher for Quantum well active layer, still higher for quantum wire lasers, and almost infinity for quantum dot.

$$J_{TH}(T) \sim J_{TH}(0)\exp\{T/T_0\}$$

Index of InGaAsP active layer $In_x Ga_{1-x} As_y P_{1-y}$

$$n(x,y) = 3.52xy + 3.39x(1-y) + 3.60y(1-x) + 3.56(1-x)(1-y) \qquad \text{(p.372)}$$

Power Output of a laser is given by

$$P_{out} = \begin{pmatrix} \text{Power emitted by stimulated} \\ \text{emisssion in the cavity} \end{pmatrix} * \left(\text{Fraction lost due to mirrors}\right)$$

$$= \left[\frac{\left(I - I_{TH}\right)\eta_{\text{int}} h\nu}{q}\right] * \left[\frac{\frac{1}{2L}\ln\left(1/R_1 R_2\right)}{\alpha + \frac{1}{2L}\ln\left(1/R_1 R_2\right)}\right] \qquad (55)$$

Active layer thickness for a single transverse mode (page 374)

$$d < \frac{m\lambda}{2\sqrt{n_r^2\big|_{active} - n_r^2\big|_{clad}}}$$

Stripe width W for a single lateral mode (page 374)

$$W < \frac{m\lambda}{2\sqrt{n_r^2\big|_{MiddleOfGainRegionInActiveLayer} - n_r^2\big|_{CornerOfActiveLayerAwayFromWhereGainIsSmall}}}$$

Beam Divergence:

Beam divergence in the junction plane $\theta_{\parallel} = \dfrac{\lambda}{W}$

The perpendicular to the junction plane $\theta_{\perp} = [4.0(n^2{}_{active} - n_{clad}^2)d/\lambda]$,

See Design Sets for reflectivity of end facets, when air is the outer medium, calculations.

$$R_1 = R_2 = R = \left(\frac{n_r - n_{air}}{n_r + n_{air}}\right)^2$$

7.13 Solved Problem SET-Lasers-I: Analysis

Q.1 (a) Compute the photon density ρ (hν)in the region shown by a box of thickness $2L_n$, width W and length L (Fig. 1) in p-GaAs side. Assume the forward current I is 10mA. The top contact stripe has a width W=5 μm and L = 500 microns (in z-direction). Assume injection efficiency to be 0.999 and quantum efficiency to be 0.95. The diffusion length L_n= 1 μm.

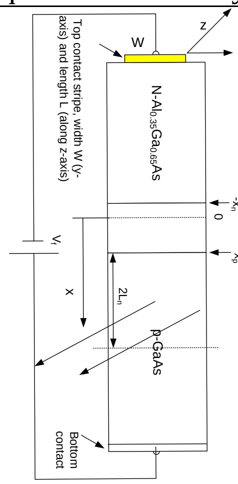

Fig. 1An abrupt n^-AlGaAs-p GaAs single heterojunction (SH) diode under forward bias.

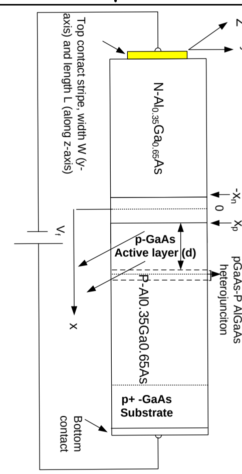

Fig. 2 An n^-AlGaAs-p GaAs-P AlGaAs double heterojunction (DH) diode under forward bias.

(b) Compute the photon density in the active layer GaAs of double heterojunction (DH) diode of Fig. 2. This device has the same contact stripe W on $Al_{0.35}Ga_{0.65}As$, and thickness of p-GaAs is d= 0.1 μm, and length L =500 μm in z-direction in the double heterojunctions (DH) diode.

(c) Find the composition of active layer InGaAsP lattice-matched to InP and emitting at 1.55 micron.

Given the 1.55 micron LED composition (HW5/Q3Note) to be $In_{0.639}Ga_{0.361}As_{0.79}P_{0.21}$.

HINT: Laser hν= E_g + 1/6 (kT/q) which is different from LED due to Bernard-Duraffourg condition.

(d) Find wavelength λ_m, λ_{m+1}, and λ_{m-1} of three successive cavity modes for the 1.55 μm InGaAsP active layer with a cavity length of 500micron The index of $In_xGa_{1-x}As_yP_{1-y}$ is given by

$$n(x,y) = 3.52xy + 3.39x(1-y) + 3.60y(1-x) + 3.56(1-x)(1-y) \qquad \text{(j)}$$

$m = \dfrac{2n_r L}{\lambda}$, or use $dn_r/d\lambda$ = 1.5 $(\text{micron})^{-1}$.

Q. 2. (a) The energy band diagrams for the diodes of Fig. 2 is shown below. Find various values.

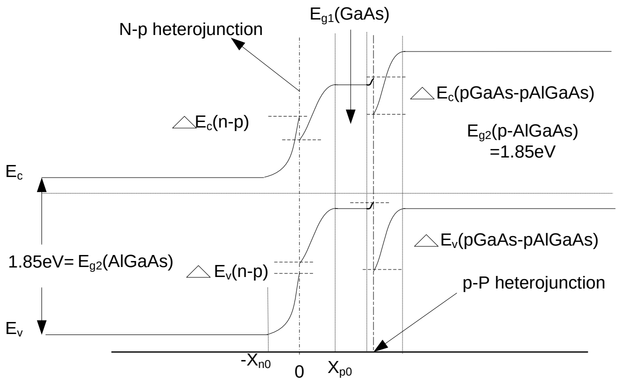

Fig. 17 Notes

(b) What is the role of pGaAs-pAlGaAs (isotype) heterojunction in confining the injected electrons in the p-GaAs layer?

(c) Find the forward bias current at a V_f =1.2V in the device Fig. 1.

Given: **n^+-side**: Donor concentration N_D= 2x 10^{18} cm^{-3}

minority hole lifetime $\tau_p=2\times10^{-9}$ sec.

Minority hole diffusion coefficient D_p=10 cm^2/sec.

Intrinsic carrier concentration n_i (AlGaAs)=300 cm^{-3}

p-GaAs : Acceptor concentration N_A= 3x10^{16} cm^{-3}, All donors/acceptors are ionized.

$\tau_n=10^{-8}$ sec. D_n=100 cm^2/sec; Junction area A=10^{-3} cm^{-2}, $\varepsilon_0=8.85\times10^{-14}$ F/cm, $\varepsilon_s=\varepsilon_r\varepsilon_0$. T=300 °K. Intrinsic carrier concentration n_i (GaAs) ~ n_i(AlGaAs) x exp[$-\Delta E_g/2kT$] = 300 $e^{-\Delta Eg/2kT}$ cm^{-3} [Here, ΔE_g = E_g(AlGaAs)- E_g(GaAs)].

p-AlGaAs: same as n+ side except it is doped with acceptors.

Additional information: Given: **n-side Al$_\xi$Ga$_{1-\xi}$As:**

Effective mass: electrons $m_e=m_n$= (0.067 + 0.083ξ)m_o, for ξ< 0.45;

Energy gap E_g (Al$_\xi$Ga$_{1-\xi}$As) = 1.424 + 1.247ξ (for ξ<0.45); and

E_g = 1.9 + 0.125ξ +0.143ξ^2 (for ξ>0.45). ΔE_g= 1.247ξ□(for ξ <0.45).

Dielectric constant: ε = 13.18 –3.12ξ, and ε_o = 8.854x10^{-14} F/cm

p-side: Effective mass of holes (density of states calculations) $m_h=m_p$= $[(m_{lh})^{3/2} + (m_{hh})^{3/2}]^{2/3}$ m_o, m_{lh} = 0.087 + 0.063 ξ, and m_{hh} = 0.62 + 0.14 ξ□[for GaAs, ξ = 0].Electron affinity in GaAs qχ = 4.07□eV. **HINT: Electron affinity of AlGaAs can be obtained from the following relation.**

$q\chi_2$□□Al$_\xi$Ga□□ξAs) = 4.07 - ΔE_c, as $q\chi_1-q\chi_2$ =ΔE_c; **ΔE_c = 0.6 ΔE_g** where ΔE_g= 1.247ξ□

[ΔE_c/□ΔE_v = 60/40 (i.e. ΔE_c = 0.6 ΔE_g where ΔE_g= 1.247ξ;

and **ΔE_v = 0.4 ΔE_g); as ΔE_c+□ΔE_v=□ΔE_g, ΔE_g = E_g(AlGaAs) – E_g (GaAs)].**

Q3. (a) Evaluate the threshold current density J_{TH} of a pAlGaAs-GaAs-nAlGaAs laser diode (Fig. 2) having an active layer thickness d=0.05 μm, cavity length of 500 μm, and cavity or contact width of 10μm.

Given: Internal quantum efficiency η_q= 0.95, Confinement factor Γ = 0.5, Reflectivity of cavity facets $R_1=R_2$=R= 0.3, Spontaneous emission line-width $\Delta\nu_s$ =6.2 x10^{12} Hz, Absorption coefficient in the cavity at the lasing wavelength α =20cm^{-1}, and, Z(T)~0.8. Dielectric constant: ε = 13.18 –3.12ξ, index of refraction n_r = (ε_r□$^{1/2}$.

[Note that Z(T) depends on quasi Fermi levels, which depend on forward current and hν].

(b) Compare J_{TH} with pAlGaAs-GaAs laser of Fig. 1.

Q.4. Estimate the minimum injected electron concentration n_e needed to satisfy Bernard-Duraffourg condition in an n^+-p InGaAsP homojunction laser diode operating at 300°K at 1.3microns. Given: n_i (GaAs at 300 °K) = 10^7 cm^{-3} with E_g=1.424 eV. The p-type concentration in the lasing layer (or active layer) can be assumed to be equal to n_e in order to maintain charge neutrality. **HINT**: Design set problem set for 1.55 micron.

Q.5(a). Of the two lasers emitting at 1.3 microns, one having a spectral width of 100MHz and the other 1KHz, which one will have higher temporal coherence.

(b) Why the laser pointer's output is full of small spots?

(c) Do any two spots or regions in the pointer's output have spatial coherent relationship?

(c) **Circle one**: Laser diodes have narrower or wider spectral width than LEDs.

Q.6 (a). Draw a distributed feedback (DFB) laser structure,

(b) How does its output differ from cavity type laser diode output?

(c) Draw cross-section of surface emitting lasers in cavity and DFB configurations.

Solution set 6 Lasers-I

Q1-(a) Photon Density in a Box $2L_n$*Area

=$2L_n$ * W * L   W width of Top Stripe

L Cavity length

Volume of Box = 2 * 10-4 * 10 * 10-4 * 500 * 10-4 cm3

=1.0*10-8 cm3

Electron Current at Junction $x=x_p$

$I_n(x_p) = I * \eta_{int} =$ 10 mA * 0.999

$I_n(x_p+2L_n) = In(x_p) * e^{-2}$

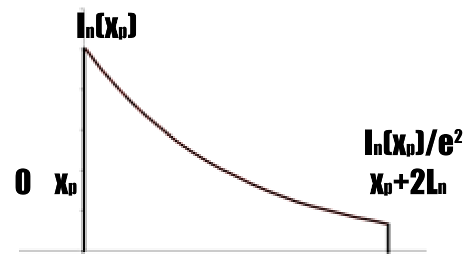

Current which generates photons is

$I_n(x_p+2L_n)$- $In(x_p) * e^{-2}$

$= I_n(x_p)[1- e^{-2}] = In(x_p)*0.8646$

No. of photons generated in $2L_n$ A volume

$$= \frac{10 \times 10^{-3} \times 0.999}{q} * 0.8646 * \eta_q$$

$$= \frac{10 \times 10^{-3} \times 0.999}{1.6 \times 10^{-19}} * 0.8646 * 0.95$$

$$= 5.1 \times 10^{16} \text{photon/Sec}$$

Approx. Simple way to find # photons/sec $= \frac{I_n(x_p) * \eta_q}{q}$ =(I * η_{int} * η_q)/q= 11.86×10^{16}(here we assume that all $I_n(x_p)$ has produced photons) Photon density $= \frac{5.1 \times 10^{16}}{1 \times 10^{-8}} = 5.1 \times 10^{24}/\text{cm}^3$

Q1-(b) Active layer d=0.1μm

Box in which photons are generated

= A*d =W*L*d=10*10^{-4} * 500 * 10^{-4} * 0.1 * 10^{-4} = 500*10^{-12} cm^3

In double heterostructure In(xp) recombine 99%or more in active" layer" d

Photons produced per second =[$I_n(x_p)$* η_q]/q =[I*η_{int}]/q

$$= \frac{(10 \times 10^{-3} \times 0.999)}{1.6 \times 10^{-19}} * 0.95 = 9.49 \times 10^{16}/\text{Sec}$$

$$\text{Photon density/Sec} = \frac{9.49 \times 10^{16}}{500 \times 10^{-12}} = 1.59 \times 10^{26}/\text{cm}^3$$

Q1-(c) Point B is corresponds to hν= E_g + kT/6.

or $E_g = \frac{1.24}{1.55\text{ um}} - \frac{0.0259}{6} = 0.795\text{ eV}$

$P\% = \frac{A \to B}{A \to \text{InP}} = \frac{0.6}{3} \times 100\%\ A \to B \Rightarrow P = 20\%\ \text{0r } 0.20$

$\text{As}\% = 0..8 \text{ as } \%\text{As} + \%\text{P} = 1$

$\text{In}\% = \frac{A \to B}{A \to \text{InP}} \times 0.47 + 0.53 = .2 \times .47 + 0.53 = 0.624$

$\text{Ga}\% = 1 - 0.71 = 0.376$

$In_{0.623}\ Ga_{0.376}\ As_{0.8}\ P_{0.2}$

Q1-(d) $m = \frac{2Ln_r}{\lambda}, \frac{\partial n_r}{\partial \lambda} = 1.5\mu m^{-1}$, L=500µm, n_r=?, Active layer $In_{.65}\ Ga_{.35}\ As_{.75}\ P_{.25}$

n_r(x,y)=3.52xy+3.39x(1-y)+3.6(1-x)y+3.56(1-x)(1-y) ; Where 'x=.65, y=.75'

Active layer n_r=1.716+0.5508+0.94+0.3115=3.5183

$$\text{Eq. 22 page 299 } \Delta\lambda = \frac{\lambda^2}{2Ln_r}\left(1 - \frac{\lambda}{n_r}\frac{\partial n_r}{\partial \lambda}\right)^{-1} = \frac{(1.55 * 10^{-4})}{2 * 500 * 10^{-4} * 3.5183}\left(1 - \frac{1.55}{3.5183} * 1.5\right)^{-1}$$
$$= 2.0133 \times 10^{-7}\text{cm} = 20.133 \times 10^{-8} = 20.13\ \text{A}^{\text{o}}$$

Q2 (a) We have computed in Q1 that the structure of Fig.2 (Double Heterojunction) has 200 times more photon density then Fig.1.

This will increase the rate of stimulated emission, which in turn will reduce the threshold current density. That is, the optical gain g will be higher at lower current in order to become $= \alpha + \frac{1}{2L}\ln(\frac{1}{R_1 * R_2})$ laser.

The structure of Fig.2 confines injected electrons in p-GaAs layer. The p-GaAs layer is made thinner than $2L_n$ by having a P-AlGaAs layer adjacent to it.

This P-AlGaAs layer stops diffusion to injected electrons n(x) or δn(x) .

How does p-GaAs- P-AlGaAs isotype heterojunction confine injected electrons in p-GaAs?

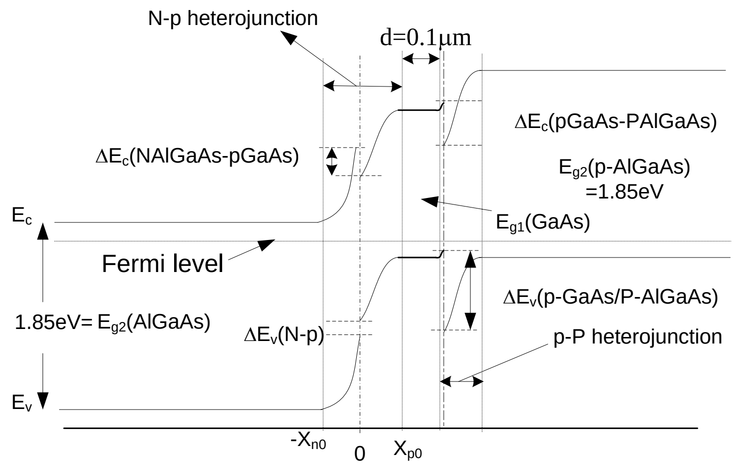

Equilibrium energy band diagram. Dotted line is Fermi Level.

Here, $\Delta E_c = 0.6\Delta E_g$, = 0.2556eV
and $\Delta E_v = 0.4\Delta E_g$ = 0.1704eV
as ΔE_g,= 1.85- 1.424 = 0.4260Ev
See Q4 Solution set #4 for E_c-E_f =0.1098eV, on N-side and E_f-E_v =0.0187eVon P-AlGaAs side.

Q2 (b) Injected electrons in P-GaAs are confined by two ΔEc's on other side of PGa layer d. Also read page 244 (last paragraph) and See Fig. 18 on page 246.

Injected holes are confined by N-AlGaAs (ΔEv) and P-AlGaAs (ΔEv)$E_{gp\text{-}AlxGa1\text{-}xAs} > Eg_{p\text{-}GaAs}$, we have assumed ΔE_g of 0.426 eV. Since $n_i^2 \big|_{pAlGaAs} << n_i^2 \big|_{pGaAs}$, we get a very small value of injected excess electron concentration Δn_{e2}, which in turn determines the excess electron concentration n_e at pGaAs-pAlGaAs boundary. This is qualitative explanation of injected electron confinements in pGaAs.

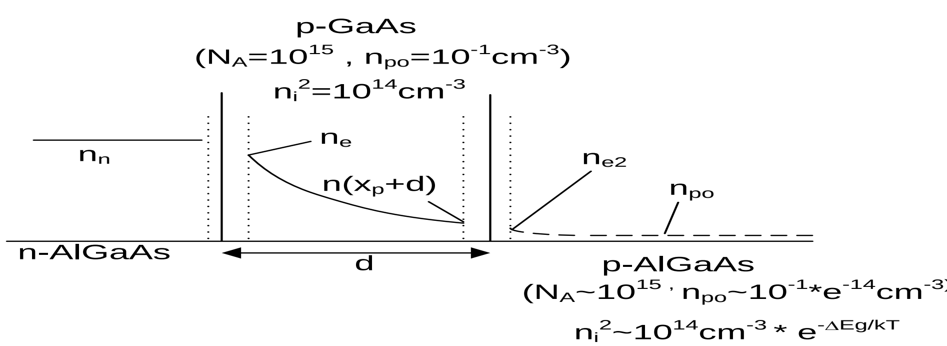

Chapter 2 Fig. 41 minority carrier profile.

In $Al_\zeta Ga_{1-\zeta}$ As the band gap is given by E_g= 1.424+0.083*ζ if ζ<0.45, ζ=0.3416

Calculation of Fermi level (E_c-E_f) in N-AlGaAs

$$n = 2\left[\frac{2\pi m_n kT}{h^2}\right]^{3/2} \times e^{\frac{-(E_c - E_f)}{KT}} \qquad - \text{Eq. 16/Page 66}$$

$$e^{\frac{E_c - E_f}{KT}} = 2\left[\frac{2\pi m_n kT}{h^2}\right]^{3/2} / n$$

m_n=(0.067+0.083*0.3416)*m_o=(0.095)*m_o=0.095*9.1*10^{-31}=8.677*10^{-32} kg

$$E_c - E_f = KT * \ln\left\{2\left[\frac{2\pi m_n kT}{h^2}\right]^{3/2} /n\right\}\ ;\ n \approx 2*10^{18}\,cm^{-3} = 2*10^{24}\,m^{-3}$$

$$= .0259 * \ln\left\{\frac{2\left[\frac{2\pi * (8.677 * 10^{-32}) * (1.38 * 10^{-23}) * 300}{(6.63 * 10^{-34})^2}\right]^{3/2}}{2 \times 10^{24}}\right\} = 0.025\ eV$$

Calculation of (E_f-E_v) in p-AlGaAs

$$p = 2\left[\frac{2\pi m_p kT}{h^2}\right]^{\frac{3}{2}} \times\ e^{\frac{-(E_f - E_v)}{KT}}$$

$p \approx N_A = 3*10^{16}\,cm^{-3} = 3*10^{22}\,m^{-3}$

$m_p=[m_{lh}^{3/2} + m_{hh}^{3/2}]^{2/3} * m_o$

m_{lh}=0.087+0.063*ζ =0.087+0.063*0.3416=0.108

m_{hh}=0.62+0.14*ζ =0.62+0.14*0.3416=0.667

$m_p=[0.108^{3/2} + 0.667^{3/2}]^{2/3} * m_o$ =[0..354 + 0.5447] $^{2/3}$ * m_o

=0.6955*9.1*10^{-31}=6.32*10^{-31} kg

$$E_f - E_v = KT * \ln\left\{\frac{2 * \left[\frac{2\pi m_p kT}{h^2}\right]^{3/2}}{p}\right\}$$

$$= .0259 * \ln\left\{\frac{2 * \left[\frac{2\pi * 6.32 * 10^{-31}\ \ * 1.38 * 10^{-23} * 300}{(6.63 * 10^{-34})^2}\right]^{3/2}}{3 \times 10^{22}}\right\} = 0.16\ eV$$

Similarly, we can calculate the Fermi level in pGaAs.

Q2 (c) Find the forward current for Fig1 diode at $V_f\ = 1.2\ V$ N $Al_{0.35}Ga_{0.65}$As- pGaAs Diode:

$$I_N \quad = \frac{q * A * D_N * n_{po}}{L_n} * \left(e^{\frac{qV_f}{kT}} - 1\right)$$

A = W*L = 10μm $* 500\mu m\ = 5000 * 10^{-8}\,cm^2\ = 5 * 10^{-5}\,cm^2$

$$D_N\ = 100\,\frac{cm^2}{sec}$$

$$n_{po} = \frac{n_{i\ (GaAs)}^2}{N_A} = \frac{(10^7)^2}{3 * 10^{16}} = 3.3 * 10^{-3} cm^{-3}$$

L_n=$\sqrt{D_N * \tau_N}$=$\sqrt{100 * 10^{-8}}\ = 10^{-3}$ cm

$$I_N = \frac{(1.6 * 10^{-19}) * (5 * 10^{-5}\,) * (100) * (3.3 * 10^{-3}\,)}{10^{-3}} * \left(e^{\frac{1.2}{0.0259}} - 1\right)$$

$$I_N = \frac{(1.6 * 10^{-19}) * (5 * 10^{-5}\,) * (100) * (3.3 * 10^{-3}\,)}{10^{-3}} * (1.3235 * 10^{20})$$

$I_N = 0.349$ A = 349 mA, (Dominant Term)

Hole current; $I_p = \frac{q*A*D_P*P_{no}}{L_p}\left(e^{\frac{qV_f}{kT}} - 1\right)$

$$A = W*L = 10\mu m * 500\mu m = 5000 * 10^{-8}\, cm^2 = 5 * 10^{-5}\, cm^2$$

$$D_P = 10 cm^2/s\ ,$$

$$P_{no}(AlGaAs) = \frac{n_{i\,(AlGaAs)}^2}{N_D} = \frac{4.88 * 10^6}{2 * 10^{18}} = 2.443 * 10^{-12}$$

$$\frac{n_{i\,(AlGaAs)}^2}{n_{i\,(GaAs)}^2} = \frac{e^{\frac{-Eg2}{2KT}}}{e^{\frac{-1.424}{kT}}}$$

$$n_{i\,(AlGaAs)}^2 = 10^{14} * e^{\frac{-(Eg2-Eg1)}{kT}} = 10^{14} * 4.887 * 10^{-8}$$

$$= 4.88 * 10^6 cm^{-3}$$

$$L_P = \sqrt{D_P * \tau_P} = 1.414 * 10^{-4}\, cm$$

$$I_p = \frac{(1.6 * 10^{-19}) * (5 * 10^{-5}) * (10) * (2.443 * 10^{-12})}{1.414 * 10^{-4}} * (1.3235 * 10^{20})$$

$$= 1.8294 * 10^{-10}\ Amp$$

Total Current I =$I_N + I_p \approx 0.349$A

Q3 (a) Double heterostructure laser of Fig. 2

$$J_{TH} = \frac{8\pi * n_r^2 * \Delta v_s * q * d * v^2}{\Gamma\eta_q z(T)\lambda^2}[\alpha + \frac{1}{2L}\text{In}\left(\frac{1}{R1\ R2}\right)]$$

Parameters:

d=0.05 μm=0.05*10^{-4}cm

L=500 μm,   W = 10μm

$n_{r(GaAs)} = 3.63$

R1, R2=0.3

$\Gamma = 0.5$

$\Delta v_s = 6.2 * 10^{12}$Hz

$Z(T) = 0.8$, $\eta_q = 0.95$, $\alpha = 20\ cm^{-1}$

$\lambda = 0.84\mu$m.

$$\frac{1}{2L}\text{In}\left(\frac{1}{R1\ R2}\right) = \frac{1}{2 * (500 * 10^{-4})}\text{In}\left(\frac{1}{0.3 * 0.3}\right) = 24.07$$

$$\alpha + \frac{1}{2L}\text{In}\left(\frac{1}{R1\ R2}\right) = 20 + 24.07 = 44.07 cm^{-1}$$

$$J_{TH} = \frac{8\pi * n_r^2 * \Delta v_s * q * d}{\Gamma * \eta_q * Z(T) * \lambda^2}[\alpha + \frac{1}{2L}\text{In}\left(\frac{1}{R1\ R2}\right)]$$

$$J_{TH} = \frac{8\pi*(3.63)^2*(6.2*10^{12})*(1.6*10^{-19})*(0.05*10^{-4})}{0.5*0.95*0.8*(0.84*10^{-4})^2}[44.07] = 26.99\ A/cm^2$$

If d is higher J_{TH} will be higher, J_{TH} is lower Γ is higher

Here Γ =0.5 for d=0.05 μm is quite small.

As you see in Q4 $\Gamma \cong 0.1$ or 0.02.

I_{TH}=$J_{TH} * w * L = 26.99 * 10\mu m * 500\ \mu m = 26.99 * 0.5 * 10^{-4} = 1.349$ mA

$E_{fn} - E_{fp} > h\nu > E_g$
E_g=1.424 eV
Approx.1 $h\nu = E_g + \frac{kT}{2}$
Approx.2 $h\nu = Eg + \frac{h\Delta\nu_s}{3} = 1.424 + \frac{h*6.2*10^{12}}{3} = 1.4325\text{eV}$
$\lambda = \frac{1.24}{1.4325}$=0.8655 μm,

Our wavelength is smaller than 0.8655 microns. We have used $\lambda = 0.84\mu\text{m}$
Q. 3b For the single heterostructure laser (Fig.1)
d=2-3*L_n
d=20*10^{-4}cm = 20μm
(use the value of Ln from Q2 InPGaAs)
L_n=$\sqrt{\tau_n * D_n} = \sqrt{10^{-8} * 100}$=10*$10^{-4}$cm
As compared to Q3 (a) d is very large
$J_{TH} = \frac{26.99}{0.05} * 20 = 1.079 * 10^4 \text{A/cm}^2$
Q4 Bernard-Duraffourg condition relates the quasi Fermi levels E_{fn} *and* E_{fp} the emission photon energy in a laser; $(E_{fn} - E_{fp}) > h\nu > E_g$
hν for 1.3 μm laser is $\frac{1.24}{1.3\mu\text{m}} = 0.9538 \sim 0.954$ eV.

$$\text{Since, } h\nu \cong E_g + \frac{kT}{3}, E_g = h\nu - \frac{kT}{3}, E_g = 0.954 - \frac{0.0259}{3} = 0.9454\text{eV}, \qquad E_g = 0.9454\text{eV}$$

The electron concentration n_e in the p-GaAs active layer is; $n_e = n_i\, e^{\frac{(E_{fn} - E_{fp})}{2KT}}$ or
$(E_{fn} - E_{fp}) > h\upsilon$; assume $(E_{fn} - E_{fp}) = 0.96\text{ev}$
$n_e = 1.28 * 10^{11} * e^{\frac{0.96}{2*0.0259}} = 1.43 * 10^{19}\text{cm}^{-3}$

Evaluation of n_i in simple form in InGaAsP

$n_i(\text{GaAs}) = 10^7\text{cm}^{-3}$ This is assumed.
$n_i \propto e^{\frac{-Eg}{2kT}}$

$$\frac{n_i\,(\text{GaAs})}{n_i(\text{InGaAsP})} = \frac{e^{\frac{-1.424}{2KT}}}{e^{\frac{-0.945}{2KT}}}$$

$n_i(\text{InGaAsP}) = 10^7 * e^{\frac{(1.424-0.945)}{2*0.0259}}$=$10^7 * e^{\frac{0.479}{2*0.0259}}$ = 1.029*10^{11}cm^{-3}
Q5 (a) The laser line width Δν= 1KHz will have a higher temporal coherence.
Q5 (b) Laser pointer output spot has speckles. This is due to multiple transverse and lateral modes.
Q5 (c) No
Q5 (d) Laser diodes have narrower spectral width than 1.3 μm LEDs.

Q. 6. (a) Distributed feedback lasers are distinct from cavity type lasers. Here a grating is created in one of the cladding layers. This is achieved by selective etching and re-growth. Figure below shows the structure. The high-low index grating is formed using Al0.07Ga0.93As and Al0.3Ga0.7As layers.

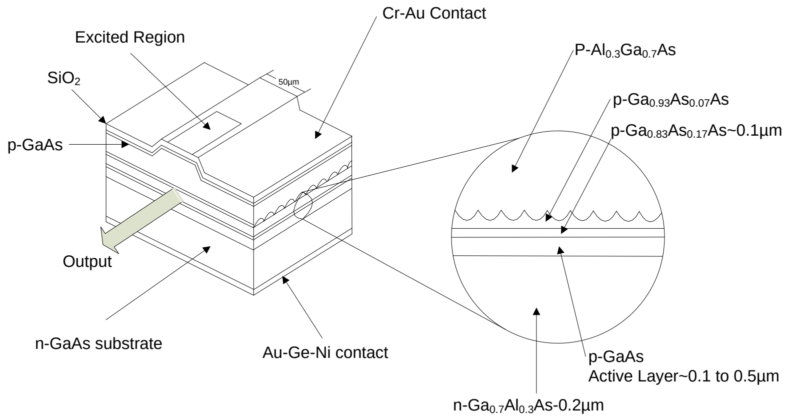

Fig. 48. 3-D view of a distributed feedback laser. The inset shows the details of cladding.

(b) Emission spectrum of a distributed feedback laser (double heterojunction type). Ref. Nakamura et al, APL 25, 487(1974). Note the absence of the axial cavity modes normally seen in heterojunction lasers with cleaved reflectors. (This is not meant to imply that the other modes are not present.)

The modes separation is higher than in cavity laser. In cavity $\Delta\lambda$ =1-2Å, in DFB it is 43Å.

(c). Surface emitting laser in a DFB configuration uses a second order grating.

In cavity type laser, as drawn on the board in the class, the active layer is sandwiched between two high low index □/4 quarter wave mirrors (the periods of this dielectric stack determines the R1 and R2). The mirrors are separated by two $\lambda/2$ spacer layers.

References

1. K. Kuhn, Laser Engineering, Prentice Hall, 1998.
2. G. P. Agrawal and N.K. Dutta, "Semiconductor Lasers", 2nd Edition, Van Nostrand Reinhold, New York, 1993.
3. S.M. Sze, "Physics of Semiconductor Devices", 2nd Edition, John Wiley & Sons, 1981.
4. L. A. Coldren and S. W. Corzine, "L.A. Coldren, S. W. Corzine and M. Mashanovitch, Diode Lasers and Photonic Integrated Circuits", John Wiley & Sons, 2012.
5. B.G. Streetman, S. Banerjee, "Solid State Electronic Devices", 5th Edition, Prentice Hall, New Jersey, 2000.
6. R.S. Muller, T. I. Williams, M. Chan, "Device Electronics for Integrated Circuits", 3rd Edition, John Wiley & Sons, 2003.
7. W. Liu, Handbook of III-V Heterojunction bipolar transistors, John Wiley, 1998.
8. A. Yariv, Introduction to Optical Electronics, Holt, Reinhart, and Winston, 1991.
9. Nakamura et al, APL 25, 487(1974).
10. H. C. Casey and M. B. Panish, Heterostructure Lasers (Part I and II), Academic Press, 1978.
11. H. Yonezu, K. Kobayashi and I. Sakuma, Threshold current density and lasing transverse mode in a GaAs-$Al_xGa_{1-x}As$ double heterostructure laser, Jap. J. Applied Phys. 12, pp. 1593-1599, October 1973.
12. T. S. Moss, G. J.Burrell, and B. Ellis, Semiconductor Optoelectronics, Wiley, 1973.
13. F. Jain, S. Srinivasan, E. Heller, R. LaComb, M. Gokhale, W. Huang, Monolithic Integration of Red, Blue and Green Lasers for Smart Projection Displays, J. Soc. Information Display (SID), 5, pp. 241-250.
14. F.C. Jain, "Transistor Lasers," U.S. Patent Number 5,239,550, August 24, 1993. Also see F. Jain et al, ISDRS conference 1991.
15. F. Jain, and W. Huang, "Modeling of Optical Gain in InGaN-AlGaN and $In_xGa_{1-x}N$-$In_yGa_{1-y}N$ Quantum Well Lasers", IEEE J. Quantum Electronics, QE-32, No. 5, pp. 859-864, May 1996.
16. R. LaComb, and F. Jain, "A Self-Consistent Model To Simulate Large-Signal Electrical Characteristics Of Resonant Tunneling Bipolar Transistors", Solid-State Electronics Vol. 39, pp. 1621-1627, November 1996.
17. W. Huang, and F. Jain, "Temperature insensitivity of threshold current density in exciton- dominated wide energy gap quantum wire lasers", Optical Engineering 40(5) 1 (May 2010).
18. S. Cheung, F. Jain, R. Sacks, D. Cullen, G. Ball, and T. Grudkowski, "High Contrast Fabry-Perot Optical Modulator Using Quantum Confined Stark Effect Tuning in InGaAs-GaAs Multiple Quantum Well Cavity", Appl. Phys. Lett., 63, July 19, 1993.
19. J. Jahns et al, Optical interconnects using top-surface-emitting microlasers and planar optics, Applied Optics, 31, pp. 592-596, 1992.

20. J. L. Jewell et al, Surface emitting microlasers for photonic switching and interchip connections, Opt. Eng. 29, pp. 210-214, 1990.

7.14. Threshold current density in Quantum wire/dot Structures

The threshold occurs when the gain becomes equal to all the losses at the operating wavelength λ.

The threshold current density is related to the excitonic gain coefficient [6]

The threshold current density J_{th} is obtained by setting the gain equal to the sum of various loss coefficients (free carrier α_f, scattering α_c and diffraction loss α_d) as expressed by Eq. (11).

$$g = \frac{1}{2L}\ln\left(\frac{1}{R_1 R_2}\right) + \alpha_f + \alpha_c + \alpha_d \qquad (3)$$

If we account for the losses in active layer as well as in the cladding layer, we get

$g = [\Gamma\alpha_{FC,AL} + (1-\Gamma)\,\alpha_{FC,CL} + \Gamma\alpha_{DIFF,AL} + (1-\Gamma)\,\alpha_{DIFF,CL} + (1/2L)\ln(1/R_1R_2)]$.

B. Here, we have used $\alpha_{FC,CL}$ for the losses in the core due to free carrier as well as other scattering losses. $\alpha_{DIFF,CL}$ is the loss due to diffraction in the cladding.

C.

D. Substituting in for J, we get

$J_{TH} = [\{q\, d\, \Delta\nu_s\, 8\, \pi\, \nu^2\, n_r^2\}/\{\eta_q\, c^2\}]$
$[\Gamma\alpha_{FC,AL}+(1-\Gamma)\alpha_{FC,CL}+\Gamma\alpha_{DIFF,AL}+(1-\Gamma)\alpha_{DIFF,CL}+(1/2L)\ln(1/R_1R_2)]\,[1-\exp\{h\nu-\Delta\zeta\}/kT]^{-1}$

Here, L is the length of the cavity and R_1 and R_2 are the mirror reflectivities.

4. Quasi Fermi Levels E_{fn}, E_{fp}, and $\Delta\zeta$

Quasi Fermi levels are evaluated using charge neutrality condition. In the case of quantum wells and wires and dots, it is given below.

Quantum Wells

$$\frac{m_e}{\pi\hbar^2 L_x}\int_E^{\infty}\frac{dE}{1+e^{(E-E_{Fn})/kT}} = \frac{m_{hh}}{\pi\hbar^2 L_x}\int_{E_{hh}}^{\infty}\frac{dE}{1+e^{(E-E_{Fn})/kT}} + \frac{m_{lh}}{\pi\hbar^2 L_x}\int_{E_{lh}}^{\infty}\frac{dE}{1+e^{(E-E_{Fn})/kT}} \quad --(4)$$

Quantum Wires

$$\frac{(2m_e)^{1/2}}{\pi\hbar L_x L_y}\int_{E_e}^{\infty}\frac{(E-E_e)^{-1/2}dE}{1+e^{(E-E_{Fn})/kT}}=\frac{(2m_{hh})^{1/2}}{\pi\hbar L_x L_y}\int_{E_{hh}}^{\infty}\frac{(E-E_{hh})^{-1/2}dE}{1+e^{(E-E_{Fn})/kT}}+\frac{(2m_{lh})^{1/2}}{\pi\hbar L_x L_y}\int_{E_{lh}}^{\infty}\frac{(E-E_{lh})^{-1/2}dE}{1+e^{(E-E_{Fn})/kT}}--(5)$$

Quantum Dots

The charge neutrality condition for dots is:

$$\frac{1}{L_x L_y L_z}\int_{E_{e(l,m,n)}}^{\infty}\frac{\delta(E-E_{e(l,m,n)})\ dE}{1+e^{(E-E_{Fn})/kT}}=\frac{1}{L_x L_y L_z}\int_{E_{hh(l,m,n)}}^{\infty}\frac{\delta(E-E_{hh(l,m,n)})dE}{1+e^{(E-E_{Fn})/kT}}$$

$$\underrightarrow{or}=\frac{1}{L_x L_y L_z}\int_{E_{lh(l,m,n)}}^{\infty}\frac{\delta(E-E_{lh(l,m,n)})\ dE}{1+e^{(E-E_{Fn})/kT}}--(6)$$

In the case of quantum dots, we take either heavy or light holes.

5. Operating Wavelength λ:

E.
F. The operating wavelength of the laser is determined by resonance condition
G. $L=m\lambda/n_r$
H. Since many modes generally satisfy this condition, the wavelength for the dominant mode is obtained by determining which gives the maximum value of the value of the gain. In addition, the index of refraction, n_r, of the active layer is dependent on the carrier concentration, and knowing its dependence on the current density or gain is important.
I. For this we need to write the continuity equation.

6. Continuity equation and dependence of index of refraction on injected carrier concentration

J.

The rate of increase in the carrier concentration in the active layer due to forward current density J can be expressed as:

$$\frac{dn}{dt}=\frac{J}{qd}-\frac{(n-n_{po})}{\tau_n}-\frac{\Gamma g_m}{E}(\beta I_{sp}+I)--(7)$$

here, n_{po} is the equilibrium minority carrier concentration, □$_n$ is the carrier lifetime, □ is the spontaneous emission coefficient which gives coupling of I_{sp} into a guided laser mode, g_m is the material gain [g_m = a (n – n_o) - a_2 (□□□□□□$_p$) ~ a (n – n_o); here a is known and n_0 is the carrier concentration at the transparency].

Equation (7) simplifies to

$$\frac{dn}{dt}=\frac{J}{qd}-\frac{(n)}{\tau_n}-\frac{\Gamma g_m}{E}(\beta I_{sp}+I_{av})--(8)$$

Equation 8 neglects equilibrium minority concentration n_{po}. We can neglect I_{av} which is the intensity from an external light signal (as in the case of a laser amplifier).

The phase condition

L= m λ/2 n_r

is modified as n_r is a function of the carrier concentration n.

K. 7. Direct computation of gain dependence on photon energy
L.
M. Gain coefficient can be calculated directly from the absorption coefficient and Fermi-Dirac distribution functions. However, it depends on the nature of transitions. We are considering free electron-hole and excitonic transitions. Of these the excitonic transitions are relevant in the case of wide energy semiconductors such as GaN, ZnSe, related ternary and quaternary compounds, and other low dielectric constant and wide energy gap semiconductors including organic semiconductors.

N. Free Carrier Transitions

C. Optical Gain in Quantum Wells

O. The gain coefficient expression is:

$$g_{free}(\omega)=\frac{2\pi e^2}{\varepsilon_0 n_r m_0 c\omega L_Z}\sum_{l,h}[\frac{m_{eh}}{\pi\hbar^2}|M_b|^2\bullet$$
$$\bullet\left|\int\Psi_e(z)\Psi_h(z)dz\right|^2\bullet\int\rho(E)\bullet L(E)dE(f_e+f_h-1)]$$

Here, the polarization factor ρ(E) for free carrier transition in quantum wire is taken from the literature [5]. L_z is the well thickness, E_e and E_h are the ground state energies for electron and hole inside the quantum well. Mb is the matrix element and L(E) is the line shape function. The summation is over the heavy hole and light hole.

D. Optical Gain in Quantum Wires

The gain coefficient due to free carrier band-to-band transitions in quantum wire lasers can be expressed by substituting for α as:

$$g_{free}(\omega)=\frac{2\pi e^2}{\varepsilon_0 n_{rm_0} c\omega L_x}\sum_{l,h}[\frac{(2m_{eh})^{1/2}}{\pi\hbar L_y L_z}|M_b|^2\bullet\left|\int\Psi_e(y)\Psi_h(y)dy\right|^2 \quad (9)$$
$$\bullet\int\Psi_e(z)\Psi_h(z)dz|^2\bullet\int(E-E_e-E_h)^{-1/2}\rho(E)\bullet L(E)dE(f_e+f_h-1)]$$

where the polarization factor ρ(E) for free carrier transition in quantum wire is taken from the literature [5]. E_e and E_h are the ground state energies for electron and hole inside the quantum wire. The summation is over the heavy hole and light hole.

E. Optical Gain in Quantum Dots

The gain coefficient in a quantum dot for free electron-hole transitions can be expressed by modifying Eq. 4 (b) .

$$g_{free}(\omega) = \frac{2\pi e^2}{\varepsilon_o n_r m_o c\omega} \sum_{l,h} [(\frac{2}{L_x L_y L_z}) | M_b|^2 \bullet | \int \psi_e(x)\psi_h(x)dx |^2$$

$$\bullet | \int \psi_e(y)\psi_h(y)dy |^2 \bullet | \int \psi_e(z)\psi_h(z)dz |^2 \rho(E)$$

$$\bullet \frac{1}{\sqrt{\pi}\delta} e^{[(\hbar\omega - \hbar\omega)^2/\delta^2]}] \quad \bullet (f_c + f_v - 1) \qquad (10)$$

Here, the polarization factor ρ(E) is for free carrier transitions and is taken from the literature [5]. The summation is over the heavy and light holes.

P. Excitonic Transitions

Optical Gain in Quantum Wire Structures

In case of quantum wires, the exciton density of states N_{ex}(wire) equals to

$2\pi^{1/2} |\phi_{ex}(0)|^2/L_y L_z$,

and the overlap function is $| \Psi_e(y)\Psi_h(y)\, dy|^2 \bullet | \Psi_e(z)\Psi_h(z)\, dz|^2$. Substituting the exciton density and overlap function in Eq. 3, we get

$$g_{ex}(\omega) = \frac{2\pi e^2}{\varepsilon_o n_r m_o c\omega L_y L_z} \sum_{l,h} [| M_b|^2 \bullet 2\pi^{1/2} |\phi_{ex}(0)|^2$$

$$\bullet (| \Psi_e(y)\Psi_h(y)dy |^2 | \Psi_e(z)\Psi_h(z)dz |^2) \bullet \rho_{ex} \bullet \mathrm{L}(E_{ex}) \bullet (f_c + f_v - 1)]$$

(11)

Here, $|\phi_{ex}(0)|^2$ is related to a, the variational parameter or exciton radius, as $(2/\square a^2)^{1/2}$. The details are given in our paper [3].

Optical Gain in Quantum dot Structures

In case of quantum dots, the exciton density N_{ex}(dot) is expressed as

$N_{ex}(dot) = 1/(L_x L_y L_z) = 1/[4\pi a^3_{Bex}]$, and the overlap function is | $\Psi_e(x)\Psi_h(x)\,dx|^2 \bullet | \Psi_e(y)\Psi_h(y)\,dy|^2 \bullet | \Psi_e(z)\Psi_h(z)\,dz|^2$. Substituting these in Eq. 3, the excitonic gain coefficient for quantum dots is expressed by

$$g_{ex}(\omega) = \frac{2\pi e^2}{\varepsilon_o n_r m_o c\omega} \sum_{l,h} [(\frac{2}{(4\pi/3) a^3_{B,ex}}) | M_b|^2 \bullet | \int \psi_e(x)\psi_h(x)dx |^2 \\ \bullet | \int \psi_e(y)\psi_h(y)dy |^2 \bullet | \int \psi_e(z)\psi_h(z)dz |^2 \rho_{ex} \\ \bullet \frac{1}{\sqrt{\pi}\delta} e^{[(\hbar\omega_{ex}-\hbar\omega)^2/\delta^2]}] \bullet (f_c + f_v - 1) \qquad (12)$$

In quantum wires, we add both free and excitonic contributions. However, in the case of quantum dots, we need to consider excitonic part only.

8. Comments

ix) The absorption coefficient α_{FC} and □α_{DIFF} which appear in the threshold condition represents the free carrier absorption and diffraction loss (they vary 20-40 cm^{-1} in value and do not represent interband transitions).

x) The confinement factor depends on the waveguide construction. It's value is 2-2.5% in quantum well, wire and dot lasers.

xi) Spontaneous line width $\Delta\nu_s$ does depend on well, wire, and dots.

xii) L_x is the active layer thickness (i.e. the thickness of well in quantum well, thickness in the transverse direction in quantum wire and dots); L_y is the wire dimension along the lateral direction; and L_z refers to the dot dimension along the length of the cavity. ***Note: I have changed L_z by L_x in the threshold equation (2). It is the same as d.***

xiii) The quasi Fermi levels are different in three cases.

xiv) For a given operational wavelength the value of material composition will be different due to shift in the energy levels.

xv) The Gain coefficient variation with λ at a given current will be different for well, wire, and dots.

xvi) The quantum efficiency η_q is somewhat different. The difference is significant in heavily dislocated materials and in which exciton transitions are dominant.

7.15. Comparison of Double Heterostructure, Quantum Well, Quantum Wire, and Quantum Dot Laser Parameters

nAlGaAs-pGaAs-pAlGaAs Double Heterostructures (DH):

This treatment is to understand the confinement of injected electrons in pGaAs layer. This is the active layer where electrons and holes recombine emitting photons. The narrowness of this active layer (lower value of d) results in reduced threshold current density J_{TH}. The introduction of P-*AlGaAs layer results in reducing the number of minority holes at the pGaAs-PAlGaAs boundary* $\boldsymbol{x=x_p+d}$. *Figure 6 shows schematically a double heterostructure diode.The details of N-p heterojunction and p-P isotype (same conductivity, p and P) heterojunction are shown in Fig. 7.*

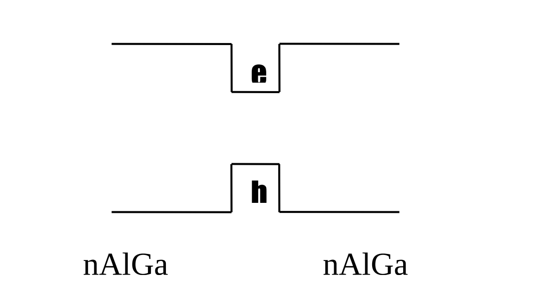

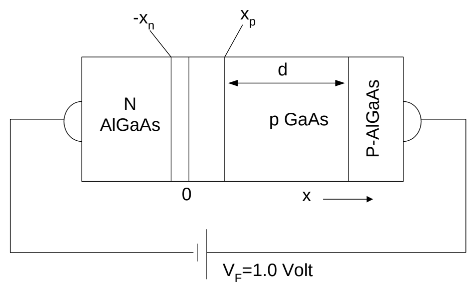

Fig. 6. A forward biased NAlGaAs-pGaAs-PAlGaAs double heterojunction diode.

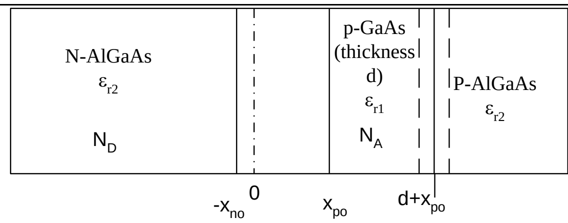

Figure. 7. A double heterostructure NAlGaAs-pGaAs-PAlGaAs diode.

The minority concentrations in various regions are shown in Fig. 8. Note that n_{e2} is determined by n_{po}(P-AlGaAs), which is quite low as compared to pGaAs. And n_{e2} determines the boundary value of n_p(at $x = x_p + d$, using the coordinate system of Fig. 7.) Thus, the addition of P-AlGaAs at x=xp+d forces the injected electron concentration quite small. That is, it forces all injected carrier to recombine in the active layer. This is known as carrier confinement.

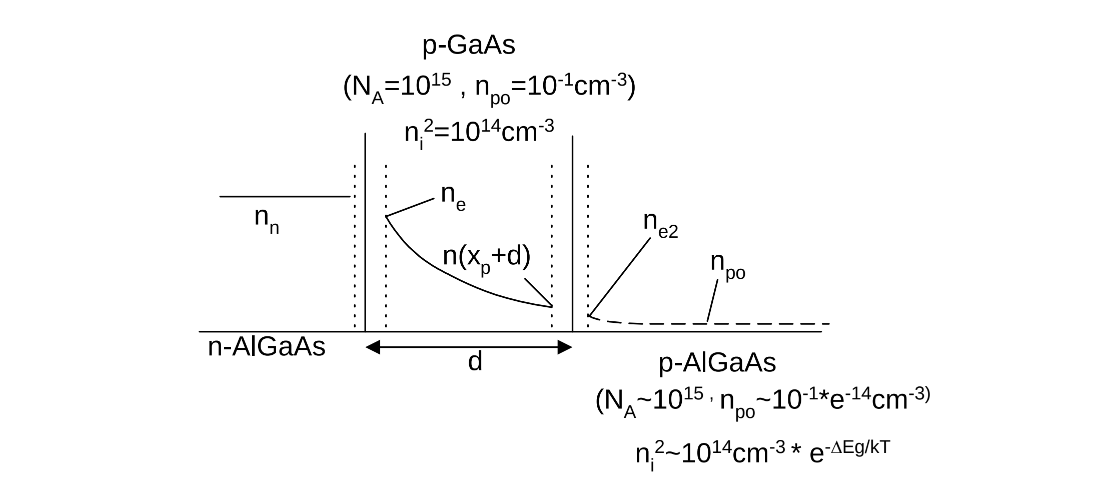

Figure 8. Minority carrier concentration in p-GaAs and in p-AlGaAs. We have assumed a bandgap difference of 0.35eV

The energy band diagram is given in Fig. 9.

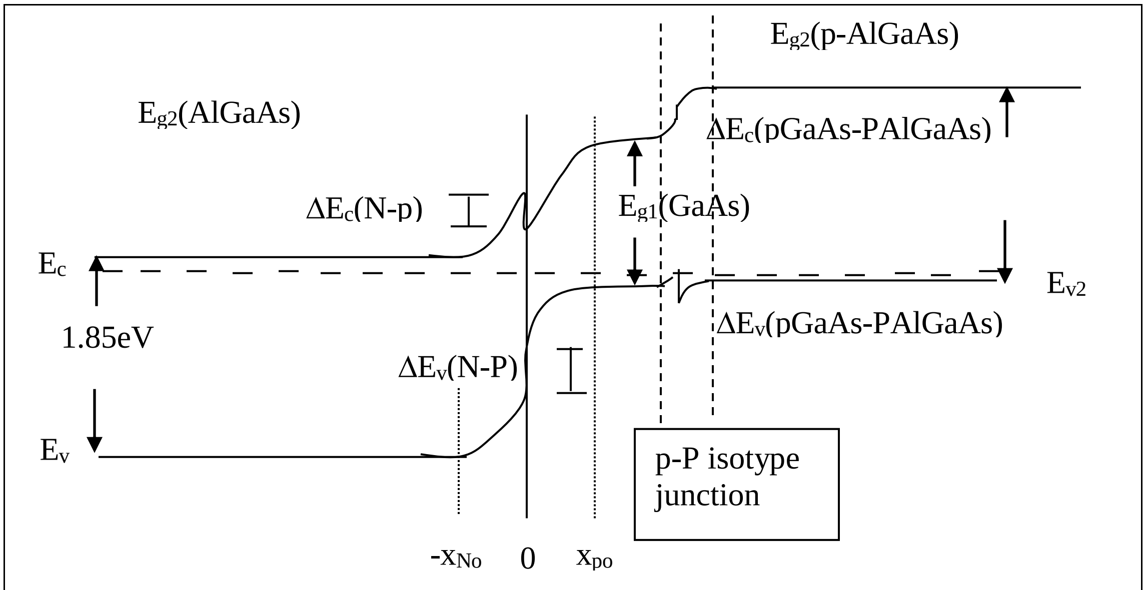

Fig. 9 Energy band diagram of a NAlGaAs-pGaAs-PAlGaAs double heterostructure diode.

Optical confinement:

As is evident from waveguiding fundamentals, we need to sandwich the active layer between two lower index of refraction layers. AlGaAs fits that requirement. In addition, it is lattice matched to GaAs. In the laser design example, we have mentioned various methods for the calculation of modes in such a slab waveguide. Also we need to calculate the confinement factor □□of the mode. Confinement factor also determines the J_{TH}. Generally, the confinement factor becomes smaller as the thickness of the active layer becomes narrower. This also depends on the index of refraction difference between the active and the cladding layers.

Photon Confinement in the Active Layer:

In this structure, p-AlGaAs and n-AlGaAs cladding layers (having lower index of refraction n_{r1}, depending on the Aluminum concentration) sandwich the nGaAs layer that has a larger index of refraction n_{r2}. As a Optical confinement:

As is evident from waveguiding fundamentals, we need to sandwich the active layer between two lower index of refraction layers. AlGaAs fits that requirement. In addition, it is lattice matched to GaAs. In the laser design example, we have mentioned various methods for the calculation of modes in such a slab waveguide. Also we need to calculate the confinement factor □□of the mode. Confinement factor also determines the J_{TH}. Generally, the confinement factor becomes smaller as the thickness of the active layer becomes narrower. This also depends on the index of refraction difference between the active and the cladding layers.

Carrier confinement in a double Heterostructure (DH) laser:

Figure 6 shows a p-AlGaAs-nGaAs-nAlGaAs DH laser structure. Here, n-GaAs is the active layer. Generally, this structure is realized on an n-GaAs substrate, and the p-AlGaAs layer has a thin p^+-GaAs cap layer. The heavy doped substrate and the cap layer serves to form Ohmic contacts. In addition, the substrate provides the mechanical support.

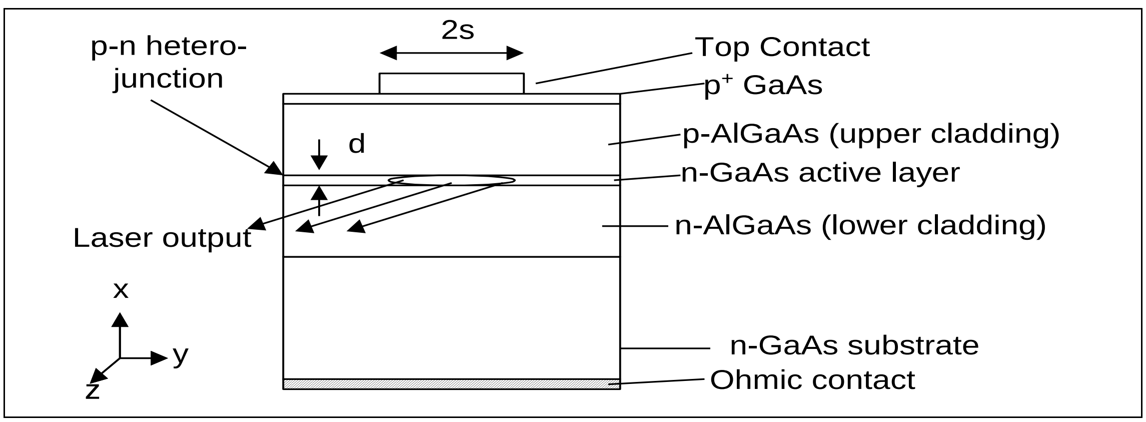

result this causes waveguiding along the x-direction. Depending on the index difference Δn and the active layer thicnkness, the waveguide will support fundamentals or higher TE (transverse electric) modes.

Electron and Hole Confinement in the Active layer:

We have seen that in a pAlGaAs-nGaAs heterojunciton, the minority carriers are not injected from a lower energy gap (E_{g2}, n-GaAs) semiconductor into a larger energy gap (E_{g1}) semiconductor (p-AlGaAs). This is due to the band discontinuity ΔE_c (or ΔE_v for holes injection from pGaAs into n-AlGaAs in nAlGaAs-pGaAs heterojunctions).

Another property of a heterojunction, in this case isotype n-GaAs/n-AlGaAs, is that the injected minority holes from the p-AlGaAs emitter are confined into the nGaAs layer only. The nAlGaAs acts as a barrier for the hole transport. This confines the injected minority holes within the nGaAs active layer. To maintain the charge neutrality, equal concentration of electrons are supplied by the Ohmic contact on the side. This aspect is illustrated in Fig. 7. Here, a p-n GaAs homojunction is compared with a p-n double heterojunction.

Once the electrons and holes are confined to the lower energy gap GaAs active layer, photons are emitted in this layer. The confinement of photons into a thinner (than homojunctions) active layer ensures reduced threshold current density J_{TH}.

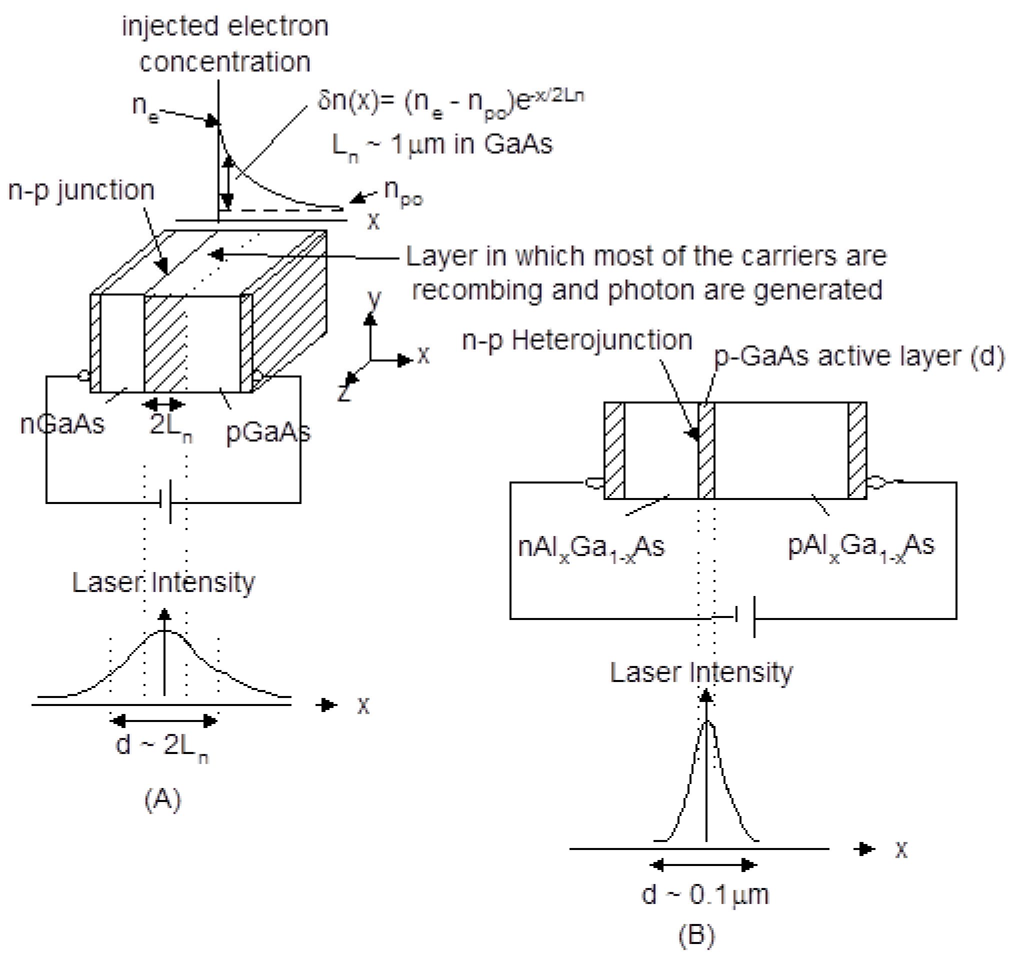

Fig. 7. Comparison of transverse lasing intensity distribution in: (A) n-p GaAs homojunction and (B) n-p double heterojunction. Note the mode confinement and increased laser intensity for the same injection current.

Homojunction Device A: Electrons are injected from the n-GaAs side into p-side. The injected minority electrons recombine with holes. The electron population declines by $1/e^2$ within a distance of $2L_n$ from the junction. Emitted photons are confined within a cavity of length L and thickness $2L_n$. The width of the cavity is determined by the top contact stripe as shown in figure6.

Double Heterojunction Device B: In contrast (to structure A), the injected electrons are confined to the p-GaAs layer of thickness d. The thickness of this layer can be made much smaller than $2L_n$. Typical value of d is 0.1μm in double Heterostructures. In the case of quantum well lasers, grown by molecular beam epitaxy or MOCVD, this thickness could be in the range of 50 – 100 Å.

As $d << L_n$, the threshold current density in DH and quantum well lasers is much smaller than homojunction lasers.

How does this happen? The role of p-$Al_xGa_{1-x}As$ is crucial in the restriction of electrons in the p-GaAs region.

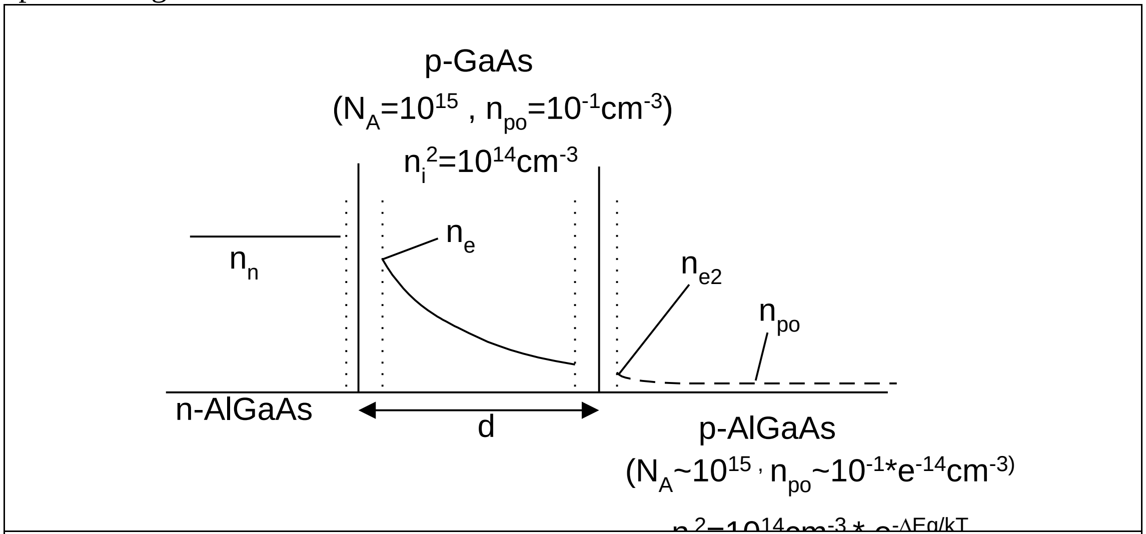

Figure8. Minority carrier concentration in p-GaAs and in p-AlGaAs. We have assumed a bandgap difference of 0.35eV

$Eg_{pAlxGa1-xAs} > Eg_{p-GaAs}$, we have assumed ΔE_g of 0.35 eV. Since $n_i^2|_{pAlGaAs} << n_i^2|_{pGaAs}$, we get a very small value of $n_{p0}|_{pAlGaAs} << n_{p0}|_{pGaAs}$. A reduced value of n_{po} in p-AlGaAs determines the value of injected excess electron concentration Δn_{e2}, which in turn determines the excess electron concentration n_e at pGaAs-pAlGaAs boundary. This is a qualitative explanation of injected electron confinement in p-GaAs.

a. Single Transverse
b. Single Lateral

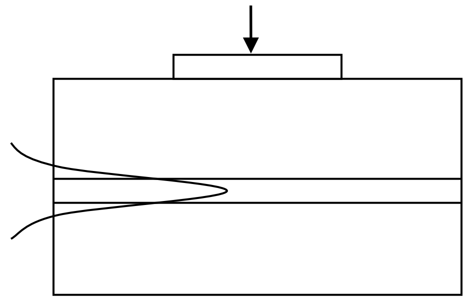

$n^{C}_{guide} < n^{middle}_{guide}$

$$W = \frac{m\lambda}{2\sqrt{(n_g^m)^2 - (n_g^c)^2}}$$

Fig. 63 Single Mode

Single Longitudinal: Large $\Delta\lambda$ separation
Cavity Lasers: 1-2Å
Distributed Feedback Lasers: ~40 Å

a.<u>Transverse Mode:</u>

Active layer thickness (d), to cut-off TE_1
(Three Slab Waveguide)

b. Lateral Mode: Stripe Geometry (width, W)

Gain Guiding
Index Guiding

Creation of Stripe

SiO_2 (oxide) mask
Buried Heterostructure (Fig 15.15, Yariv)
Etching to create a ridge (waveguide)

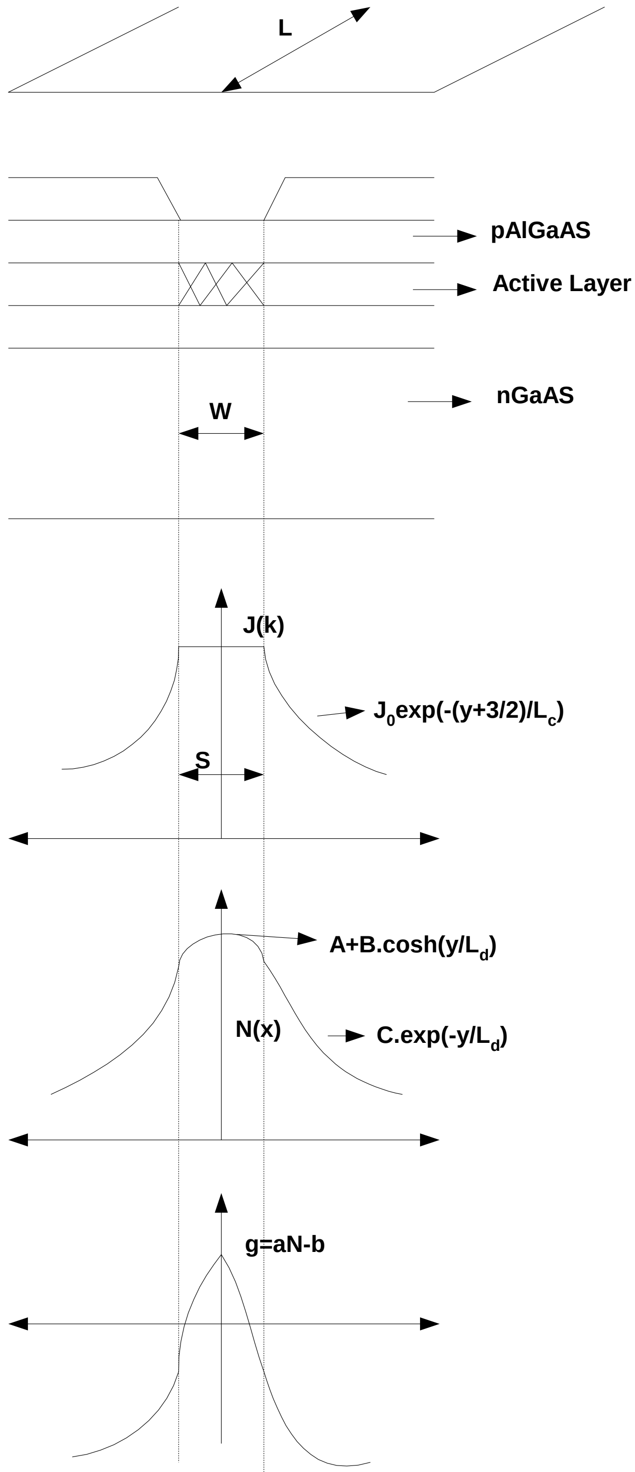

Fig.64 Basic Laser Parameters

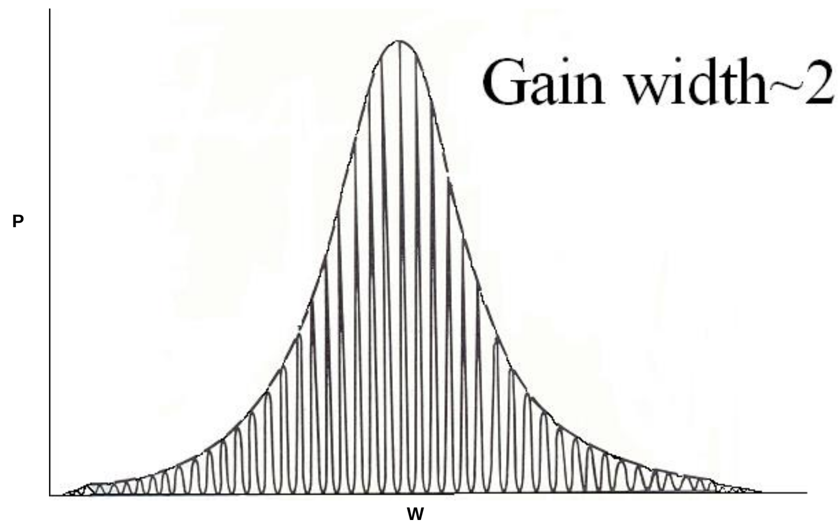

Fig.65 Laser Output Characteristics

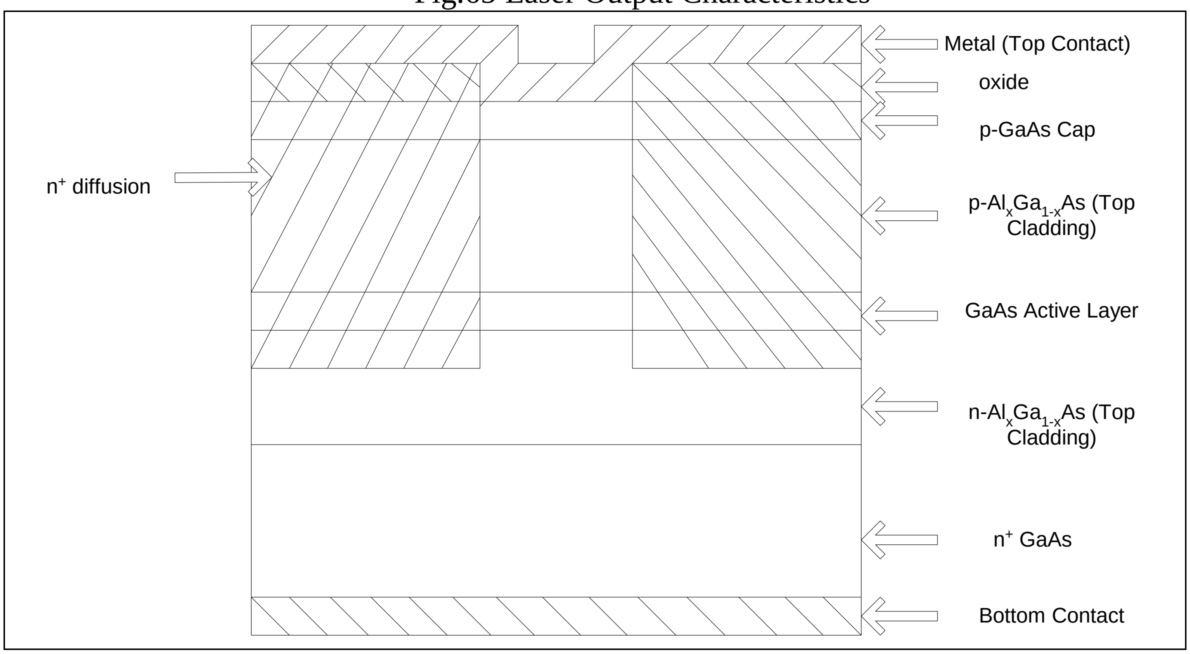

Fig.65 Buried Heterostructure Laser

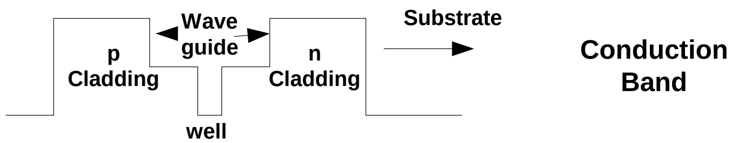

Fig.66 Abrupt Quantum Well

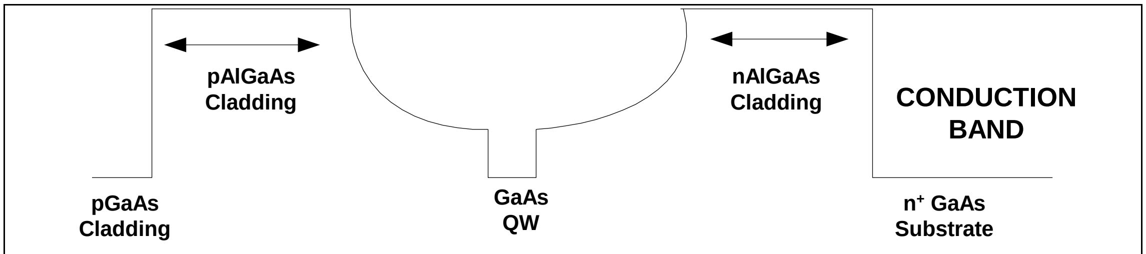

High Power lasers

Fig.67 Graded Index Seperately Confined Heterostructure (GRINSCH)

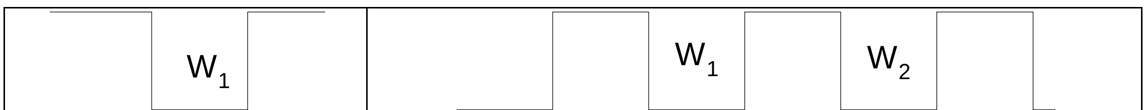

Single Quantum Well	3-4 wells are generally used

Fig.68 Singular Quantum Well vs. Multiple Quantum Wells

Gain is higher in QW than in Double Heterostructure.

<u>Double Heterostructure versus Quantum Well</u>

1) Threshold

$J_{TH}\big|_{DH} > J_{TH}\big|_{QW}$

2) Confinement Factor

$$\Gamma_{DH}(\sim 0.3 - 0.7) > \Gamma_{QW}(\sim 0.02 - 0.4)$$

3) Operating Wavelength

$\lambda_{DH} > \lambda_{QW}$ for the same material